Durham University

Durham E-Theses

A study of the non-equilibrium response of an mos device subjected to a triangular voltage wave form.

Rahman, M.I

How to cite:

Rahman, M.I (1983) *A study of the non-equilibrium response of an mos device subjected to a triangular voltage wave form.*, Durham theses, Durham University. Available at Durham E-Theses Online: http://etheses.dur.ac.uk/7214/

Use policy

The full-text may be used and/or reproduced, and given to third parties in any format or medium, without prior permission or charge, for personal research or study, educational, or not-for-profit purposes provided that:

- a full bibliographic reference is made to the original source
- a link is made to the metadata record in Durham E-Theses
- the full-text is not changed in any way

The full-text must not be sold in any format or medium without the formal permission of the copyright holders.

Please consult the full Durham E-Theses policy for further details.

Academic Support Office, The Palatine Centre, Durham University, Stockton Road, Durham, DH1 3LE
e-mail: e-theses.admin@durham.ac.uk Tel: +44 0191 334 6107
http://etheses.dur.ac.uk

A STUDY OF THE NON-EQUILIBRIUM RESPONSE OF AN MOS DEVICE SUBJECTED TO A TRIANGULAR VOLTAGE WAVE FORM.

M.I.RAHMAN.

The copyright of this thesis rests with the author.
No quotation from it should be published without
his prior written consent and information derived
from it should be acknowledged.

A thesis submitted in accordance with the regulations for the degree of Master of Science;in the University of Durham.

1983

-5. DEC. 1983

Thesis
1983/RAH

ABSTRACT

This thesis is concerned with the study of the response of an MOS device subjected to a triangular voltage waveform of such frequency as to take the device into the non-equilibrium mode of operation.

A new technique,called the drop-back technique,is developed and used to measure device characteristics,such as the depletion width within the semiconductor bulk region, the generation current and generation rate of bulk traps.

A direct plot of surface potential versus the gate voltage is obtained by using an analogue circuit and the results are compared with the similar plot obtained by the dropback technique.

ACKNOWLEDGEMENTS

I would like to take this opportunity to thank my Supervisor, Dr. P.G.C. Allman, for his helpfulness and guidence throughout both my work and preparation of this thesis.

I would also like to thank Dr.M.J. Morant for all of his help and suggestions.

I also extend my gratitude to Mr. John Gibson for all help received.

LIST OF SYMBOLS

A	MOS device gate area, cm^2.
A_v	Operational amplifier voltage gain.
C	Capacitance, F.
C_f	Feedback capacitance, F.
C_{ox}	Oxide capacitance, F/cm^2.
C_{min}	Minimum high frequency capacitance, F/cm^2.
d	Oxide thickness, cm.
e_n	Emission probability for electrons.
e_p	Emission probability for holes.
E_c	Energy of bottom of conduction band, eV.
E_f	Energy of fermi level in semiconductor bulk region, eV.
E_{fs}	Energy of fermi level at oxide-semiconductor interface, eV.
E_{fB}	Energy of fermi level at the bulk of the semiconductor, eV.
E_i	Energy of the midgap level, eV.
E_t	Trapping energy level in the bulk of the semiconductor, eV.
E_v	Energy of top of the valence band, eV.
f	Probability of occupation of trapping centre by an electron
F	Frequency, Hz.
G_{th}	Thermal generation rate, $cm^{-3}sec^{-1}$.
i	Current, A.
I	Current per area unit, A/cm^2.
I_d	Depletion current, A/cm^2.
$\|I_d\|_f$	Depletion current during the forward sweep, A/cm^2.
$\|I_d\|_r$	Depletion current during the reverse sweep, A/cm^2.
$\|I\|_f$	Gate current during the forward sweep, A/cm^2.
$\|I_g\|$	Gate current, A/cm^2.
$\|I\|_r$	Gate current during the reverse sweep, A/cm^2.

$\|I_{gen}\|$	Generation current,A/cm^2.
$\|I_{ox}\|$	Oxide current,A/cm^2.
$\|I_q\|$	Current due to the flow of the inversion charge from the interface to the bulk of the semiconductor,A/cm^2.
K	Boltzman constant,eV/K.
L_E	Normalized steady-state depletion width,cm.
m*	Effective mass of electron,Kg.
n	Free electron density,cm^{-3}.
n_i	Intrinsic carrier concentration,cm^{-3}.
N_A	Acceptor concentration of substrate,cm^{-3}.
N_c	Effective density of states in the conduction band,cm^{-3}.
N_D	Donor concentration of substrate,cm^{-3}.
N_t	Bulk trap density in the semiconductor,cm^{-3}.
N_v	Effective density of states in the valence band,cm^{-3}.
p	Free hole density,cm^{-3}.
q	Electronic charge,c.
Q_G	Gate charge,C.
Q_d	Semiconductor space charge per unit area,C/cm^2.
Q_g	Gate charge,C.
Q_i	Inversion charge per unit area,C/cm^2.
Q_s	Total charge per unit area,C/cm^2.
r_a	Rate of capture of electron by trapping centre,cm^{-3}sec^{-1}
r_b	Rate of emission of electron by trapping centre,cm^{-3}sec^{-}
r_c	Rate of capture of hole by trapping centre,cm^{-3}sec^{-1}.
r_d	Rate of emission of hole by trapping centre,cm^{-3}sec^{-1}.
R	Total rate of recombination.
R_{ext}	Operational amplifier circuit external resistance,Ω.
R_i	Operational amplifier circuit input resistance,Ω..

R_L	Operational amplifier circuit load resistance, Ω.
R_o	Operational amplifier circuit output resistance, Ω.
t	Time, sec.
t_B	Time at the onset of sweep reversal, sec.
T	Absolute temperature, K.
U_g	Bulk trap generation rate, $cm^{-3} sec^{-1}$.
$\mathcal{V}_i$	Operational amplifier circuit input voltage, V.
$\mathcal{V}_o$	Operational amplifier circuit output voltage, V.
$\mathcal{V}_s$	Operational amplifier circuit signal voltage, V.
$\mathcal{V}_{th}$	Thermal velocity of the carriers, cm sec^{-1}.
V	Gate voltage above, V_o, V.
V_d	Diode voltage, V.
V_g	Gate voltage, V.
V_B	Gate voltage at the instant of the sweep reversal, V.
V_o	Gate voltage at onset of generation, V.
$\mathcal{V}_R$	Reference voltage, V.
$\mathbf{V}$	Certain constant voltage value, V.
X	Distance into semiconductor bulk from S_i/S_iO_2 interface, cm.
X_{dB}	Semiconductor depletion width at $V=V_B$, cm.
X_d	Semiconductor depletion width, cm.
X_E	Average value of the depletion width between two points, cm
X_o	Depletion width at onset of generation, cm.
Z	Normalized depletion width.
Z_B	Normalized depletion width at instant of sweep reversal.
α	Voltage sweep rate, V/sec.
ψ	Electrostatic potential in semiconductor bulk, V.
ψ_s	Semiconductor surface potential, V.
ψ_f	Fermi potential, V.
ψ_i	Surface potential at onset of inversion, V.
ψ_B	Potential difference between the fermi level and the intrinsic fermi level in bulk, V.

ε_s	Silicon permitivity, F/cm.
ε_{ox}	Oxide permitivity, F/cm.
τ_g	Generation life-time, sec.
σ	Capture cross section for holes and electrons, cm^2.
$\Delta\lvert I\rvert$	Drop in gate current at sweep reversal, A/cm^2.

CONTENTS

	page
Absract.	i
Acknowledgements.	ii
List of symbols.	iii
CHAPTER ONE "INTRODUCTION"	
1.1 Introduction.	1
1.2 Review of the field.	1
CHAPTER TWO "THEORY OF THE NON-EQUILIBRIUM RESPONSE"	
2.1 Introduction.	5
2.2 Review of the generation and recombination processes.	5
2.3 Non-equilibrium fast ramp (I-V) analysis.	11
2.4 Theory of the drop-back technique.	21
CHAPTER THREE "INSTRUMENTATION AND PROGRAMING"	
3.1 Introduction.	33
3.2 The Triangle Wave Generator.	33
3.3 Direct measurement of ($\psi_s - V_g$) by Tonner & Simmons technique.	36
3.4 The drop-back experimental setup .	38
3.5 The drop-back technique program.	40
CHAPTER FOUR "MEASUREMENT AND RESULTS"	
4.1 Introduction.	43
4.2 The High frequency bridge measurements.	43
4.3 The drop-back technique experimental measurements.	47

4.4 Surface potential measurement. 68

4.5 Discussion. 79

CONCLUSIONS 80

REFERENCES 82

APPENDIX ONE

A-1 The Clock circuit. 84

A-2 Some electronic circuit fundamentals. 84

A-3 The analogue to digital Converter circuit. 93

APPENDIX TWO "LISTING OF THE EXPERIMENTAL RESULTS" 100

APPENDIX THREE "LISTING OF THE PROGRAM"

CHAPTER ONE

INTRODUCTION

1.1 Introduction

The study of simple metal-oxide-semiconductor MOS structures can help towards the understanding of interface and bulk effects in more complicated semiconductor devices.

This thesis is concerned with the application of a new experimental technique, designated the drop-back technique, which can be used to obtain rapid information about the processes occurring in an MOS device.

The parameters which can be measured are depletion width in the semiconductor, bulk trap generation current and bulk trap generation rate.

Chapter Two is concerned with bulk traps in the semiconductor and we discuss the use of the fast ramp technique in determining the properties of these traps, the second section of the chapter describing in detail the drop-back theory.

The Third Chapter considers the instrumentation used to obtain the experimental results and the computer program developed to analyse the data.

In Chapter Four the experimental results are presented and general conclusions follow at the end of the thesis.

1.2 Review of the field

In 1959 the MIS structure was first proposed by Moll [2] and Pfann and Garrett [3], as a voltage variable capacitor.

Frankel [4] and Lindner [5] subsequently presented

an analysis to describe the characteristics of the device.

Terman [6] studied the structure when he worked on thermally oxidized silicon surfaces.

Since that time, many experiments and techniques have been developed to investigate MOS device characteristics, the early works being mainly concerned with the evaluation of the interface density. The high frequency capacitance technique was presented by Terman [6], in which he compared the theoretical capacitance vs. voltage curve without interface states and a measured high frequency capacitance vs. voltage curve, and was able to obtain the distribution of the states.

In 1965 Gray and Brown [7] presented the temperature variation technique in which they varied the temperature while maintaining the flat band condition by observing the change in capacitance and continuously adjusting the bias. They recorded the flat-band voltage versus the temperature and then converted the resulting data to surface charge versus surface potential, and finally deduced the surface density.

Nicollian and Goetzberger [8] proposed a measurement method called the Admittance Technique, which gives accurate and reliable results. The conductance of the MOS device is measured and directly related to the surface states. The disadvantage of this technique lies in the fact that only a small portion of the energy gap can be studied and information about the bulk semiconductor properties are lost.

Another technique was proposed by Berglund [9], called the integration technique, in which he applied a voltage to

the gate of the MOS device at a low enough frequency to maintain electrical equilibrium.

Kuhn [10] made use of the Berglund technique. In this technique , where a slow voltage ramp is applied to the gate of the MOS device , it is possible to measure the interface state density over large parts of the energy gap.With all of the above technique it is not possible to study the bulk properties of the semiconductor and so obtain information about the generation-recombination processes in the bulk.

Later work was,therefore,concerned with the study of the bulk properties of the MOS device . This is achievable by driving the device into the non-equilibrium mode of operation . Many experiments and techniques have been carried out with this end in mind.

Rupprecht [11] Jund and Poirier [12] and Zerbst [13] studied the generation properties of the surface states, measuring the carrier concentrations and the minority life-time,using the pulsed MOS structure.

Heiman [14] used a large voltage step, which is applied in a direction as to take the device into deep depletion.

Huang [15] used again the large voltage step and applied it to the MOS gate while the device was biased in strong inversion (to eliminate the interface state effect) From the transient wave form he deduced a life time value.

Hofstein [16] used a small voltage step and included the effect of the surface states , the accuracy of this technique therefore depended on the density of the surface states.

Kuper and Grimbergen [17] measured both the current and the capacitance of an MOS device in response to a depleting linear voltage ramp.Starting in inversion,

a rapid measurement of the life-time can be obtained by using their analysis.

Board and Simmons [1] presented a study of the MOS device subjected to a triangular voltage wave form, the sweep rate being of such magnitude as to take the device into the non-equilibrium mode of operation. They present analytical equations relating the current, and hence the small signal capacitance, and the gate voltage to the depletion width.

In 1978, Board, Simmons and Allman [18] presented experimental verification of this technique.

Allman and Simmons [19 & 20] suggested the use of a constant-current instead of constant-voltage ramp bias.

CHAPTER TWO

THEORY OF THE NON-EQUILIBRIUM RESPONSE

2-1 Introduction

A fast voltage ramp is applied to the gate of the (MOS) device of such magnitude as to drive the device into the non-equilibrium mode, that is, the minority carrier generation rate cannot maintain the device in equilibrium for that given rate of change of voltage bias. Hence, the depletion width (X_d) will be wider at any given gate voltage (V_g) than the corresponding value in equilibrium.

Figure(2.1) shows clearly the effect of increasing ramp frequency, so taking an (MOS) device into the deep depletion mode. It is very important to understand the non- equilibrium mode of operation because of its use in device applications, (eg, charge coupled devices).

The dynamic aspect of traps is lost when the (MOS) device is operated in the quasi-equilibrium mode.

2-2 Review of the generation and recombination processes

At equilibrium there is continuous thermal agitation which excites electrons and makes them leave the valence band and rise up to the conduction band, thus forming holes in the valence band. Mathematically, this can be expressed as,

$np = (ni)^2$, where the letters have their usual notation.

But as the device is driven into non-equilibrium the condition

$np = (ni)^2$ is violated.

There are two possible cases which can be considered:

a)) When $np > (ni)^2$, called the injection of excess carriers.

b)) When $np < (ni)^2$, called the extraction of carriers from the semiconductor.

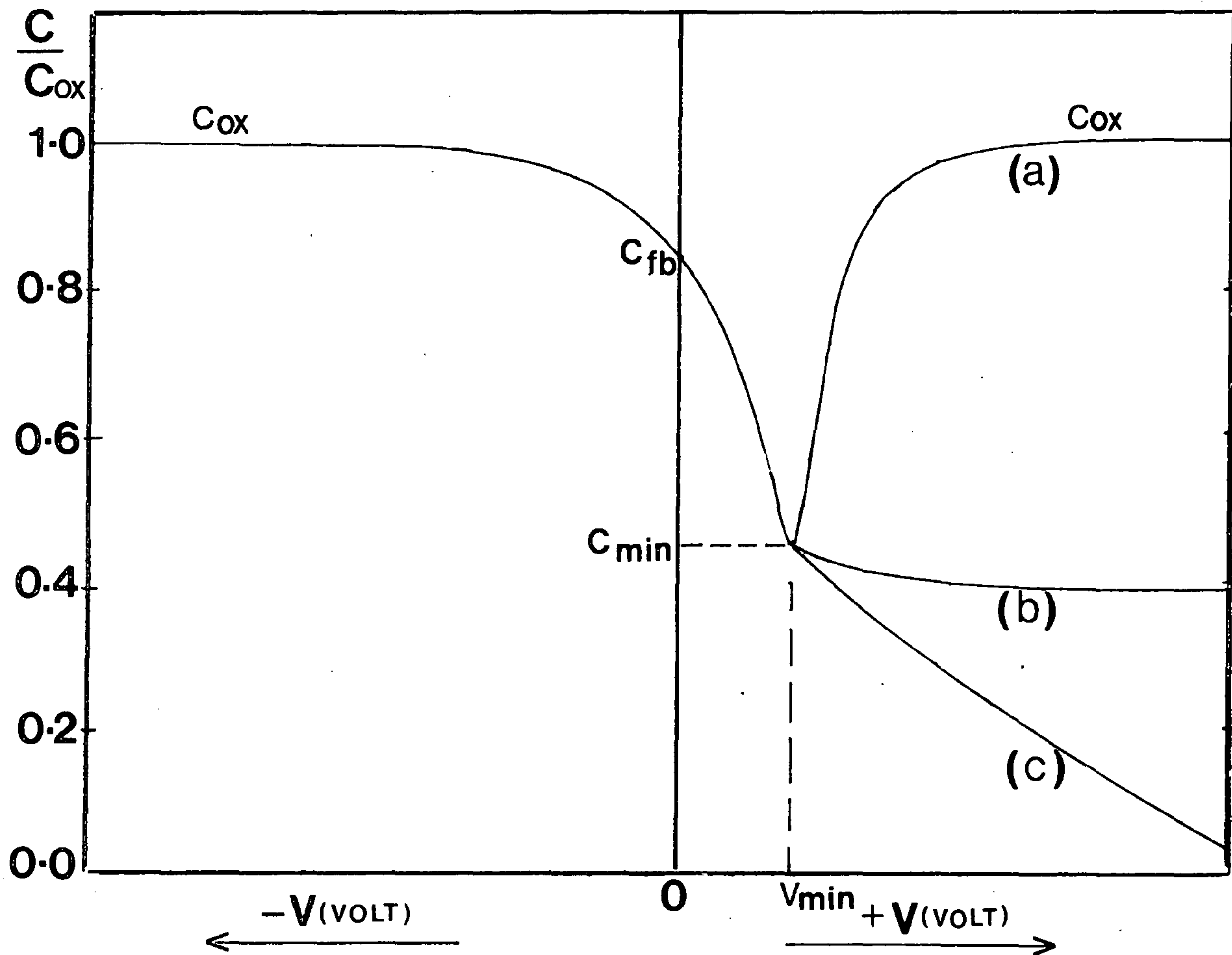

Figure (2.1)

MOS capacitance-voltage curves (after Grove et al [ref 30])
a) Low frequency , b) High frequency , c) Deep depletion .
(p-type substrate).

Whenever the carrier concentrations are disturbed from their equilibrium values,in time and given the right conditions, $np = (ni)^2$ will be re-established.

In case (a) the return will be through the recombination process , while in case (b) the return will be through the generation process.

Briefly , generation occurs due to the transfer of the electrons from the valence band up to the conduction band under excitation (thermal or electrical .....etc), while recombination is the process of returning the electrons from the conduction band down to the valence band.

The generation-recombination processes can be classified into two types :

(1) The band to band process.

(2) The generation-recombination through intermediate traps.

Shockley and Read [ref 21] in their paper describe the generation-recombination processes inside a semiconductor and show that these processes mainly occur due to type(2), especially when the traps lie at or near midgap. Let us consider the recombination process. Shockley and Read divided the processes occuring into four steps :

(a) Electron Capture(from the conduction band to the traps.)

(b) Electron Emission (from the traps up to the conduction band.

(c) Hole Capture (from the traps to the valence band.)

(d) Hole Emission (from the valance band to the traps) In fig (2-2), (r_a) is the rate of capture of electrons, (r_b) is the rate of emission of electrons, (r_c) is the rate of capture of holes and (r_d) is the rate of emission of the holes, all of which can be described by the following expressions:

$$r_a = \mathcal{V}_{th} \cdot \delta_n \cdot n \cdot N_t \cdot (1-f)$$
$$r_b = e_n \cdot N_t \cdot f$$
$$r_c = \mathcal{V}_{th} \cdot \delta_p \cdot p \cdot N_t \cdot f$$
$$r_d = e_p \cdot N_t \cdot (1-f)$$

f is the probability of occupation of the trap by an electron and in equilibrium is given by

$$f = \frac{1}{1 + e^{(E_t - E_f)/KT}}$$

$\mathcal{V}_{th}$ is the thermal velocity of the carriers and is given by $\sqrt{3KT/m^*}$, and (δ_n) is the capture cross section which is a measure of how close the electron has to come to the trap to be captured (which is of the order of atomic dimensions, 10^{-15} cm^2). (e_n), (e_p) are the emission probabilities of electrons and holes and are the probabilities of a jump from an occupied trap to the conduction band and down to the valence band , respectively, (N_t) is the bulk trap density.
The net recombination rate can be written as:

$$U = G_{th} - R \qquad \text{----------------2-1}$$

where (R= total rate of recombination, and G_{th} is the rate of generation due to the thermal mechanism.) Using the

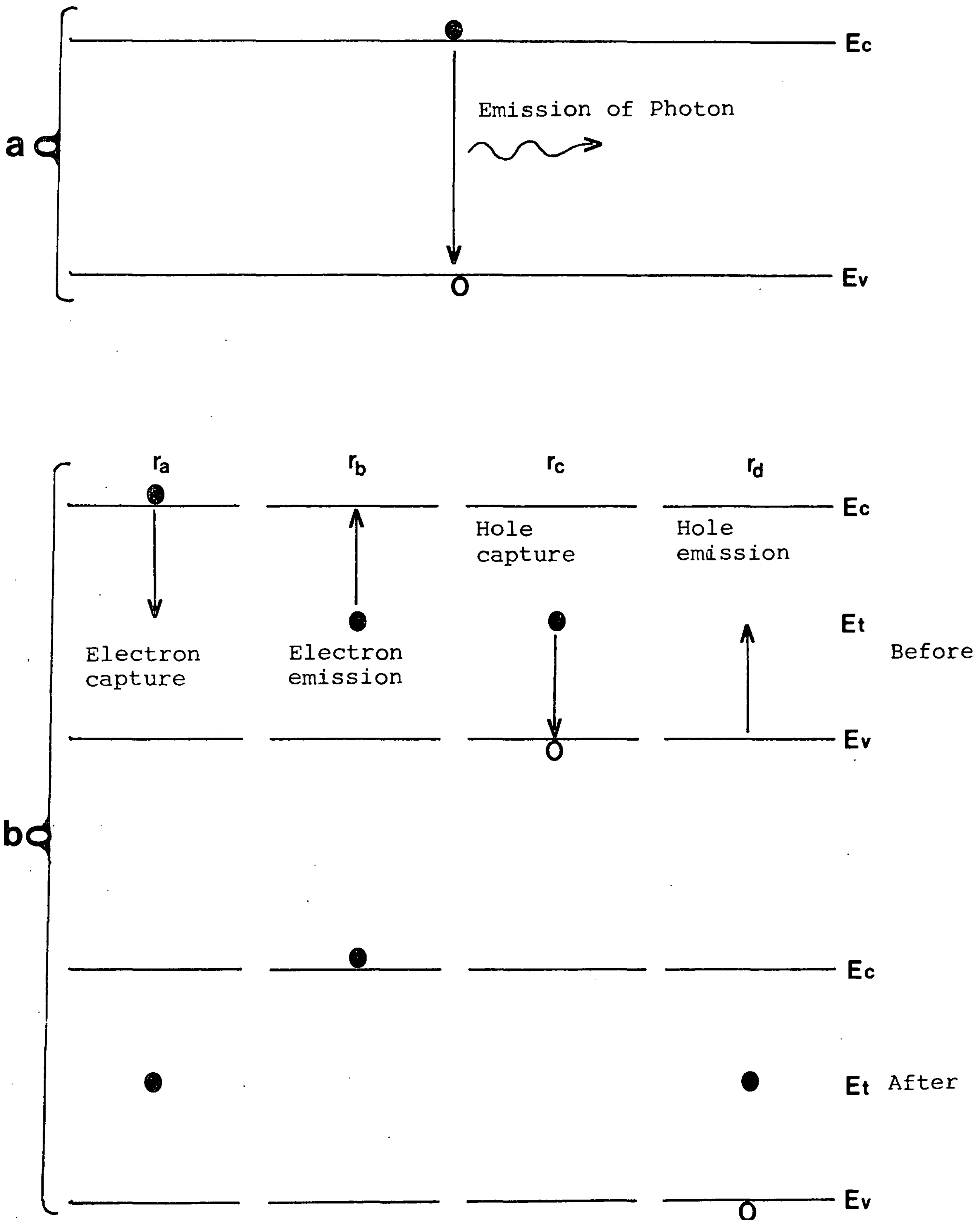

Figure(2.2) The recombination processes through intermediate levels.

a. Band to band recombination.

b. Single level recombination.

expressions above , equation (2-1) becomes:

$$U = r_a - r_b + r_c - r_d \quad \text{---------2-2}$$

In the equilibrium mode of operation , we have that:

$r_a = r_b$, and $r_c = r_d$, so that U = o,

that is, zero net recombination. Howevwr, in the non-equilibrium mode (with a steady-state trap occupancy) we have:

$$r_a - r_b = r_c - r_d \quad \text{and so}$$

$$U = r_a - r_b = r_c - r_d \quad \text{-----------2-3}$$

Upon substitution from above, this expression becomes

$$U = \frac{\sigma_p \cdot \sigma_n \cdot V_{th} \cdot N_t \, (pn - n_i^2)}{\sigma_n \left(n + N_c e^{-(E_c - E_t)/KT}\right) + \sigma_p \left(p + N_v e^{-(E_t - E_v)/KT}\right)}$$

------------2-4

which simplifies (with $\sigma = \sigma_p = \sigma_n$) to

$$U = \frac{\sigma \cdot V_{th} \cdot N_t \, (pn - n_i^2)}{n + p + 2n_i \cdot \cosh (E_t - E_i /KT)}$$

---------2-5

From equation (2-5), it is clear that;

1) U = 0 at thermal equilibrium, i.e., at $np = ni^2$.

2) U is its maximum value when E_t is at midgap, i.e., at $E_t = E_i$.

3) If U is positive then we have net recombination and if it is negative we have net generation.

The traps which are involved in the generation-recombination processes occur due to many reasons, e.g

faults in the crystal structure, foreign atoms, dangling bonds between two layers ..etc.

2-3 Non-equilibrium fast ramp (I-V) Analysis

Simmons & Board [ref 1], investigated the (I-V) characteristic of (MOS) devices subjected to fast voltage ramps. They show in their paper that over the region $0 < X < (X_d - X_o)$, (figure 2.3), the generation rate is high compared to the recombination rate and is dominent in this region, while over the region $(X_d - X_o) < X < X_d$, the generation rate is comparable with the recombination rate, so causing the net generation rate over this region to be small.

The Triangular Wave form voltage applied to the MOS device is shown in figure(2·4) over the interval $0 < t < t_B$ the device is being driven into depletion and is designated the forwared sweep, whereas over the interval $t_B < t$ the device is being driven towards accumulation and is called the reverse sweep.

In order to analyse the I-V curve (figure 2·5), let us start from the basic equations .

The inversion charge over the region $0 < X < (X_d - X_o)$ is given by :

$$Q_i = q \cdot U_g \cdot (X_d - X_0) \cdot dt \quad \text{------- 2-6}$$

or

$$I_i = q \cdot U_g \cdot (X_d - X_0) \quad \text{------- 2-7}$$

The expression for the space charge Q_d is

$$Q_d = q \cdot N_A \cdot X_d \quad \text{------------- 2-8}$$

and for the surface potential

$$\Psi_s = \frac{q \cdot N_A \cdot X_d^2}{2 \cdot \mathcal{E}_s} \quad \text{--------------- 2-9}$$

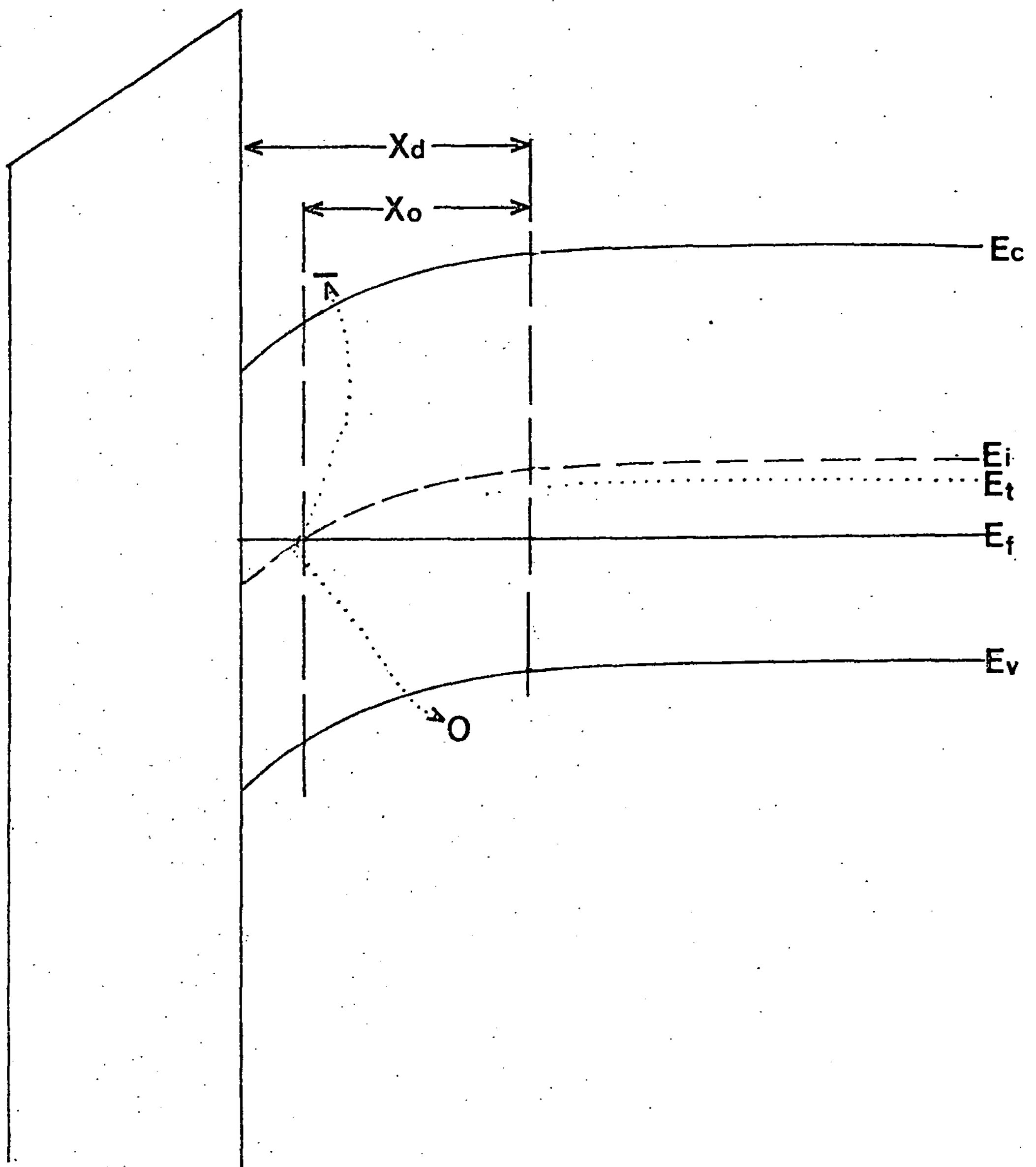

Figure (2.3)

Band diagram of the p-type MOS device structure.

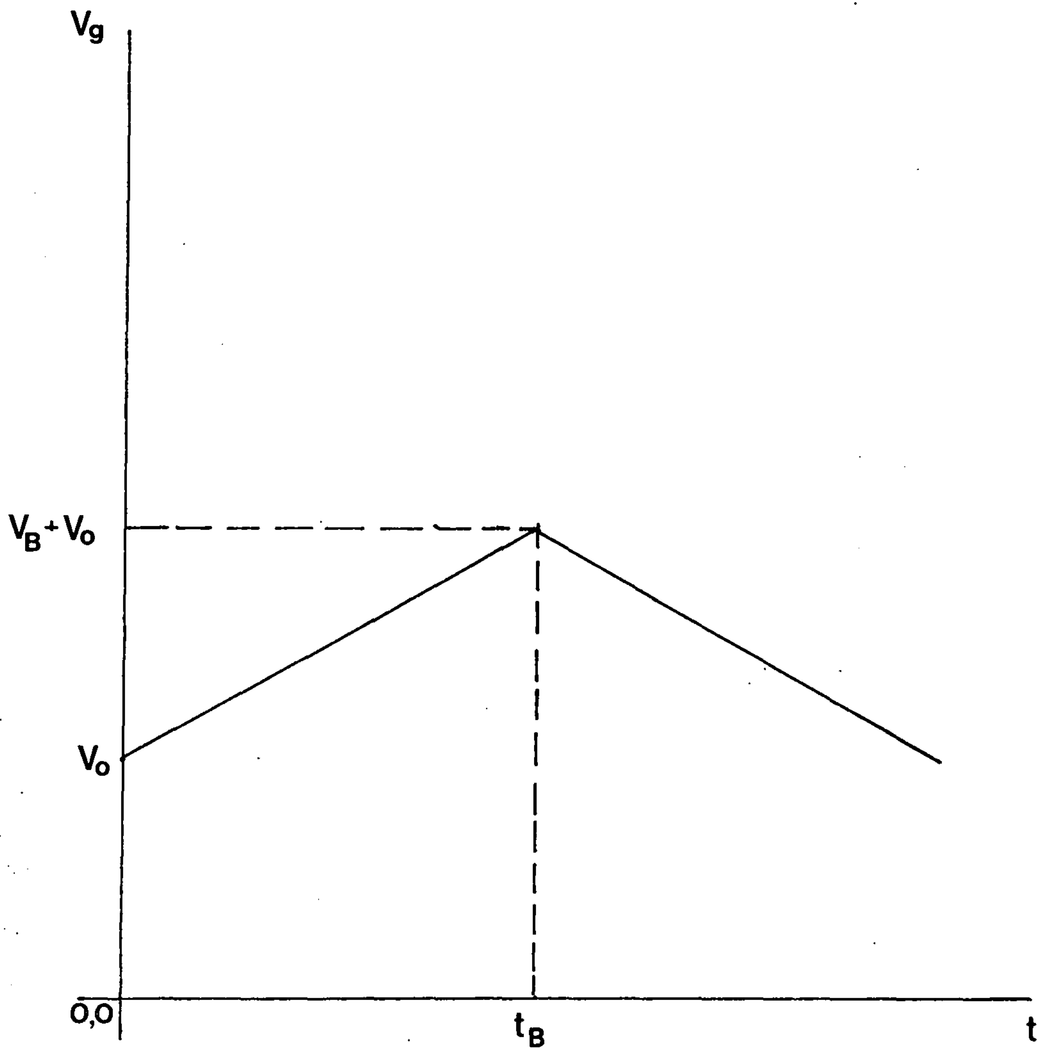

Figure (2.4)

The triangular voltage wave form applied to the MOS device.

It is convenient to study the I-V characteristic in two parts, the forward (point a to c of figure 2.5) and the reverse sweep (point c to f).

1) <u>The Forward Sweep</u>

As the forward sweep voltage is applied to the p-type MOS device, positive charge will be accumulated on the gate, and an equal negative charge will accumulate on the semiconductor side, these negative charges coming mainly from two sources, namely, the charge in the space charge region and that from the generation process [ref 1], figure (2.6a). In fact, there is a third source of charge, that being due to the interface traps which emit electrons at the beginning of the sweep. These interface traps effect only the low voltage portion of the forward sweep region i.e region (a-b) of figure (2.5), after which, their contribution is negligible. Therefore, we can write

$$|Q_g| = |Q_i| + |Q_d| \qquad \text{2-10}$$

which, upon differentiating with respect to time, becomes;

$$|I_g| = |I_{gen}| + |I_d|_f \qquad \text{2-11}$$

where $|I_d|_f$ is the depletion current and $|I_{gen}|$ the generation current.

The gate voltage is given by

$$V_g = V_{ox} + \psi_s \qquad \text{2-12}$$

where (V_{ox}) is the voltage drop across the insulator and is equal to (Q_g/C_{ox}) and (ψ_s) is the surface potential of the semiconductor, (see figure 2.7).

After substitution equation (2-12) becomes;

$$V_g = \frac{Q_g}{C_{ox}} + \frac{q \cdot N_A \cdot X_d^2}{2 \cdot \varepsilon_s} \qquad \text{2-13}$$

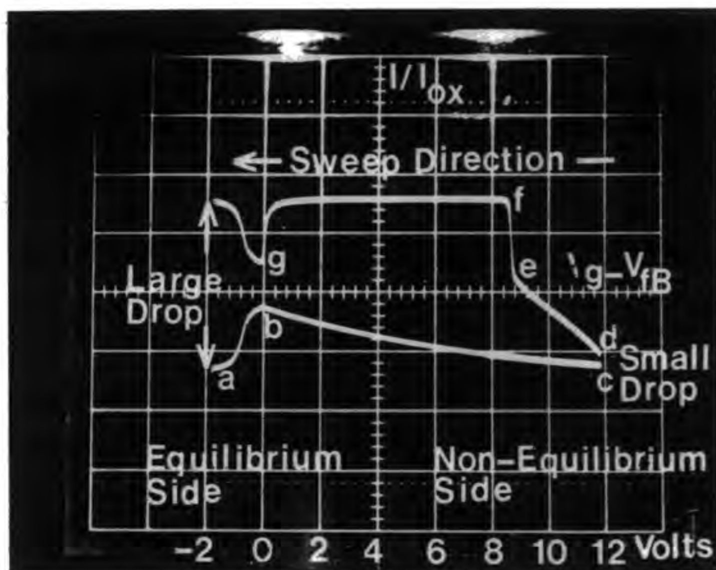

Figure(2.5) The I-V curve(p-type MOS device at sweep rate value of 0.92V/s.).

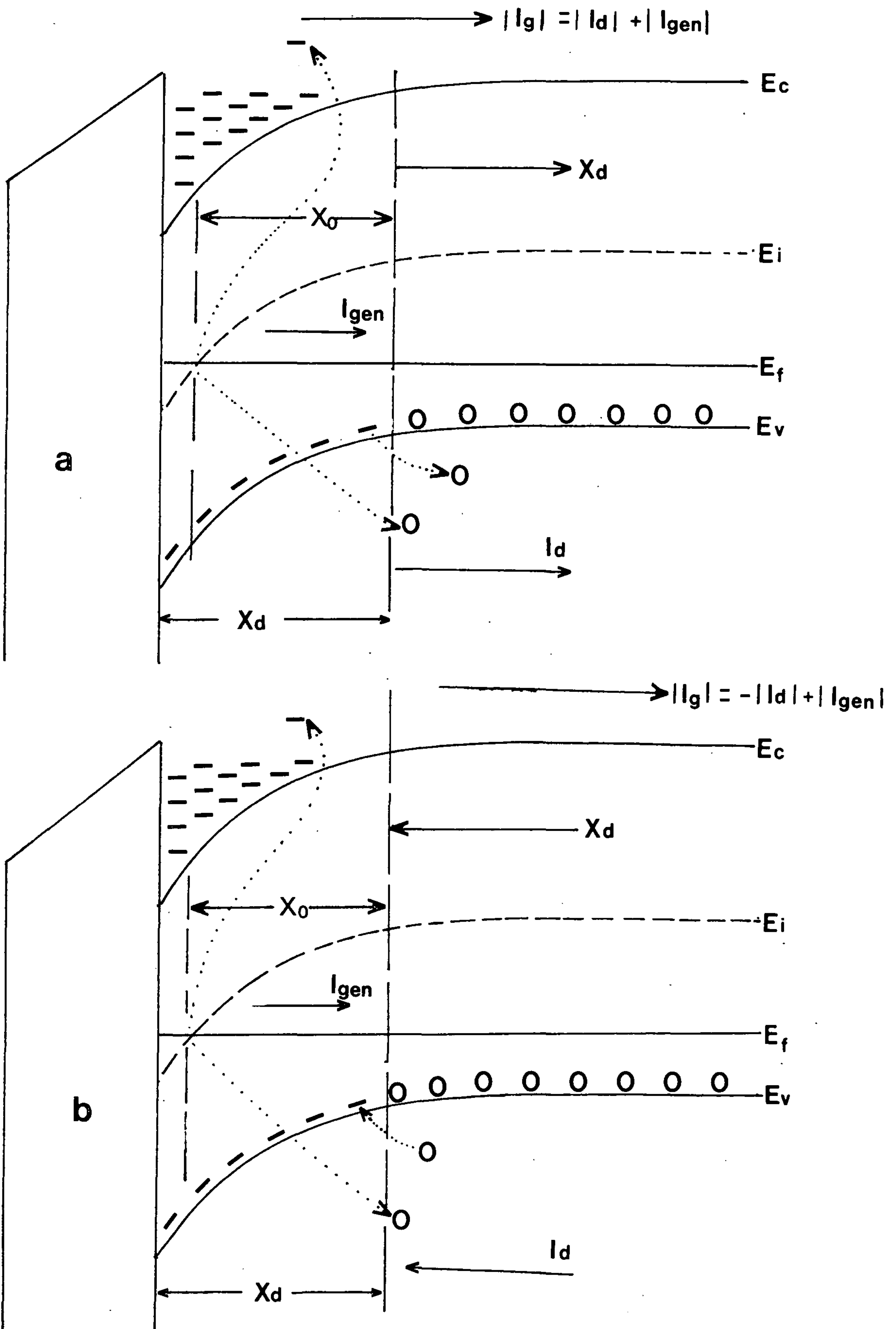

Figure(2.6a) The band diagram of a p-type MOS system during the forward sweep.

Figure(2.6b) The band diagram of a p-type MOS system during the reverse sweep.

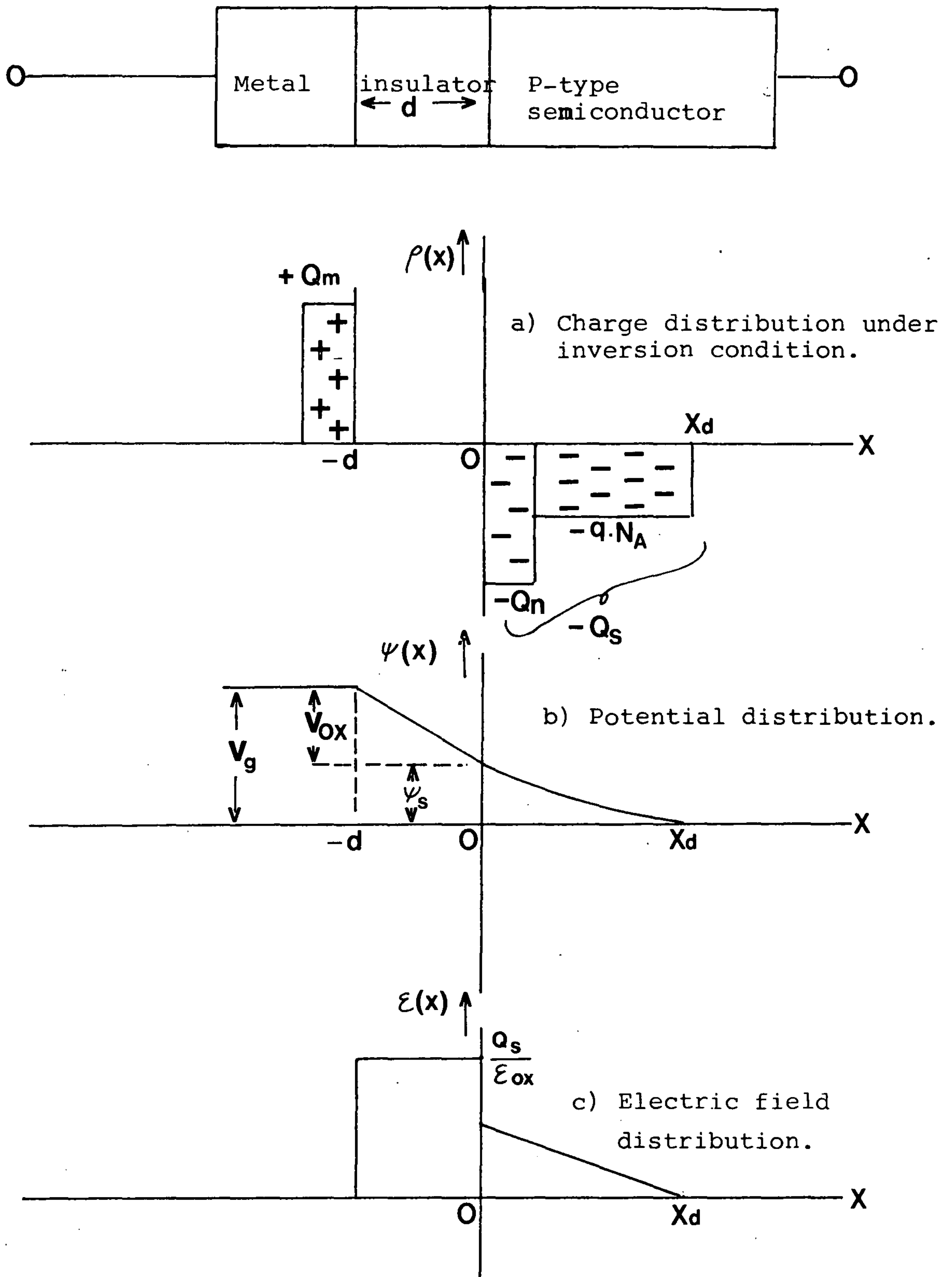

Figure(2.7)

Ideal P-type MOS structure and characteristic distributions.

and, upon differentiating with respect to time, we obtain

$$\frac{dV_g}{dt} = |\alpha| = \left(\frac{1}{C_{ox}} \cdot \left|\frac{dQ_g}{dt}\right|\right) + \left(\frac{q \cdot N_A \cdot X_d}{\mathcal{E}_s} \cdot \left|\frac{dX_d}{dt}\right|\right)$$

------------------2-14

$$= \frac{1}{C_{ox}} \cdot |I|_f + \frac{q \cdot N_A \cdot X_d}{\mathcal{E}_s} \cdot \left|\frac{dX_d}{dt}\right|$$

------------------2-15

Rearranging equation (2-15) we obtain

$$\frac{dX_d}{dt}\left(1 + \frac{C_{ox} \cdot X_d}{\mathcal{E}_s}\right) = \frac{U_g}{N_A} \cdot \left(L_E + X_O - X_d\right)$$

------------------2-16

where the substitutions,

$$L_E = \frac{|\alpha| \cdot C_{ox}}{q \cdot U_g}$$

$$Z = \frac{(X_d - X_o)}{L_E}$$

$$V = V_g - V_o$$

have been used.

By applying the boundary condition $X_d = X_o$ at $t=0$ Equation (2-16) can be solved to obtain,

$$\left(1 + \frac{C_{ox}(X_o + L_E)}{\mathcal{E}_s}\right) \cdot \mathrm{Ln}(1-Z) + \frac{L_E \cdot C_{ox} \cdot Z}{\mathcal{E}_s} = \frac{- C_{ox} \cdot V}{q \cdot N_A \cdot L_E}$$

------------------2-17

Equation (2-17) gives the relationship between the gate voltage and the depletion width. In order to obtain an expression for the gate current we differentiate equation

(2-17) to give

$$\frac{dZ}{dt} = \frac{C_{ox} \cdot (1-Z)}{q \cdot N_A \cdot L_E \cdot \left(1 + \frac{C_{ox}}{\mathcal{E}_s}(X_o + Z \cdot L_E)\right)} \quad \text{------------2-18}$$

then by rewriting equation (2-17) we obtain

$$|I|_f = |\alpha| \cdot C_{ox} \cdot Z + q \cdot N_A \cdot L_E \cdot |\alpha| \cdot \frac{dZ}{dV} \quad \text{------- 2-19}$$

By using equations (2-18), (2-19) and solving for $|I|_f$ we obtain

$$|I|_f = |\alpha| \cdot C_{ox} \cdot \left(Z + \frac{1 - Z}{1 + \frac{C_{ox}}{\mathcal{E}_s}(X_o + Z \cdot L_E)} \right) \quad \text{----------------2-20}$$

or

$$\frac{|I|_f}{|\alpha| \cdot C_{ox}} = \left(Z + \frac{1 - Z}{1 + \frac{C_{ox}}{\mathcal{E}_s}(X_o + Z \cdot L_E)} \right) \quad \text{----------------2-21}$$

The above equations relate the normalised gate current to the parameter Z (and therefore depletion width).

2) <u>The Reverse Sweep</u>

At $t = t_B$, the reverse sweep begins (point C of figure 2.5) and the space charge region in the semiconductor begins to collapse. Therefore, the generation charge (Q_i) contribution starts to decline and the system moves closer to quasi-equilibrium (see figure 2.6b). In this condition the gate current is given by

$$|I_r| = |I_{gen}| - |I_d|_r \quad \text{...........2-22}$$

By considering equations (2-12) and (2-22), we observe that a sudden change occurs in the gate current at sweep reversal. The equations that were derived above for the non-equilibrium forward sweep can be similarly obtained for the reverse sweep. By changing the sign of the sweep rate (α), putting $Z=Z_B$, $t=t_B$ and $V=V_B$ we can obtain

$$\left(1 + \frac{C_{ox}}{\mathcal{E}_s} \cdot (X_o - L_E)\right) \cdot Ln\left(\frac{1+Z}{1+Z_B}\right) + \frac{(Z - Z_B) \cdot L_E \cdot C_{ox}}{\mathcal{E}_s} = \frac{-C_{ox} \cdot (V_B - V)}{q \cdot N_A \cdot L_E} \qquad \text{2-23}$$

for the gate voltage and

$$|I|_r = (|\alpha| \cdot C_{ox} \cdot Z) - \left(q \cdot N_A \cdot L_E \cdot |\alpha| \cdot \frac{dZ}{dV}\right) \qquad \text{2-24}$$

with

$$\frac{dZ}{dV} = \frac{C_{ox} \cdot (1+Z)}{q \cdot N_A \cdot L_E \cdot \left(1 + \frac{C_{ox}}{\mathcal{E}_s} (X_o + L_E \cdot Z)\right)} \qquad \text{2-25}$$

to give

$$\frac{|I|_r}{|I_{ox}|} = \left(Z - \frac{1+Z}{\left(1 + \frac{C_{ox}}{\mathcal{E}_s} (X_o + L_E \cdot Z)\right)}\right) \qquad \text{2-26}$$

for the gate current.

The expression for the abrupt change of the gate curremt can be obtained from equations (2-21) and (2-26), that is

$$\frac{\Delta |I|}{|I_{ox}|} = \frac{2}{1 + \frac{C_{ox} \cdot X_{dB}}{\mathcal{E}_s}} \quad \text{---------------2-27}$$

which is region d-e of figure(2.5).

During the reverse sweep, the contribution of the generation current $|I_{gen}|$ keeps decreasing until $|I_{gen}| = |I_d|_r$ i.e., $|I_r| = 0$ (the point when the I-V curve cuts the X-axis), region e-f of figure(2-5). As time progresses we will eventually reach the condition that the fermi level of the bulk of the semiconductor and the fermi level of the surface are equal in energy, i.e. $E_{fB} = E_{fS}$ in figure(2.8) The system is now in quasi-equilibrium as shown by region f-g of figure(2.5). In this region the system is in quasi-equilibrium and the equations for the equilibrium condition hold.

2.4 Theory of the drop-back technique

This method is a simple and direct way of obtaining the values of the depletion width X_d, bulk generation current $|I_{gen}|$ and bulk generation rate U_g in an MOS device. In order to derive the required equations that give these quantities we look to the equations for the fast ramp technique. Consider the same triangular voltage wave form applied to a (p-type MOS) device, and let us divide the resulting (I-V) curve into two parts, the forward sweep and the reverse sweep.

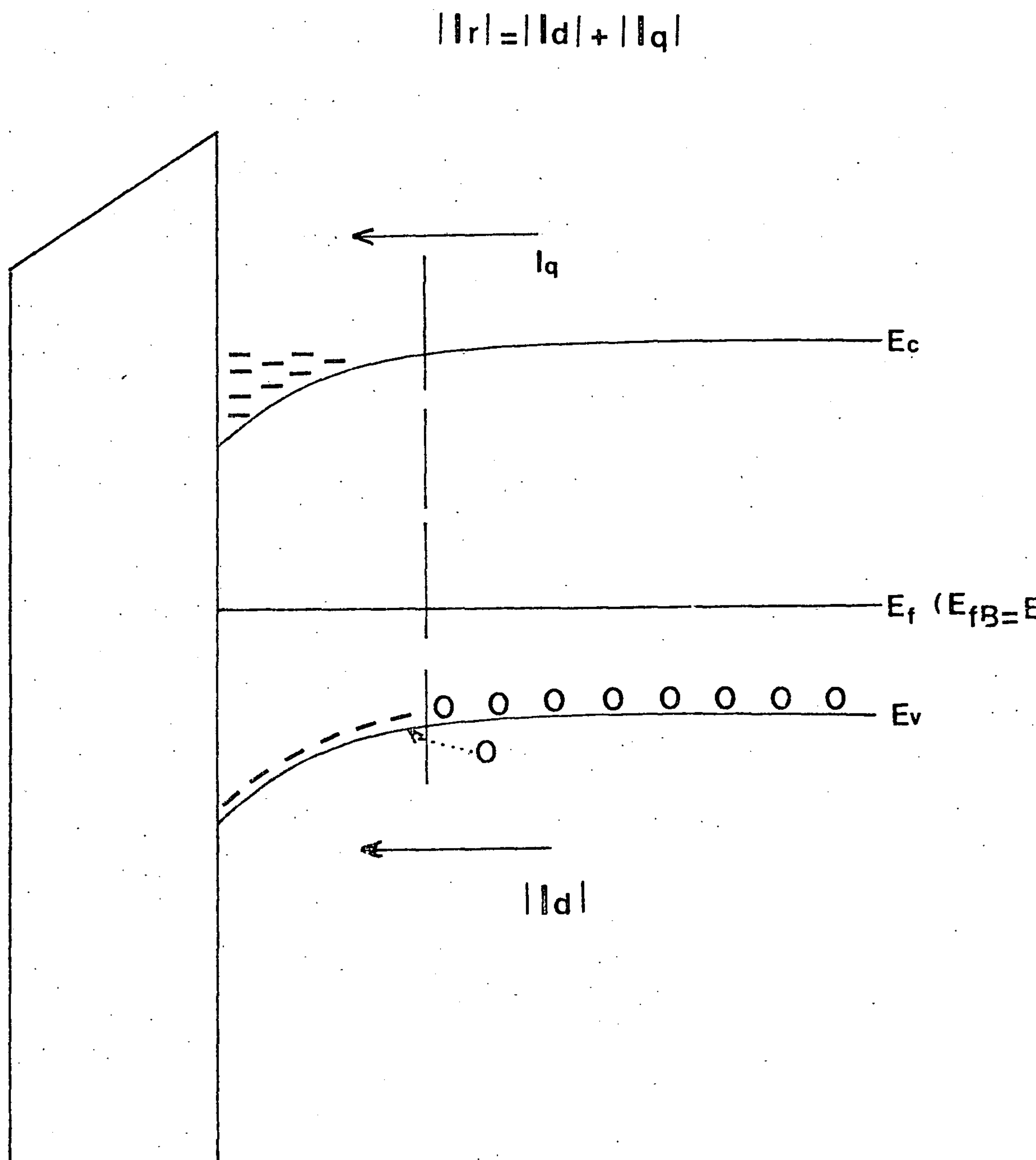

Figure(2.8)

Band diagram of a p-type MOS device at the return to equilibrium i.e., region e-f of figure(2.5).

1) The Forward Sweep

For the electrical neutrality condition

$$+\overleftarrow{|I_g|} - \overrightarrow{|I_{gen}|} - \overrightarrow{|I_d|} = 0 \qquad \text{-------------- 2-28}$$

or

$$|I_g| = |I_{gen}| + |I_d| \qquad \text{-------------- 2-29}$$

and

$$|Q_g| = |Q_i| + |Q_d| = |Q_s| \qquad \text{-------------- 2-30}$$

Where Q_g is the charge per unit area accumulated in the metal adjacent to the insulater, Q_i is the inversion charge per unit area, Q_d is the ionized acceptor charge per unit area in the space charge region and Q_s is the total charge per unit area in the semiconductor. The arrows above the currents signify the direction in which they flow (see figure 2.9).

The total voltage across the device is

$$V_g = V_{ox} + \psi_s \qquad \text{-------------- 2-31}$$

Where V_{ox} is the oxide voltage drop and is equal to $\frac{|Q_g|}{C_{ox}}$ and ψ_s is the surface potential in the semiconductor, (see figure 2.6).

So

$$V_g = \frac{|Q_g|}{C_{ox}} + |\psi_s| \qquad \text{-------------- 2-32}$$

Differentiating this equation with respect to time yields

$$\alpha = \frac{dV_g}{dt} = \frac{1}{C_{ox}} \cdot \frac{d|Q_g|}{dt} + \frac{d|\psi_s|}{dt} \qquad \text{------ 2-33}$$

and since $\psi_s = \frac{q.N_A.X_d^2}{2.\varepsilon_s}$ we obtain

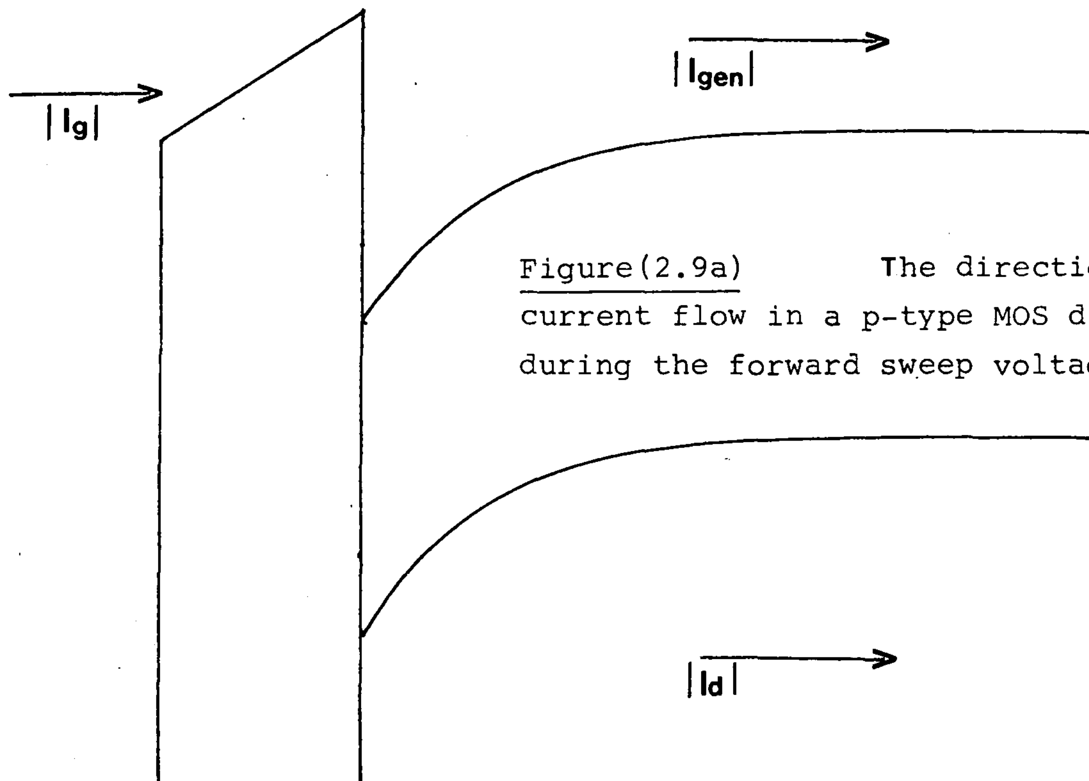

Figure(2.9a) The direction of current flow in a p-type MOS device during the forward sweep voltage.

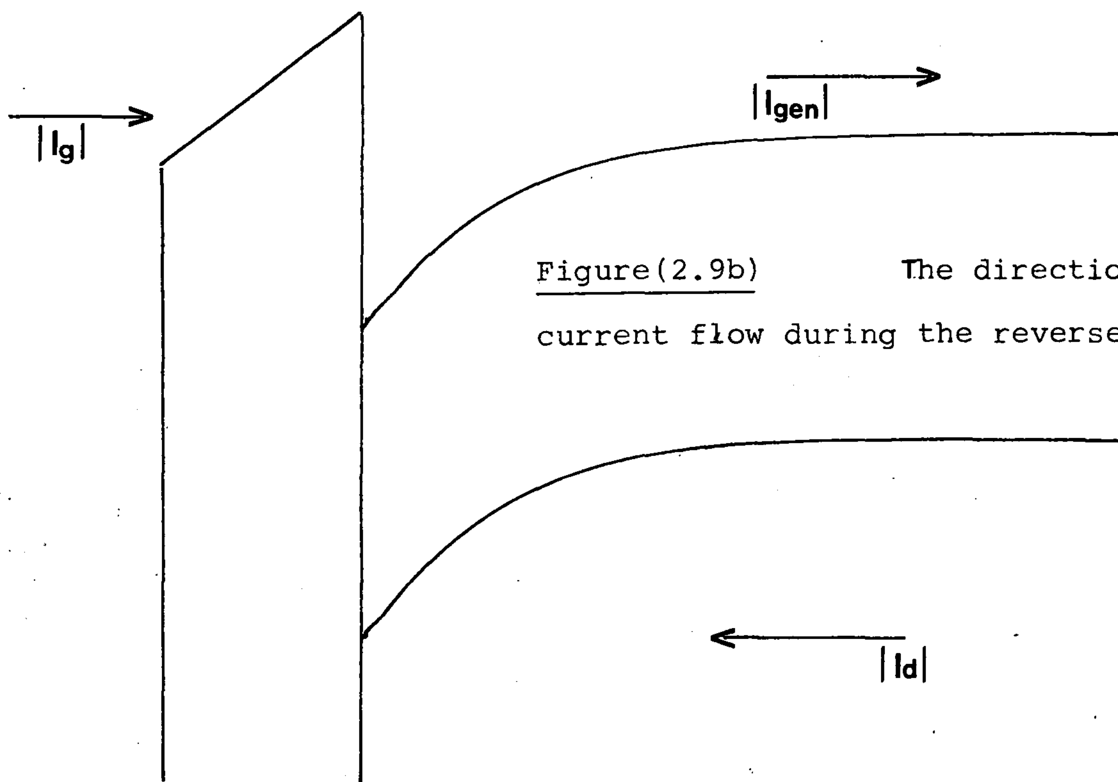

Figure(2.9b) The direction of current flow during the reverse sweep.

$$\frac{d|\psi_s|}{dt} = \frac{q \cdot N_A \cdot X_d}{\varepsilon_s} \cdot \left|\frac{dX_d}{dt}\right|,$$

So equation (2-33) becomes

$$+\alpha = -\frac{|I_g|}{C_{ox}} - \frac{q \cdot N_A \cdot X_d}{\varepsilon_s} \cdot \left|\frac{dX_d}{dt}\right| \qquad \text{------- 2-34}$$

The first term $\frac{|I_g|}{C_{ox}}$ deals with the gate current which flows in a direction shown in figure (2-9) i.e., towards the metal gate which is designated the negative direction. The second term of equation (2-34);

$\left(\frac{q \cdot N_A \cdot X_d}{\varepsilon_s} \cdot \left|\frac{dX_d}{dt}\right|\right)$ deals with the current

generated through the discharging of the acceptor states $|I_d|$ and it flows toward the right and should be negative. So using equations (2-29) and (2-34), equation (2-34) becomes;

$$+\alpha = \frac{-1}{C_{ox}} \cdot (|I_{gen}| + |I_d|) - \left(\frac{q \cdot N_A}{\varepsilon_s}\right) \cdot X_d \cdot \left|\frac{dX_d}{dt}\right| \qquad \text{------- 2-35}$$

and since $|I_d| = q \cdot N_A \cdot \left|\frac{dX_d}{dt}\right|$ we obtain

$$+\alpha = \frac{-1}{C_{ox}} (|I_{gen}| + |I_d|) - \left(\frac{X_d}{\varepsilon_s}\right) \cdot (|I_d|) \qquad \text{------- 2-36}$$

or

$$-\alpha \cdot C_{ox} = +|I_{gen}| + |I_d| + \left(\frac{X_d \cdot C_{ox}}{\varepsilon_s}\right) \cdot (|I_d|) \qquad \text{------- 2-37}$$

Solving for $(|I_d|)$ we obtain

$$|I_d| \cdot \left(1 + \frac{C_{ox} \cdot X_d}{\mathcal{E}_s}\right) = -\alpha \cdot C_{ox} - |I_{gen}| \qquad \text{2-38}$$

or

$$|I_d|_f = \frac{-\alpha \cdot C_{ox} - |I_{gen}|}{\left(1 + \frac{C_{ox} \cdot X_d}{\mathcal{E}_s}\right)} \qquad \text{2-39}$$

Where $|I_d|_f$ is the depletion current during the forward sweep.

2) <u>The reverse sweep</u>

The reverse sweep depletion current relationship can be obtained in a similar manner to the forward sweep with the appropriate changes of sign.Hence equation(2-34)becomes

$$-\alpha = -\left(\frac{|I_g|}{C_{ox}}\right) + q \cdot N_A \cdot \left(\frac{X_d}{\mathcal{E}_s}\right) \cdot \left(\frac{dX_d}{dt}\right) \qquad \text{2-40}$$

The first term on the right hand side $\left(\frac{|I_g|}{C_{ox}}\right)$ is the gate current term and is negative in direction . The gate current term is negative when this current does not cross the voltage axis on sweep reversal .For faster voltage sweep rates there is a possibility that the gate current will cross the voltage axis on sweep reversal .The gate current term would in this case be positive.However,which-ever case is taken equation (2-40) is unchanged.

The second term is related to the depletion current and is positive in direction.Following the same analysis as used for the forward sweep we obtain

$$|I_d|_r = \frac{-\alpha \cdot C_{ox} + |I_{gen}|}{\left(1 + \frac{C_{ox} \cdot X_d}{\mathcal{E}_s}\right)} \qquad \text{2-41}$$

If we compare equations (2-39) and (2-41) it is clear that $|I_d|_f \neq |I_d|_r$,i.e the current due to discharging the acceptor states does not equal the current due to filling the states , at the same value of X_d.

There are two distinct conditions for the current drop on sweep reversal :

(1) Firstly, when the drop length (c-d) is above the voltage axis gate (current always in the same direction).which happens at low sweep rates, (see figure 2.10a).In this condition, let the gate current $|C|$ at point c have a value $|I_g|_1$

So $|C| = |I_g|_1 = |I_{gen}| + |I_d|_f$ ------------------------2-42

The gate current $|D|$ at point d represents the current after sweep reversal and we call this value ($|I_g|_2$), so

$$|D| = |I_g|_2 = |I_{gen}| - |I_d|_r \qquad \text{------------------------2-43}$$

The sum of the two current values is

$$|C|+|D| = |I_g|_1 + |I_g|_2 = |I_{gen}| + |I_d|_f + |I_{gen}| - |I_d|_r$$

$$= 2 \cdot |I_{gen}| + |I_d|_f - |I_d|_r \qquad \text{----------2-44}$$

and the difference between the two values is

$$|C|-|D| = |I_g|_1 - |I_g|_2 = |I_{gen}| + |I_d|_f - |I_{gen}| + |I_d|_r$$

$$= |I_d|_f + |I_d|_r \qquad \text{-----------------2-45}$$

(2) The second condition is when the current drop extends across the voltage axis (that is the gate current reverses direction on sweep reversal) and this happens at high values of sweep rate, (figure 2.10b).

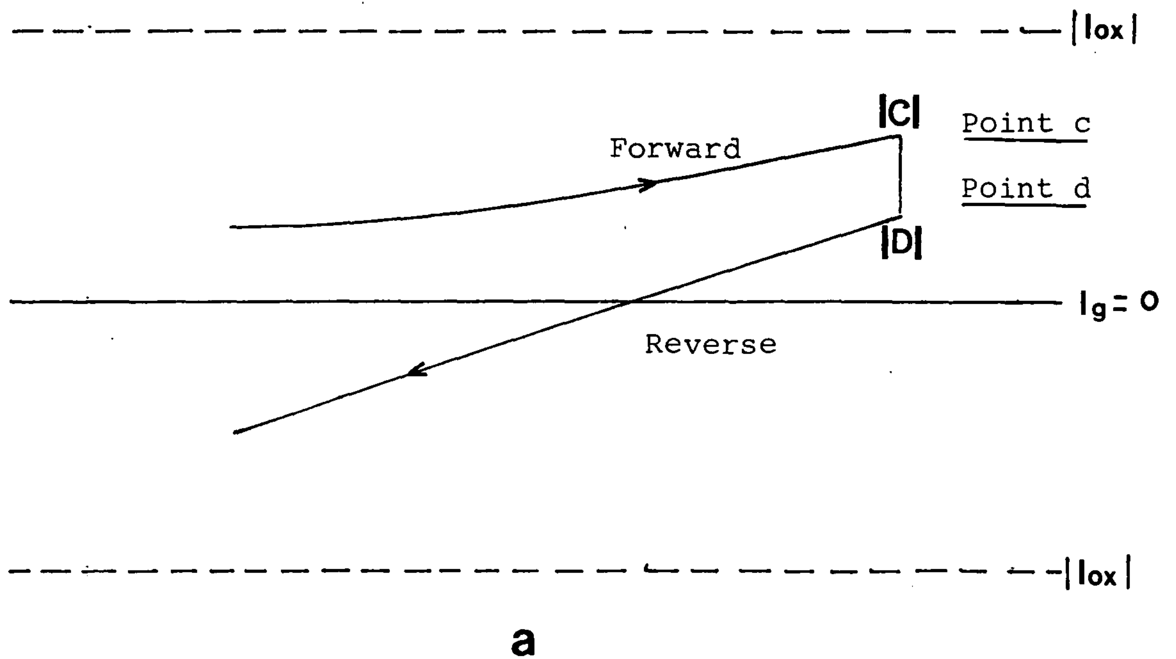

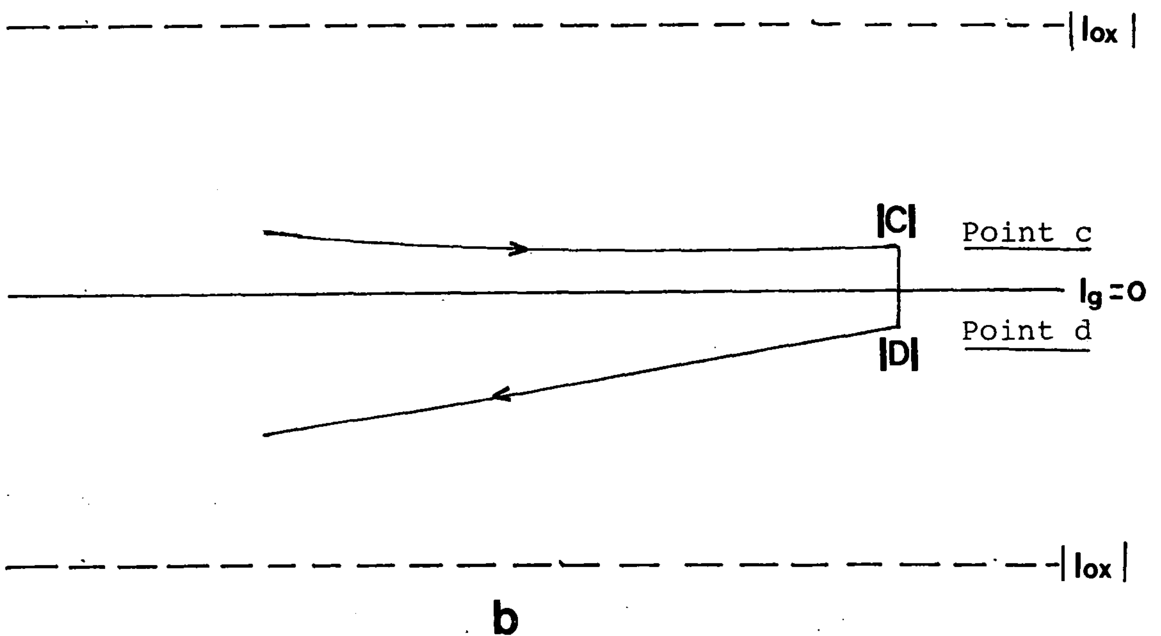

Figure (2.10) The current drop-back position for:

a. Low sweep rates.

b. High sweep rates.

Here let the gate current at point **c** be called $|I_g|_3$ and given by;

$$|C| = |I_g|_3 = |I_{gen}| + |I_d|_f \qquad \text{-------------- 2-46}$$

The gate current at **d** called $|I_g|_4$ is equal to

$$|D| = |I_g|_4 = -(|I_{gen}| - |I_d|_r) \qquad \text{-------------- 2-47}$$

The sum of the two currents is

$$|C| + |D| = |I_g|_3 + |I_g|_4 = |I_{gen}| + |I_d|_f - |I_{gen}| + |I_d|_r$$

$$= |I_d|_f + |I_d|_r \qquad \text{-------------- 2-48}$$

and the difference

$$|C| - |D| = |I_g|_3 - |I_g|_4 = |I_{gen}| + |I_d|_f + |I_{gen}| - |I_d|_r$$

$$= 2 \cdot |I_{gen}| + |I_d|_f - |I_d|_r \qquad \text{------------2-49}$$

Let us represent the expression $(2 \cdot |I_{gen}| + |I_d|_f - |I_d|_r)$ by the factor $\Delta|I|$. This factor represents the sum of the gate currents $|I_g|_1 + |I_g|_2$ at the low sweep rate condition, and the difference between the gate currents $|I_g|_3 - |I_g|_4$ at high sweep rate condition, so

$$\Delta|I| = 2 \cdot |I_{gen}| + |I_d|_f - |I_d|_r \qquad \text{-------------2-50}$$

substituting the values of $|I_d|_f$ and $|I_d|_r$ given in equations (2-39) and (2-41) into the above equation yields

$$\Delta|I| = 2 \cdot |I_{gen}| + \frac{-\alpha \cdot C_{ox} - |I_{gen}|}{\left(1 + \dfrac{C_{ox} \cdot X_d}{\mathcal{E}_s}\right)} - \frac{-\alpha \cdot C_{ox} + |I_{gen}|}{\left(1 + \dfrac{C_{ox} \cdot X_d}{\mathcal{E}_s}\right)}$$

$$\text{---------------------2-51}$$

Letting $B = \left(1 + \frac{C_{ox} \cdot X_d}{\mathcal{E}_s}\right)$, equation (2-51) becomes;

$$\Delta|I| = 2.|I_{gen}| - \left(\frac{-\alpha \cdot C_{ox}}{B}\right) - \left(\frac{1}{B}\right).|I_{gen}| + \left(\frac{-\alpha \cdot C_{ox}}{B}\right)$$

$$-\left(\frac{1}{B}\right).|I_{gen}| \quad \text{------------------------ 2-52}$$

or

$$\Delta|I| = 2.|I_{gen}| - \left(\frac{2}{B}\right).|I_{gen}| \quad \text{------------- 2-53}$$

Rearranging for $|I_{gen}|$ we obtain

$$|I_{gen}|.\ 2\ .\ \left(1 - \frac{1}{B}\right) = \Delta|I| \quad \text{------------ 2-54}$$

or

$$|I_{gen}| = \frac{\Delta|I|}{2\ .\ \left(1 - \frac{1}{B}\right)} \quad \text{------------------ 2-55}$$

Substituting for B we obtain

$$|I_{gen}| = \left(\frac{\Delta|I|}{2\ .\ \left(1 - \frac{1}{1 + \frac{C_{ox} \cdot X_d}{\mathcal{E}_s}}\right)}\right) \quad \text{---------- 2-56}$$

The above equation gives the value of the generation current $|I_{gen}|$ if X_d is known. C_{ox} is obtained by using the high frequency C-V technique and $\Delta|I|$ is measured directly from the I-V characteristic. Now, since

$$|I_{gen}| = q\ .\int U_g\ .X_d \quad \text{------------------- 2-57}$$

By differentiation we obtain

$$\frac{1}{q} \cdot \frac{d|I_{gen}|}{dX_d} = U_g(X_d) \qquad \text{-----------------------2-58}$$

From equation(2-56)we can obtain a plot of $|I_{gen}|$ versus X_d. Graphically differentiating and using equation(2-58)will give us a plot of U_g versus X_d,that is the generation rate profile in the bulk of the semiconductor.

To find X_d at sweep reversal let us represent the expression $|I_d|_f+|I_d|_r$,which represents the difference between the gate currents $|I_g|_1$and $|I_g|_2$at low voltage sweep,and the sum of the gate current values $|I_g|_3$and $|I_g|_4$at high voltage sweep, by the factor $|I|_{drop}$.

Therefore

$$|I|_{drop} = |I_d|_f + |I_d|_r \qquad \text{-----------------------2-59}$$

and,upon substituting the values of $|I_d|_f$and $|I_d|_r$from equations (2-39)and(2-41),we obtain

$$|I|_{drop} = \left(\frac{|\alpha|.C_{ox} - |I_{gen}|}{\left(1 + \frac{C_{ox} \cdot X_d}{\varepsilon_s}\right)}\right) + \left(\frac{|\alpha|.C_{ox} + |I_{gen}|}{\left(1 + \frac{C_{ox} \cdot X_d}{\varepsilon_s}\right)}\right)$$

$$\text{---------------------2-60}$$

Or

$$|I|_{drop} = \frac{|\alpha|.C_{ox} - |I_{gen}|}{B} + \frac{|\alpha|.C_{ox} + |I_{gen}|}{B}$$

$$\text{--------------------2-61}$$

Where the expression $(B=1+\frac{C_{ox} \cdot X_d}{\varepsilon_s})$ has been used.

Expanding equation (2-61) yields

$$|I|_{drop} = \frac{|\alpha| \cdot C_{ox}}{B} - \frac{|I_{gen}|}{B} + \frac{|\alpha| \cdot C_{ox}}{B} + \frac{|I_{gen}|}{B} \qquad \text{-------------- 2-62}$$

$$= \frac{2 \cdot |\alpha| \cdot C_{ox}}{\left(1 + \frac{C_{ox} \cdot X_d}{\varepsilon_s}\right)} \qquad \text{--------------- 2-63}$$

Rearranging to solve for X_d

$$|I|_{drop} + |I|_{drop} \cdot \frac{C_{ox} \cdot X_d}{\varepsilon_s} = 2 \cdot |\alpha| \cdot C_{ox} \qquad \text{--------------- 2-64}$$

Or

$$X_d \cdot \left(\frac{|I|_{drop} \cdot C_{ox}}{\varepsilon_s} \right) = 2 \cdot |\alpha| \cdot C_{ox} - |I|_{drop}$$

therefore

$$X_d = \frac{2 \cdot |\alpha| \cdot \varepsilon_s}{|I|_{drop}} - \frac{\varepsilon_s}{C_{ox}} \qquad \text{------------- 2-65}$$

Equation (2-65) gives the value of the depletion region width, if $|I|_{drop}$ is known. Since $|I|_{drop}$ can be measured from the experimental curve we can obtain a value for X_d. The value of X_d obtained can be substituted into equation (2-65) to obtain the value of $|I_{gen}|$ at that depletion width. For different voltage drop-back positions $|I_{gen}|$ can then be plotted against X_d and equation (2-58) used to obtain $U_g(X_d)$.

CHAPTER THREE

INSTRUMENTATION AND PROGRAMING

3-1 Introduction

This chapter deals with the details of the electronic circuits constructed in order to enable the experimental measurements to be performed.

The latter portion of the chapter describes the computer program used to log and analyse the experimental curves. Appendix (1) considers some fundemental electronic circuit principals which would be inapropriate to include in the main body of the work .

3-2 The Triangular Wave Generator

A basic triangular wave form generator is shown in figure(3.1) It consists of two operational amplifiers , one of them acting as an integrator and the other as a comparator.The output of the integrator is retured to the non-inverting input of the first operational amplifier to eliminate the 180° phase shift.

The generator which was built is more sophisticated and is shown in figure(3.2).A multi-turn potentiometer supplies the dual polarity offset voltage to the comparator . The output of the circuit is clamped by two Zener diodes connected in series to each other but in opposite directions . These help to improve the linearity of the comparator and to make the output voltage virtually independent of the supply voltage.

Waveform symmetry can be obtained by making sure that the magnitude of the two voltages supplied to the comparator is the same.The 2.2kΩ preset potentiometers will facilitate this.

The integrator circuit is built with switchable capacitors in order to give decade changes in frequency.

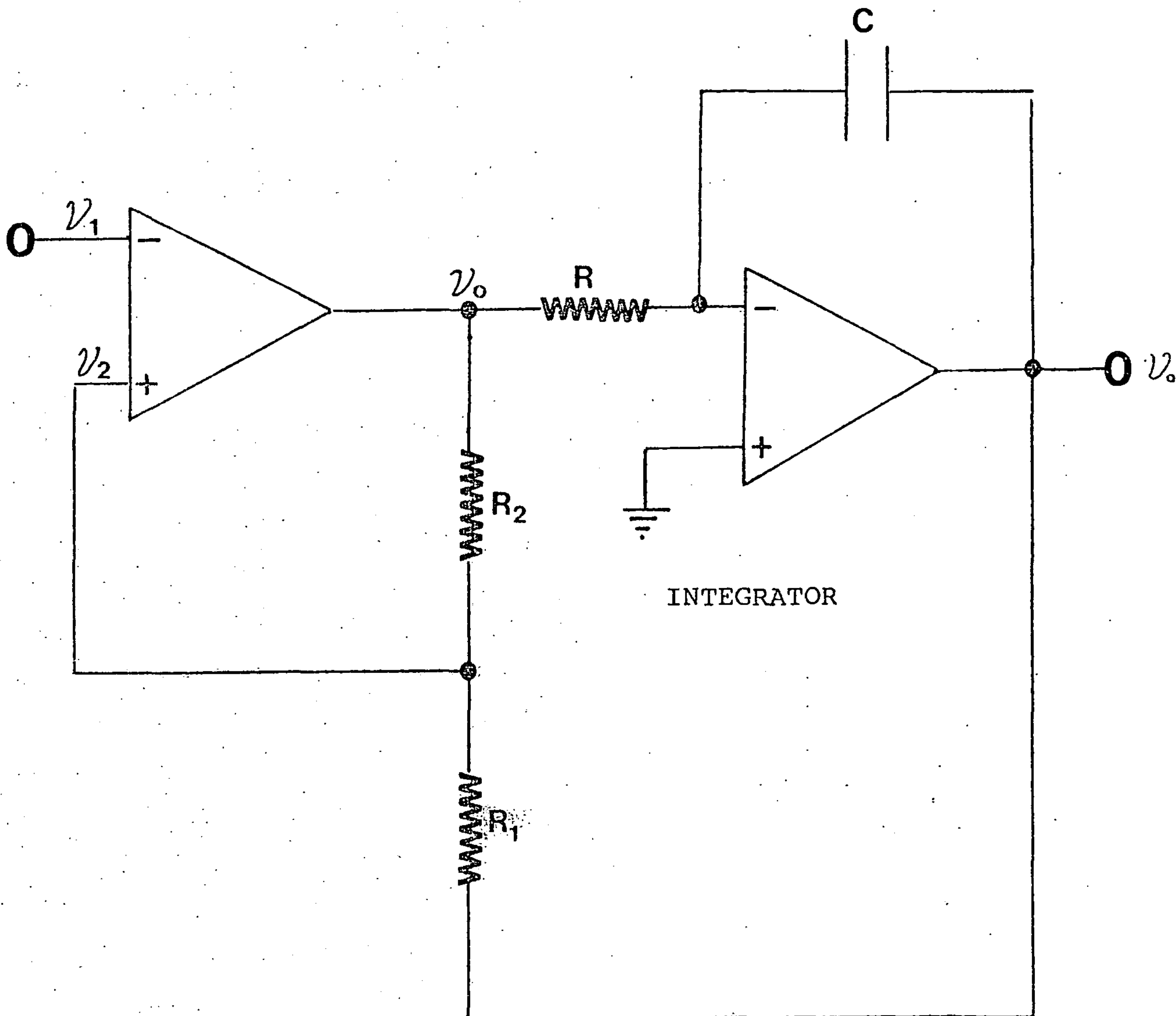

Figure (3.1)

A Basic Triangular Wave form Generator Circuit.

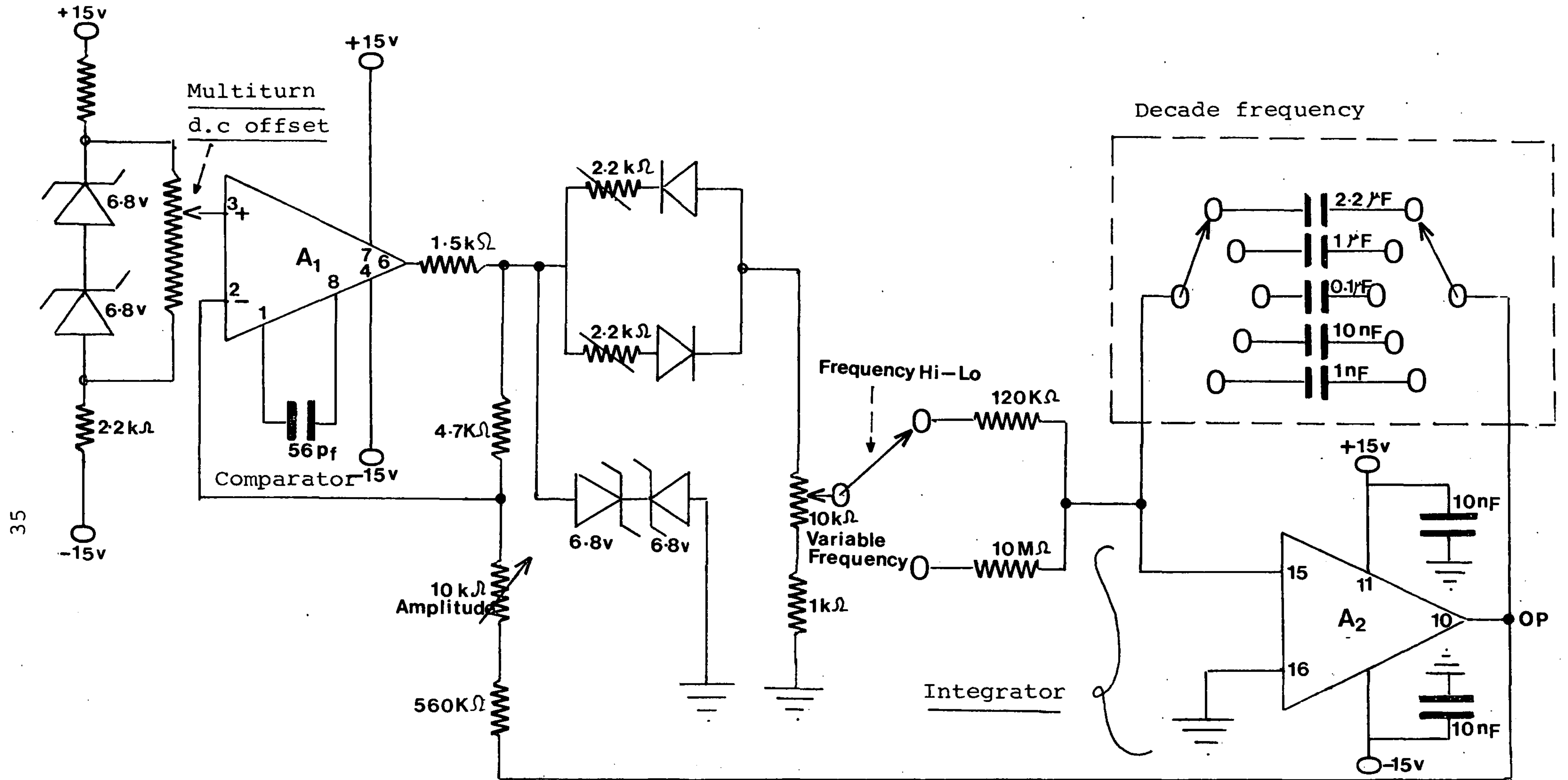

Figure (3.2)

Sophisticated Triangular-Wave Generator.

3-3 Direct measurement of ($\psi_s - V_g$) by Tonner & Simmons technique

Tonner & Simmons [ref 27] presented a new circuit technique which allows the direct plotting of a $\psi_s - V_g$ characteristic. The technique measures the MOS capacitor gate charge in response to a linear voltage ramp. The circuit diagram is shown in figure(3.3). The charging current of the MOS device passes into the electrometer, the output voltage of which is

$$\mathcal{V}_o = \frac{1}{C_f} \int_o^t i \cdot dt = \frac{-Q_G}{C_f}$$

Where C_f is the value of the feedback capacitor in the electrometer (value of 224pf)

The output current of the electrometer is fed into a voltage follower so as not to load it. This voltage follower output is applied to a summing amplifier configuration (the other portion of which is fed by the triangle wave form generator). The equations governing the configuration of summing amplifiers are :-

$$\mathcal{V}_2 = R_3 \cdot i_3 = R_3 \cdot (i_1 - i_2) \qquad \text{---------- 3-1}$$

and since

$$i_1 = \frac{V_g}{R_1} = \frac{-Q_G}{C_f \cdot R_1}$$

and

$$i_2 = \frac{V_g}{R_2}$$

therefore

$$\mathcal{V}_2 = - \left(\frac{V_g}{R_2} - \frac{Q_G}{C_f \cdot R_1} \right) \cdot R_3 \qquad \text{--------- 3-2}$$

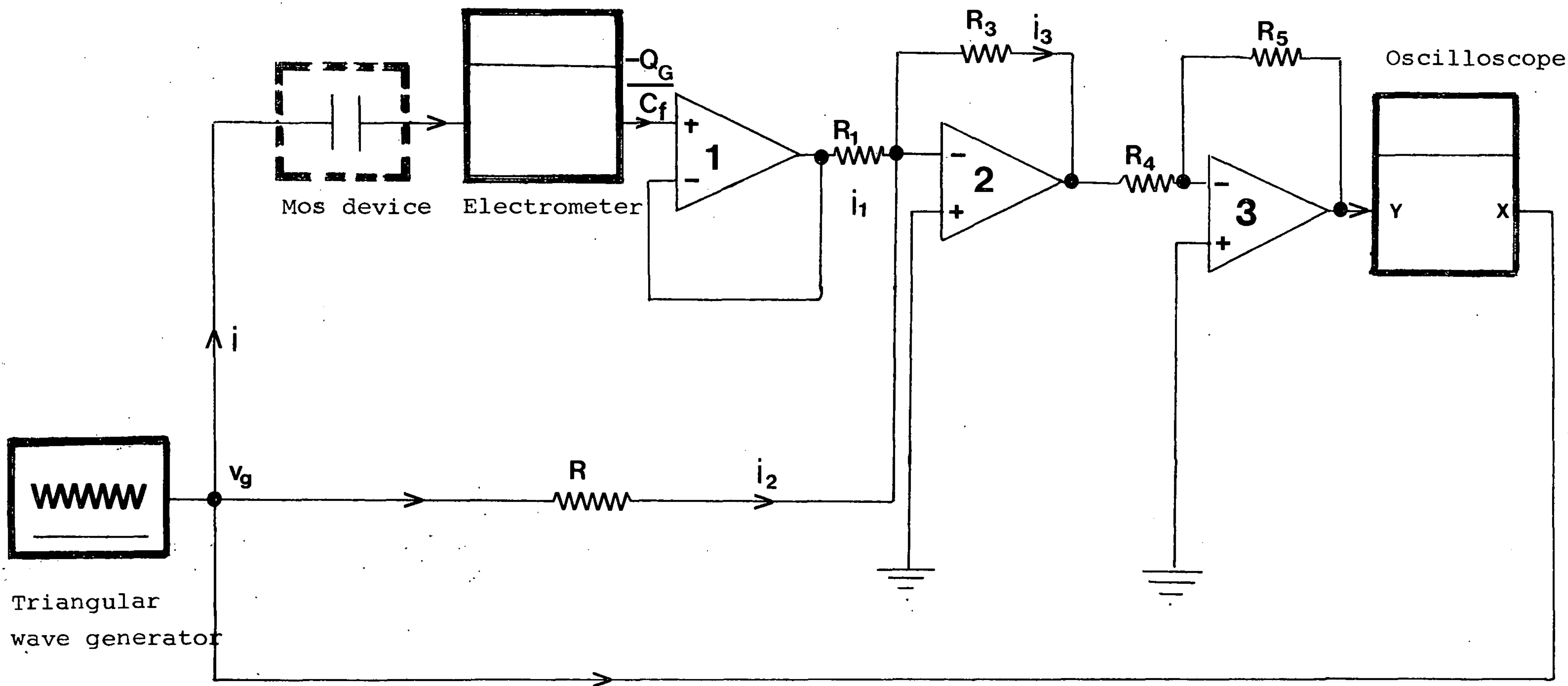

Figure(3.3)

Tonner & Simmons circuit to generate directly the ψ_s-V_g characteristic.

By putting $R_2 = R_3$ and $R_1 = \frac{C_{ox}}{C_f} \cdot R_3$,equation(3-2) becomes;

$$= - \left(\frac{V_g}{R_2} \right) \cdot R_2 + \left(\frac{Q_G}{C_f \cdot R_1} \right) \cdot \left(\frac{C_f \cdot R_1}{C_{ox}} \right)$$

$$= - V_g + \left(\frac{Q_G}{C_{ox}} \right) \qquad \text{------------------------ 3-3}$$

The final operational amplifier acts simply as a phase reversal with a gain of -1 (where $R_4 = R_5$).

So,

$$\mathcal{V}_3 = V_g - \left(\frac{Q_G}{C_{ox}} \right) \qquad \text{--------------------- 3-4}$$

Now, the surface potential is given by

$\Psi_s = V_g - \left(\frac{Q_G}{C_{ox}} \right)$,and we clearly recognise that $\mathcal{V}_3$ represents the surface potential directly.By supplying $\mathcal{V}_3$ to the Y-plates and the triangle voltage V_g to the X-plates of an oscilloscope it is possible to obtain direcly a $\Psi_s - V_g$ characteristic.

3.4 The drop-back experimental setup

The equipment setup for the drop-back experimental technique is shown in figure(3.4).The triangular wave-form generator supplies a signal to the MOS device and to the X-plates of an oscilloscope The Keithley electrometer measures the resulting MOS current and provides an output voltage propportional to the current.This voltage is then applied to the Y-plates of the oscilloscope to provide a current versus voltage characteristic.The analogue to digital converter ADC digitizes this signal,which is then read into the PET computer.A program stored within the computer then anal-

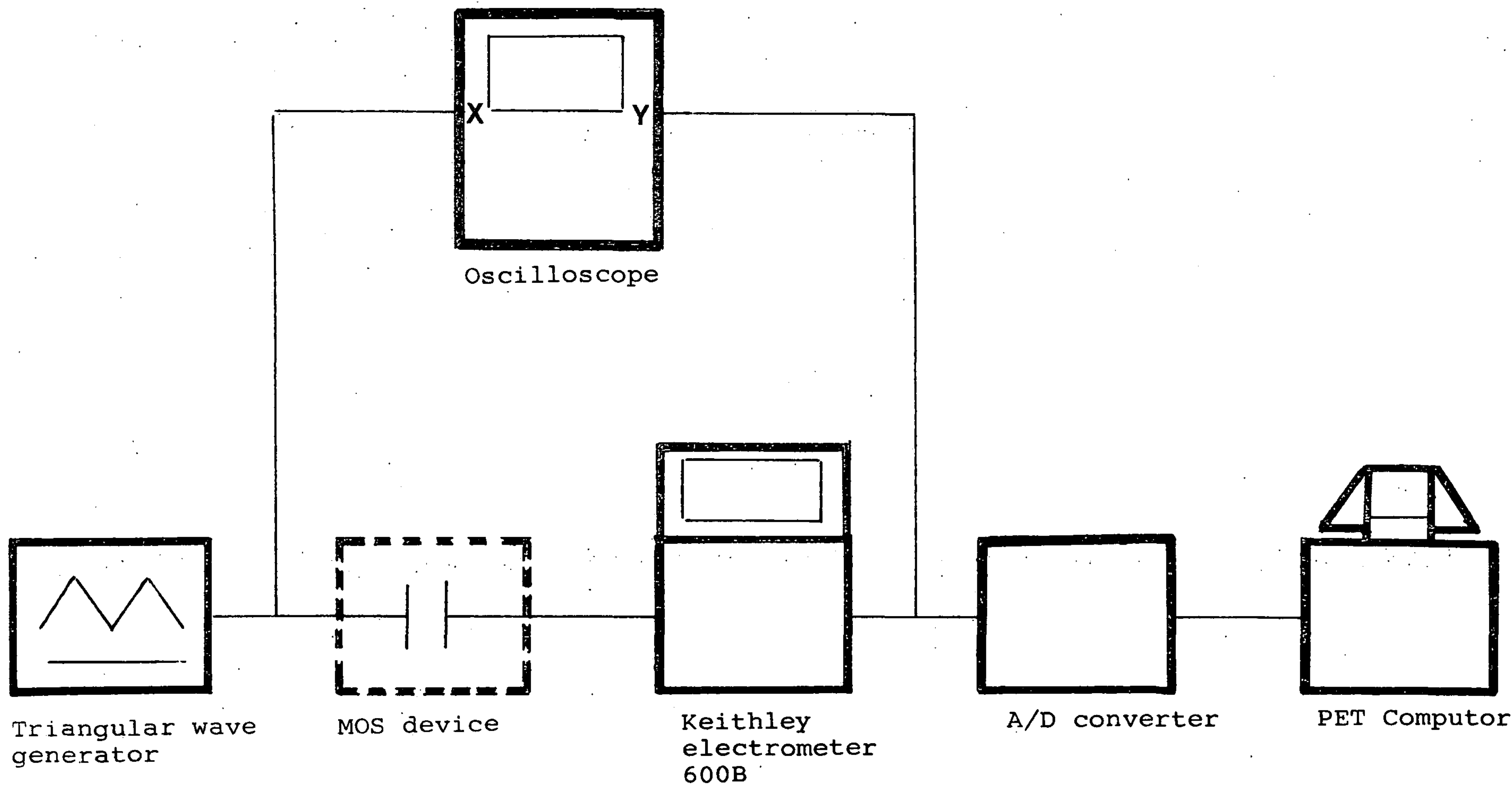

Figure(3.4) Showing the drop-back experimental setup.

-ses the results.Much work was performed in optimising the experimental setup and form of the program in order that the current drop(measured as a voltage on the output of the electrometer)on sweep reversal could be logged and analysed accurately.

3.5 The Drop-back technique program

This section is concerned with the details of a program which has been developed to log and analyse the experimental results . A full listing of the program is given in appendix two.The program involves four main steps:-

1. Latching the output of the ADC into the input register .
2. Reading the input register .
3. Checking for valid inputs :
   a. By timing the full cycle from the end of the large drop(figure 2.5).
   b. Obtaining the correct point by working in the region of approximatly half full cycle .
4. Measuring the drop-back height.

The details of the program are as follows(see figure 3.5):-

(a) Send a'Convert'command to A/D converter by toggling peripheral control register PCR at address 59468,i.e by writing the binary 11000000,(i.e the dec 192)and then writing the binary 11100000,(i.e the dec 224)into address No 59468.This gives an output on CB2 which starts the'Convert'command.The command used is; POKE 59468,192:POKE 59648,224.

(b) Read the input register at the address 59457 by the command PEEK 59457(when the conversion has taken place).

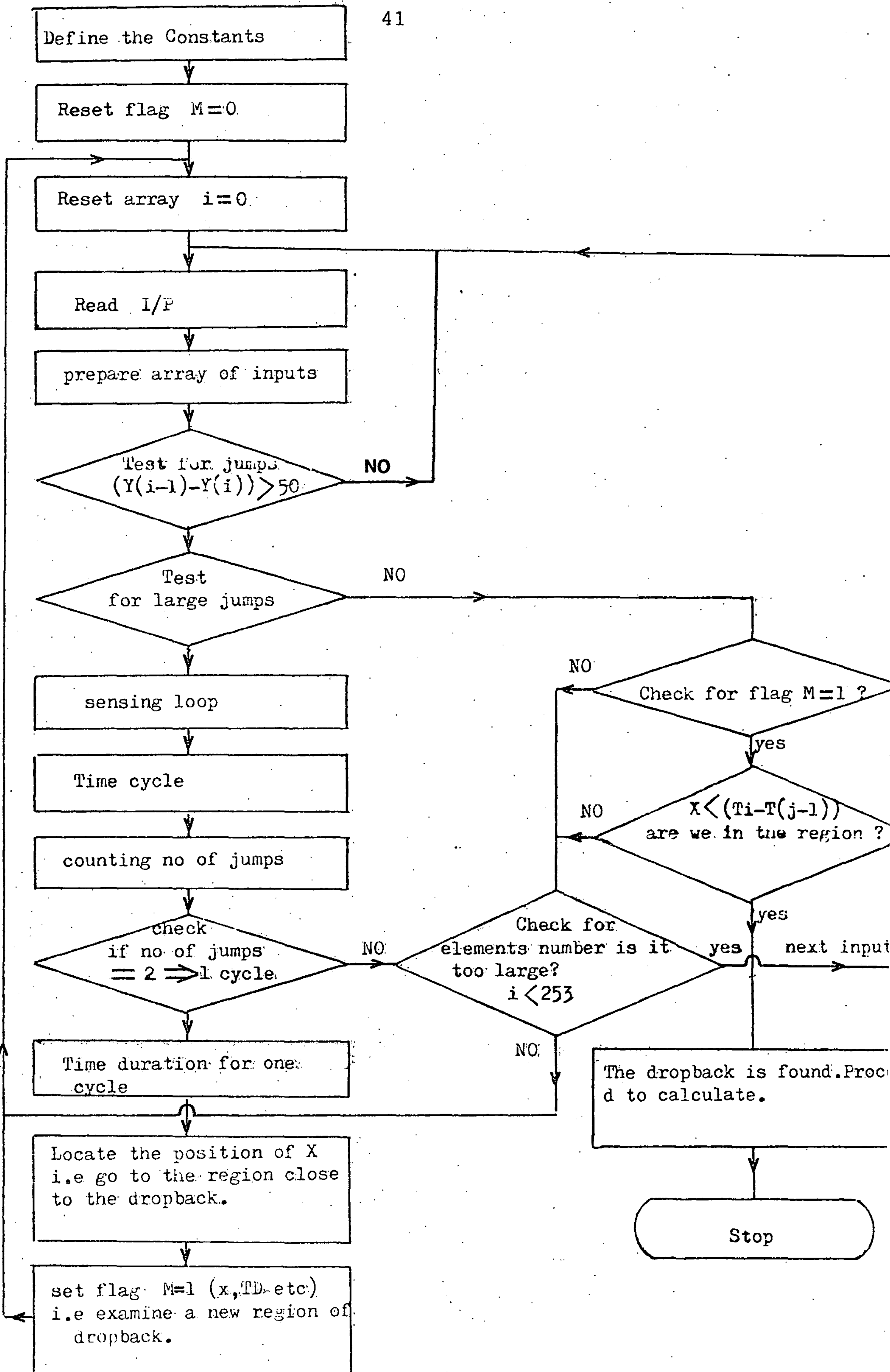

Figure (3.5) Showing the program algorithm.

(c) Log the different input values into an array Y(i).

(d) Test the array elements(i.e the inputs)for the large drop, which is the start of the sensing loop.

(e) Note the initial time when this occurs.

(f) Test for the next large drop.

(g) When this occurs,the time difference is that for one full cycle.

(h) Examine the region close to the half full cycle,both before and after the small drop.In this region,test to determine exactly the drop-back height i.e to determine points **c** and **d**.

(j) Once C and D are known,solve the equation for X_d, $I_g(X_d)$ and $U_g(X_d)$ as given in chapter two.

CHAPTER FOUR

MEASUREMENT AND RESULTS

4.1 Introduction

This chapter is concerned with the experimental measurements of the drop-back technique . The technique is based on applying a triangular waveform voltage to an MOS device, and by using a preprogrammed PET computer to analyse the resulting current-voltage characteristic . The main region of concern is the current drop-back at the end of the forward sweep where the applied voltage changes its direction.

The technique reveals important information about the Mos device and provides a mathematical relation between the depletion width X_d, the generation current and the genration rate U_g.

4.2 The High frequency bridge measurements [ref 27]

The high frequency bridge experimental setup is illustrated in figure(4.1), where a triangular wave form voltage is fed to the X-input of the Bryans plotter and to the metal gate of the MOS device, via the h.f generator. The device is housed in an electrically and optically isolated chamber, in which there is a stainless steel vacuum chuck to support the device substrate. A probe is contacted to the device gate.

4.2.1 H.F Measurements on a p-type MOS device

The p-type MOS device used during the experimental work has a gate area of $18.385 \times 10^{-3} cm^2$ and aluminium gate and substrate contact.

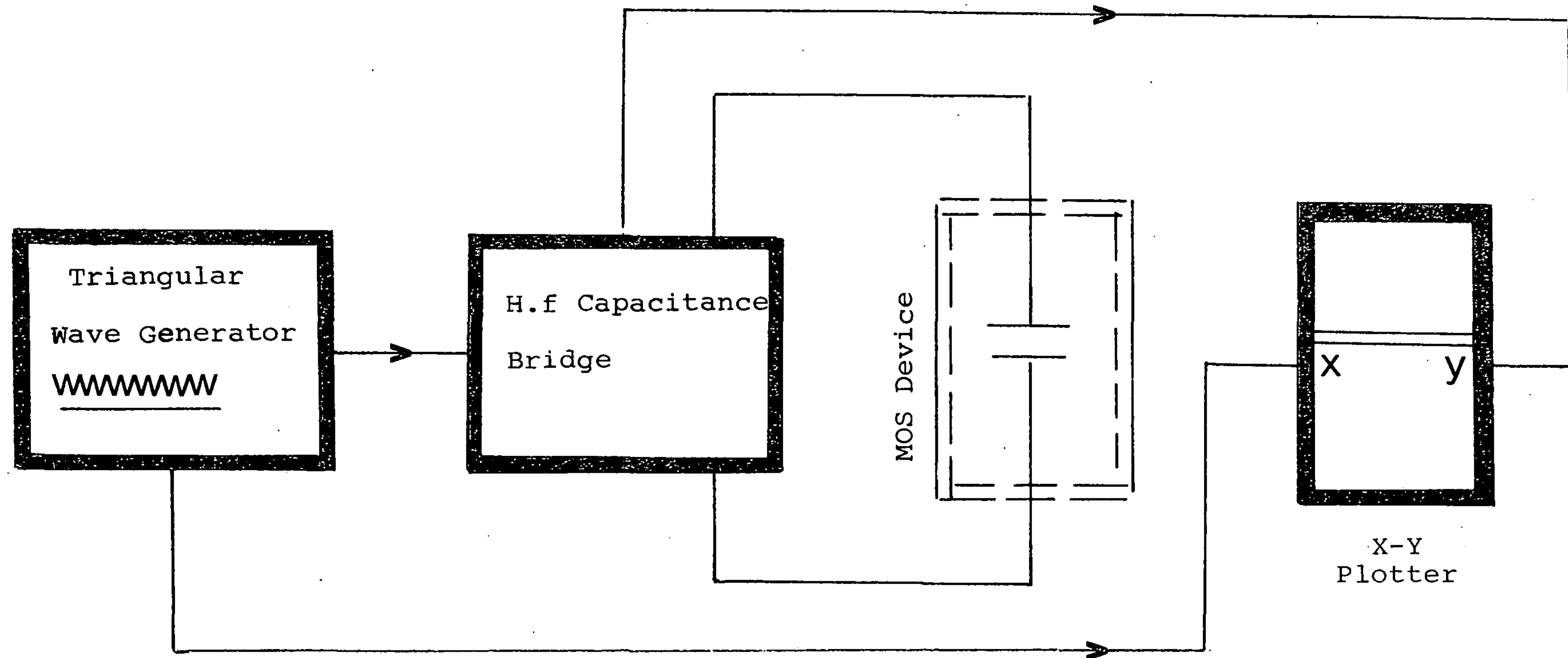

Figure(4.1) Showing the experimental setup for the high frequency C-V characterisation.

The obtained high frequency C-V curve is shown in figure (4.2).From the strong accumulation region of the curve the oxide capacitance value C_{ox} is obtained as 867 pF, and by the substitution of this value in equation(4.1), the oxide thickness d is calculated as 773 x 10^{-8}cm, that is,

$$d = \frac{\varepsilon_{ox} \cdot A}{C_{ox}} \qquad ....4.1$$

and with the help of equation (4.2).

$$C_{min} = \frac{\varepsilon_{ox}}{d + \frac{\varepsilon_{ox}}{\varepsilon_s} \cdot X_{dm}} \qquad ....4.2$$

the maximum depletion width is calculated as 0.827 x10^{-4}cm in equilibrium. C_{min} is the minimum capacitance value which is obtained directly from the experimental curve as 182 pF.The maximum depletion width is given by:-

$$(X_d)_{max} = \left(\frac{4 \cdot \varepsilon_s \cdot K \cdot T \cdot Ln(N_A/n_i)}{q^2 \cdot N_A} \right)^{\frac{1}{2}} \qquad ....4\text{-}3$$

By using equation(4.3)the acceptor state density N_A is calculated as 1.1 x 10^{15}cm^{-3}.The total capacitance at the flat-band condition is

$$C_{fB} = \frac{\varepsilon_{ox}}{d + \frac{\varepsilon_{ox}}{\varepsilon_s} \cdot \sqrt{\frac{K \cdot T \cdot \varepsilon_s}{q^2}}} \qquad ....4\text{-}4$$

Using equation (4.4) we calculate the total flat band voltage shift to be(-0.85 volts).

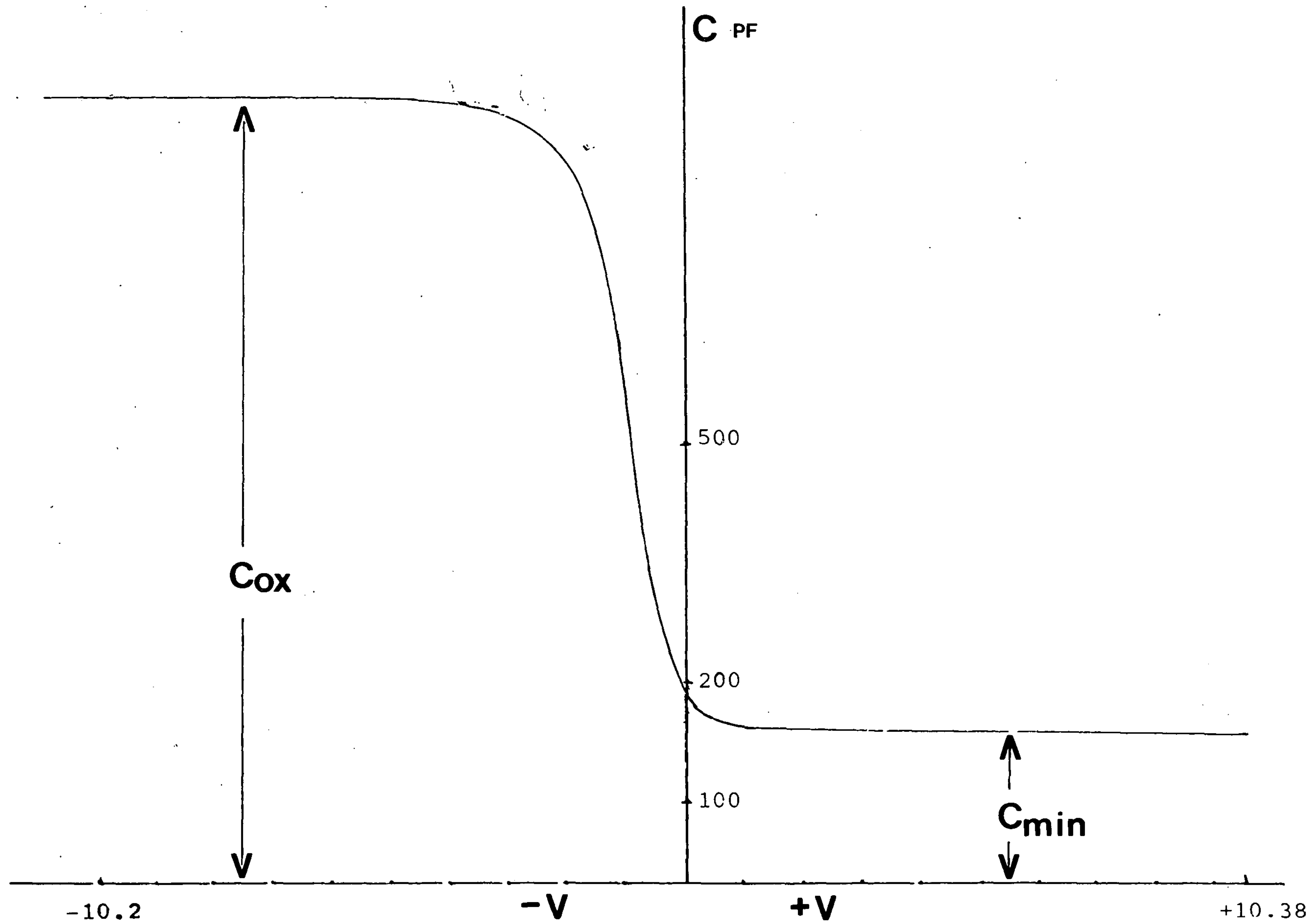

Figure(4.2) High frequency C-V curve for the p-type MOS device.

4.2.2 H.F. Measurements on an n-type MOS device

The same analytical procedure is followed for the n-type device(gate area of 4.83 x $10^{-3}cm^2$)as for the p-type.The experimental high frequency C-V curve is shown in figure (4.3).The oxide thickness is calculated as 980 x 10^{-8}cm, the maximum depletion width at equilibrium as 5.63 x 10^{-5} cm and the doping density N_D as 2.5 x $10^{15}cm^{-3}$.The total capacitance at the flat-band condition is 133.5 pF wihch yields a flat band voltage shift of -0.42 V.

4.3 The Drop-back technique experimental measurements

The experimental setup of the drop-back technique is shown in figure(3.4),and consists of:-

a) Triangular wave-form generator.

b) Probe chamber.

c) Keithley electrometer(model 600B).

d) Oscilloscope.

e) Analogue to digital converter.

f) CBM-PET desk top computer.

As we mentioned in detail in chapter three,the triangular wave-form voltage is of such a rate as to take the device into the non-equilibrium mode of operation.A voltage proportional to the gate current is fed into the preprogrammed PET computer(through an A/D converter)and analysis then takes place.As its name implies,the drop-back technique is concerned with the part of the I-V curve where a sudden drop in the gate current occurs due to the changing of the applied voltage polarity(i.e.,at $t = t_B$ in figure 2.4).The PET computer starts to sense the region of the curve between points **c** (just before the sweep reversal)and point **d** (just after the sweep reversal).These two points determine the current

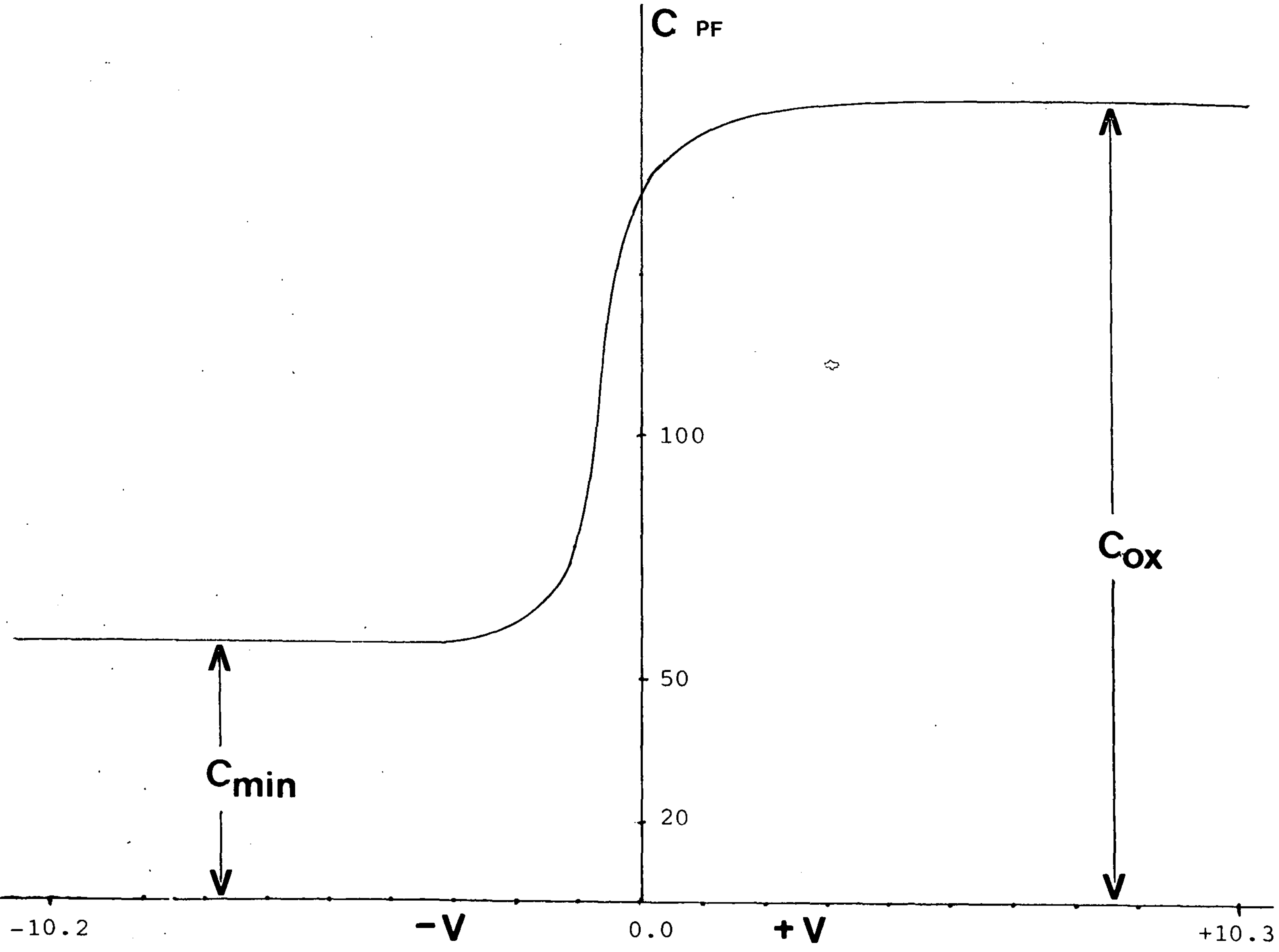

Figure(4.3) High frequency C-V curve for the n-type MOS device.

drop-back magnitude.

4.3.1 The p-type MOS device measurements

The device is placed in the probe chamber on a stainless steel vacuum chuck(substrate connection)with a movable microscopic tungsten probe contacting the metal gate of the device,the whole chamber being purged with dry nitrogen gas. This latter precaution reduces surface leakage effects across the device.

In the work on the p-type device,two values of sweep rate are chosen,one of them a high value of sweep rate(3.05 V/s),and the other a low value of sweep rate(1.03 V/s)and the electrometer range is arranged to be 0.3×10^{-8}A for the first value of sweep rate and 0.1×10^{-8}A for the latter. Figure(4.4)shows the I-V curves for these two values of sweep rate.The first recorded drop-back points occurs at a gate voltage of 2V($V_g - V_{fB} = 1.15$V),and at every 0.2V until V_g=7V. The corresponding values of point|C|and|D|are recorded as shown in figure(4.5).(full listing of results is given in appendix three).

It is clear from the curves of figure(4.5)that at the high sweep rate of 3.05 V/s,the drop-back extends across the voltage axis as shown in figure(2.10),and in this case the sum of the two values |C| and |D| is called $\Delta|I|$ and the difference between them |C| - |D| called the $|I|_{drop}$.At the lower sweep rate of 1.03 V/s the factor |C| + |D| is called the $|I|_{drop}$ and |C| - |D| is called $\Delta|I|$.By using equations (2.56)and(2.65)the values of the depletion width X_d inside the bulk of the semiconductor and the generation current $|I_g|$ are obtained.

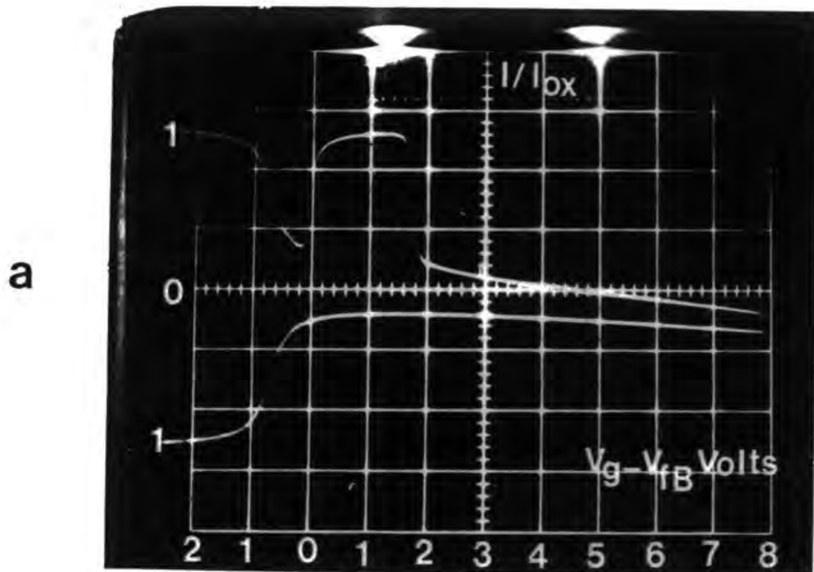

Figure(4.4a) The I-V curve for the p-type MOS device at a sweep rate value of 3.05V/s(the electrometer range is 0.3×10^{-8}A.).

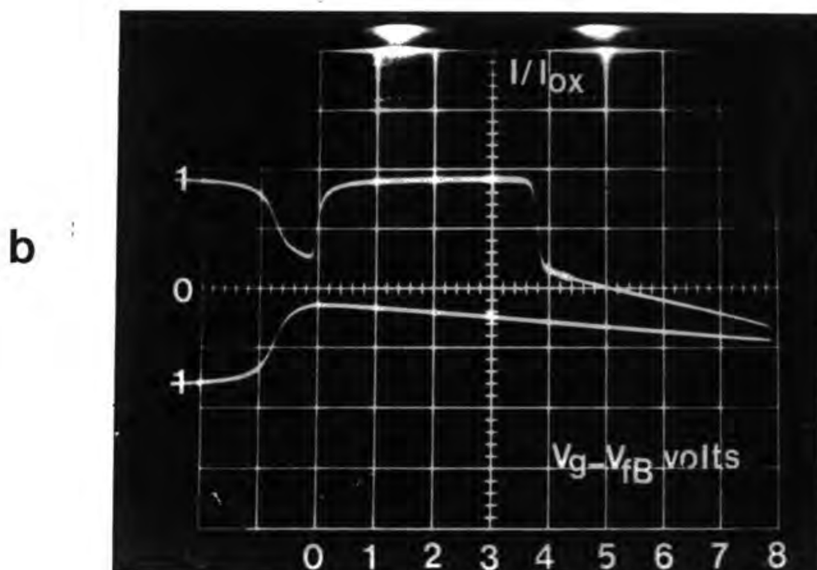

Figure(4.4b) The I-V curve for the p-type MOS device at a sweep rate value of 1.03V/s(the electrometer range is 0.1×10^{-8}A.).

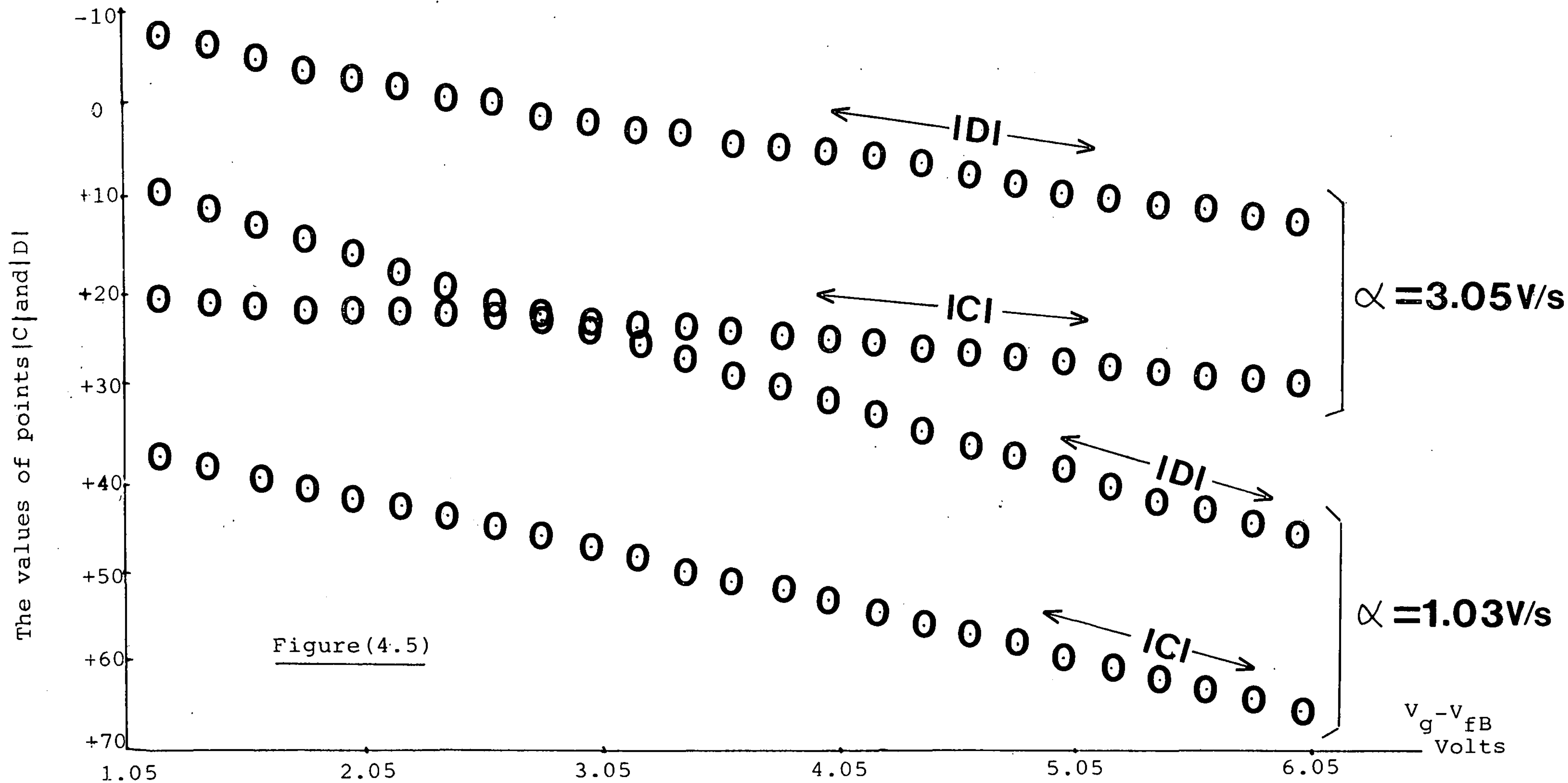

The gate current values just before and after the sweep reversal: this is represented digitally by points |C| and |D| versus the applied gate voltage V_g for an p-type MOS device at two sweep rate values of 3.05V/s and 1.03V/s.

As the applied gate voltage increases(i.e as the device is driven from accumulation towards depletion)additional charge (opposite in polarity to that demanded in accumulation)is demanded in accumulation)is demanded by the semiconductor. The generated charge supplied by the bulk and surface traps becomes insufficient to maintain a full inversion layer.As a result,the depletion width increases more rapidly than in equilibrium as shown in figures(4.6)and(4.7),thus allowing more bulk traps to rise above the fermi level and hence generate more minority carriers(electrons in the p-type device). The generation current will therefore be higher as the depletion width increases.Figures(4.8)and(4.9)show the depletion width value X_d(y-axis)obtained by the drop-back technique for two different sweep rate values.

It can be noticed that at the higher sweep rate of 3.05 V/s there are higher values of depletion width X_d and therefore higher values of generation current $|I_g|$ than that at the lower sweep rate of 1.03 V/s.This is due to the fact that at the lower sweep rate the generation rate of the traps has the ability(at least in part)to keep up with the small signal variation which leads to a charge exchange with the inversion layer almost in step with measurement signal,while at higher sweep rates the capability of the generated minority carriers(electrons)to follow the applied signal is less and so the system moves towards the deep depletion condition [ref 26].

Using equation(2.58)the generation rate value is calculated,figures(4.10)and(4.11)are showing the resulting curves.These are seen to be roughly straight lines(as may be expected in the bulk of the semiconductor),any variation

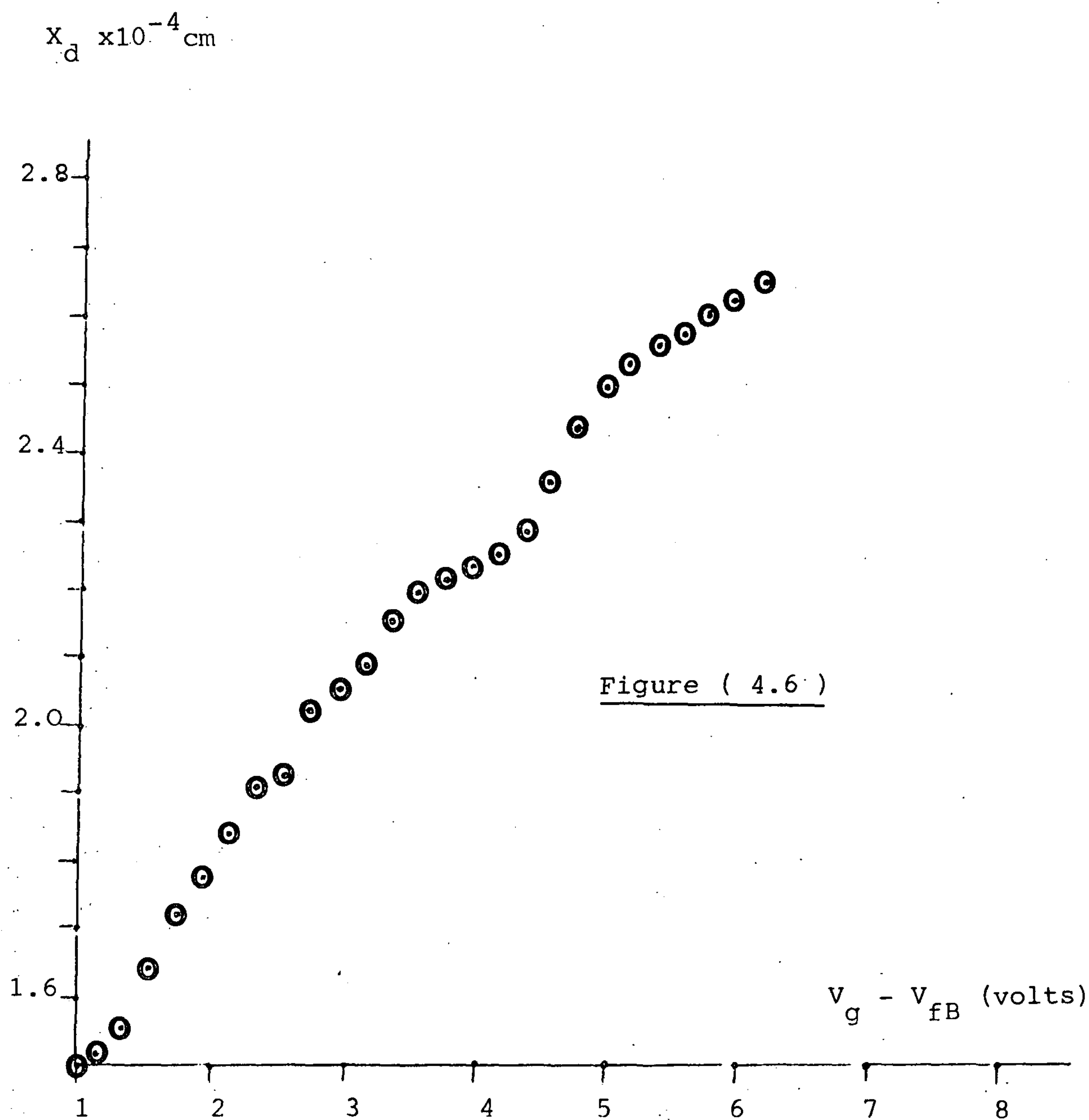

The depletion width X_d versus the applied gate voltage V_g curve for the p-type MOS device at a sweep rate value of 3.05V/s as obtained by the drop-back technique.

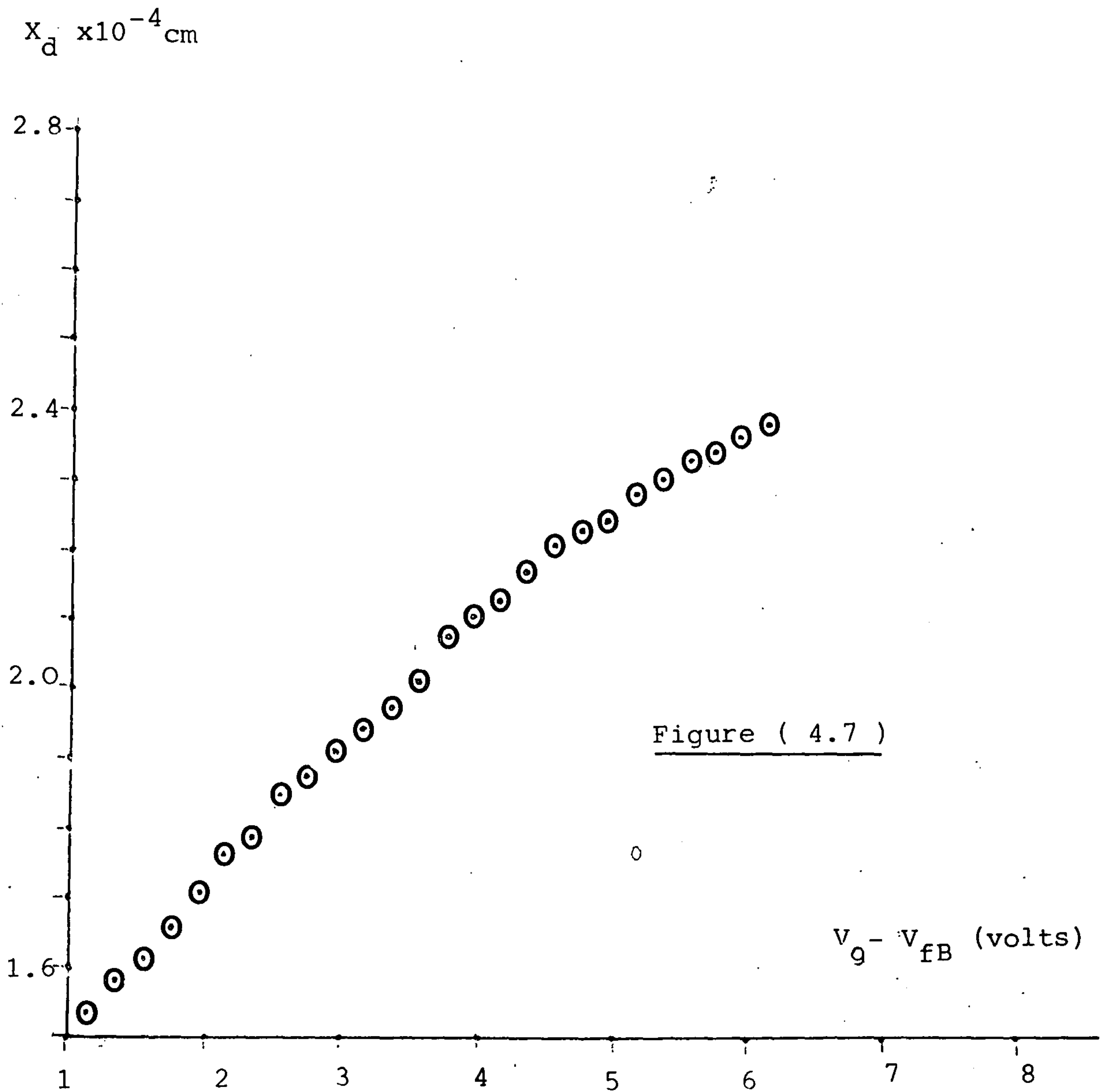

The depletion width X_d versus the applied gate voltage V_g curve for the p-type MOS device at a sweep rate of 1.03V/s as obtained by the drop-back technique.

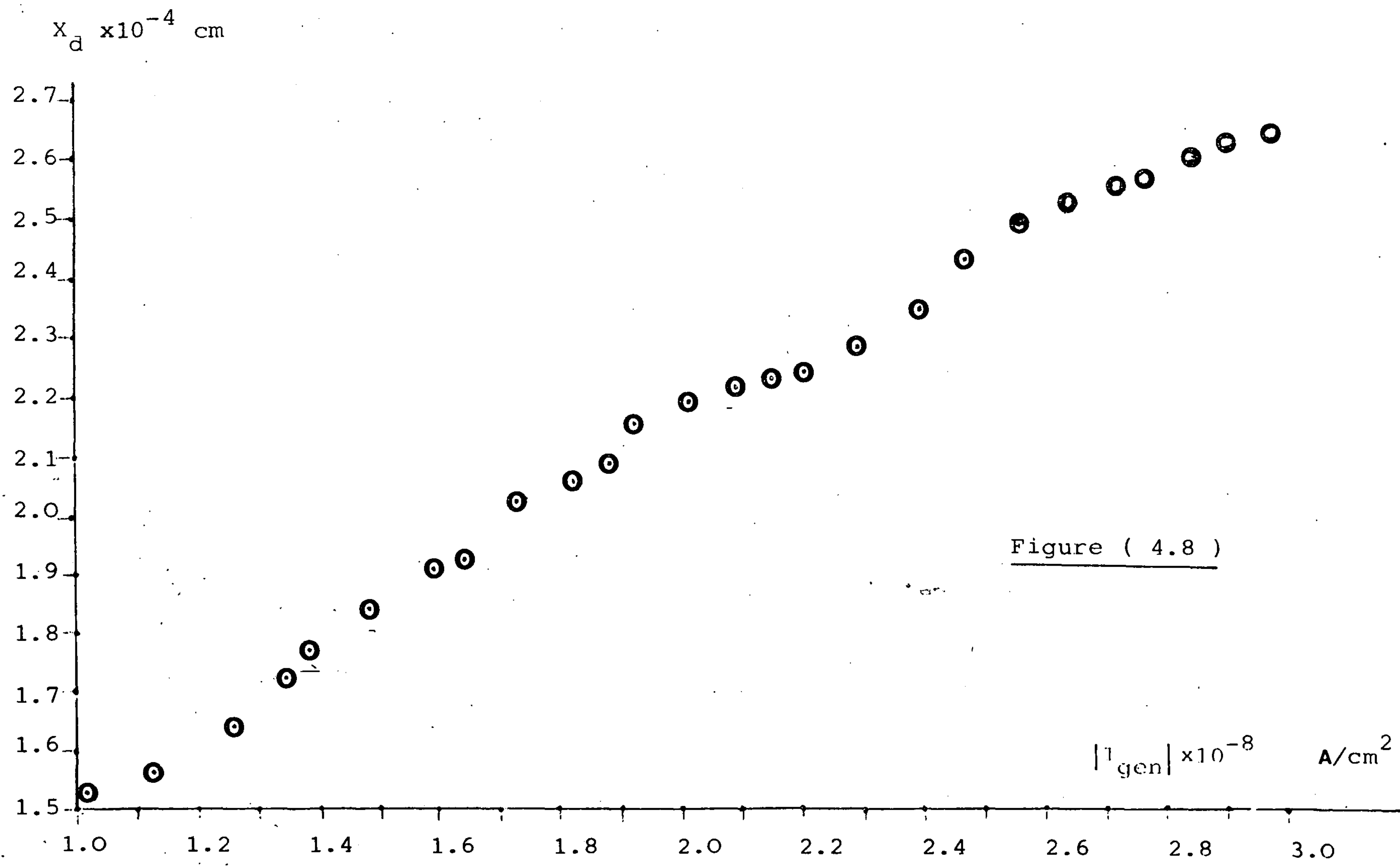

Figure (4.8)

The depletion width X_d versus the generation current $|I_{gen}|$ for the p-type MOS device at a sweep rate of 3.05V/s as obtained by the drop-back technique.

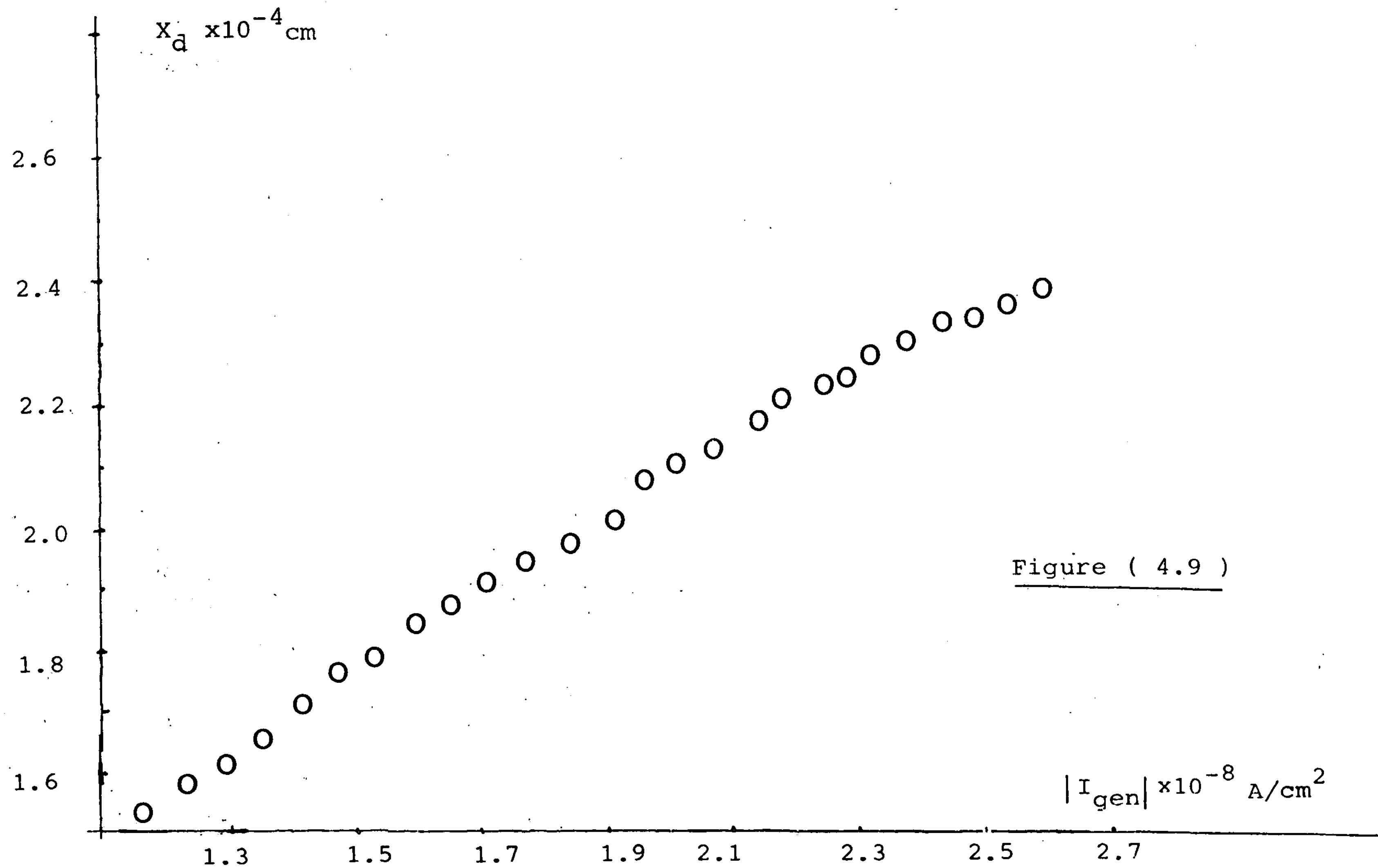

The depletion width X_d versus the generation current $|I_{gen}|$ for the p-type MOS device at a sweep rate of 1.03V/s as obtained by the drop-back technique.

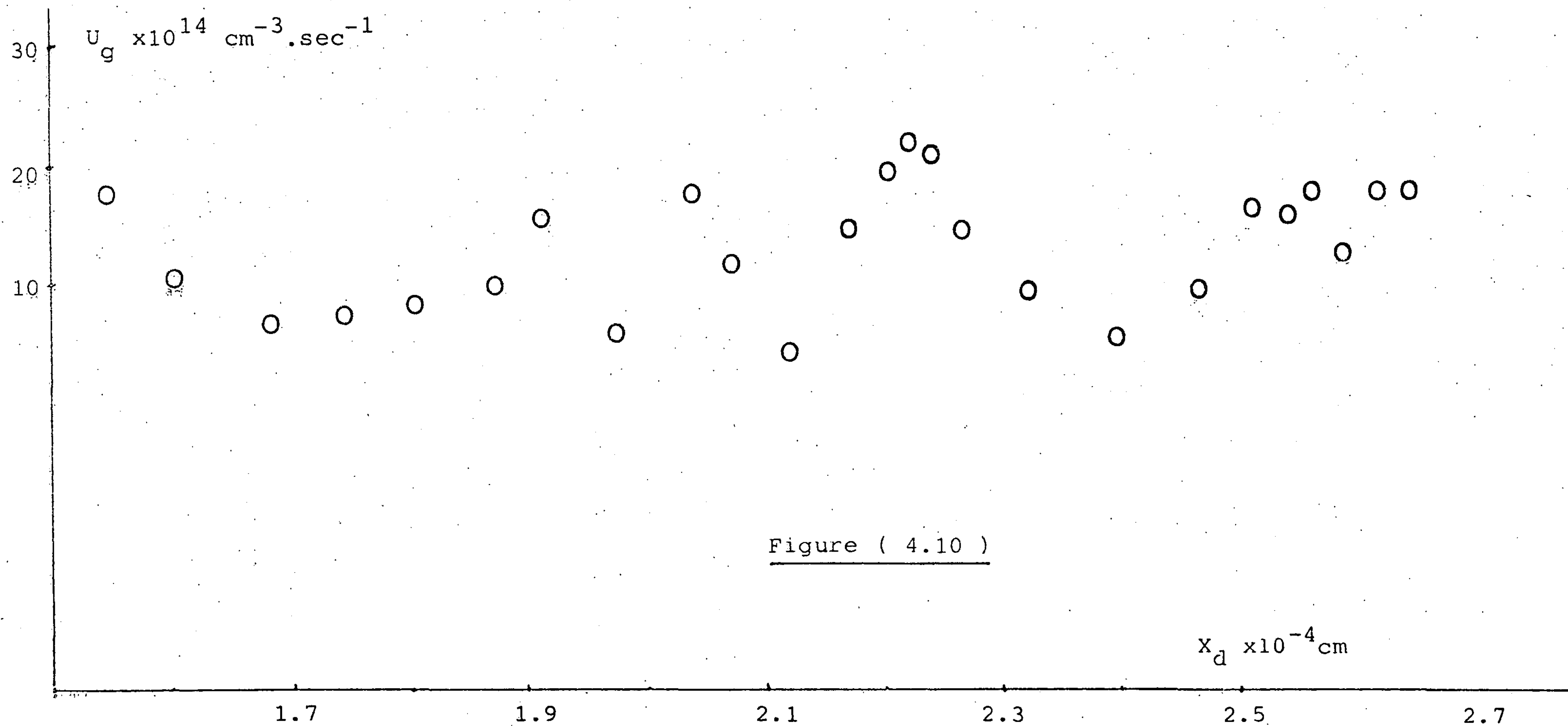

Figure (4.10)

The bulk generation rate U_g versus the depletion width X_d for the p-type MOS device obtained at a sweep rate of 3.05V/s.

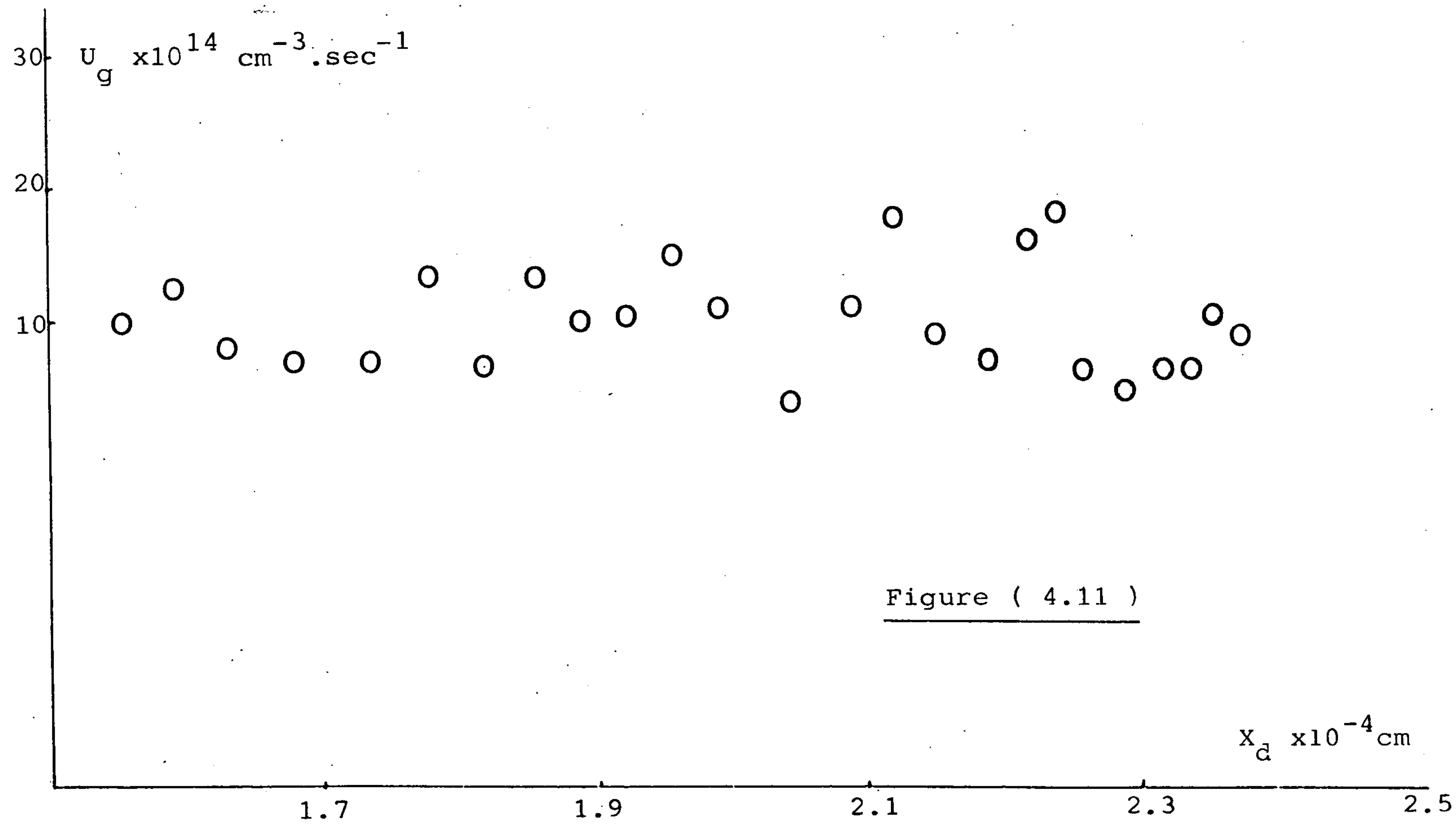

<u>Figure (4.11)</u>

The bulk generation rate U_g versus the depletion width X_d for the p-type MOS device obtained at a sweep rate of 1.03V/s.

from this probably being due to inaccuracy in measurement rather than real differences in the bulk trap generation rate.

The best straight line fit values of the generation rate U_g for the p-type device at the two values of sweep rate of 3.05 V/s and 1.03 V/s are $1.34 \times 10^{15} sec^{-1} cm^{-3}$ and $1.11 \times 10^{15} sec^{-1} cm^{-3}$, respectively, together yielding an average value of $1.23 \times 10^{15} sec^{-1} cm^{-3}$.

4.3.2 The n-type MOS device measurement

The same procedure was followed for the n-type device as for the p-type device, all of the data obtained being tabulated in appendix three and shown diagramatically in figure 4.12. The two chosen values of the sweep rates are 5.72 V/s for the higher sweep rate and 1.72 V/s for the lower sweep rate as shown in figure (4.13).

By using equations (2.56) and (2.65), the values of the depletion width and the generation current are obtained. Figures (4.14) and (4.15) show the form of the d-pletion width curves and how this value increases as the applied voltage increases in the negative direction. As expected, for the higher sweep rate, at the same voltage, the depletion width is larger.

The curves of the generation current versus the depletion width are given in figures (4.16) and (4.17). They are seen to be similar form except that the higher value of sweep rate extends the depletion width further.

The generation rate versus depletion width curves are obtained by differentiating the $|I_g|$ versus X_d characteristic, the resulting plots being shown in figures (4.18) and (4.19) for the two rates.

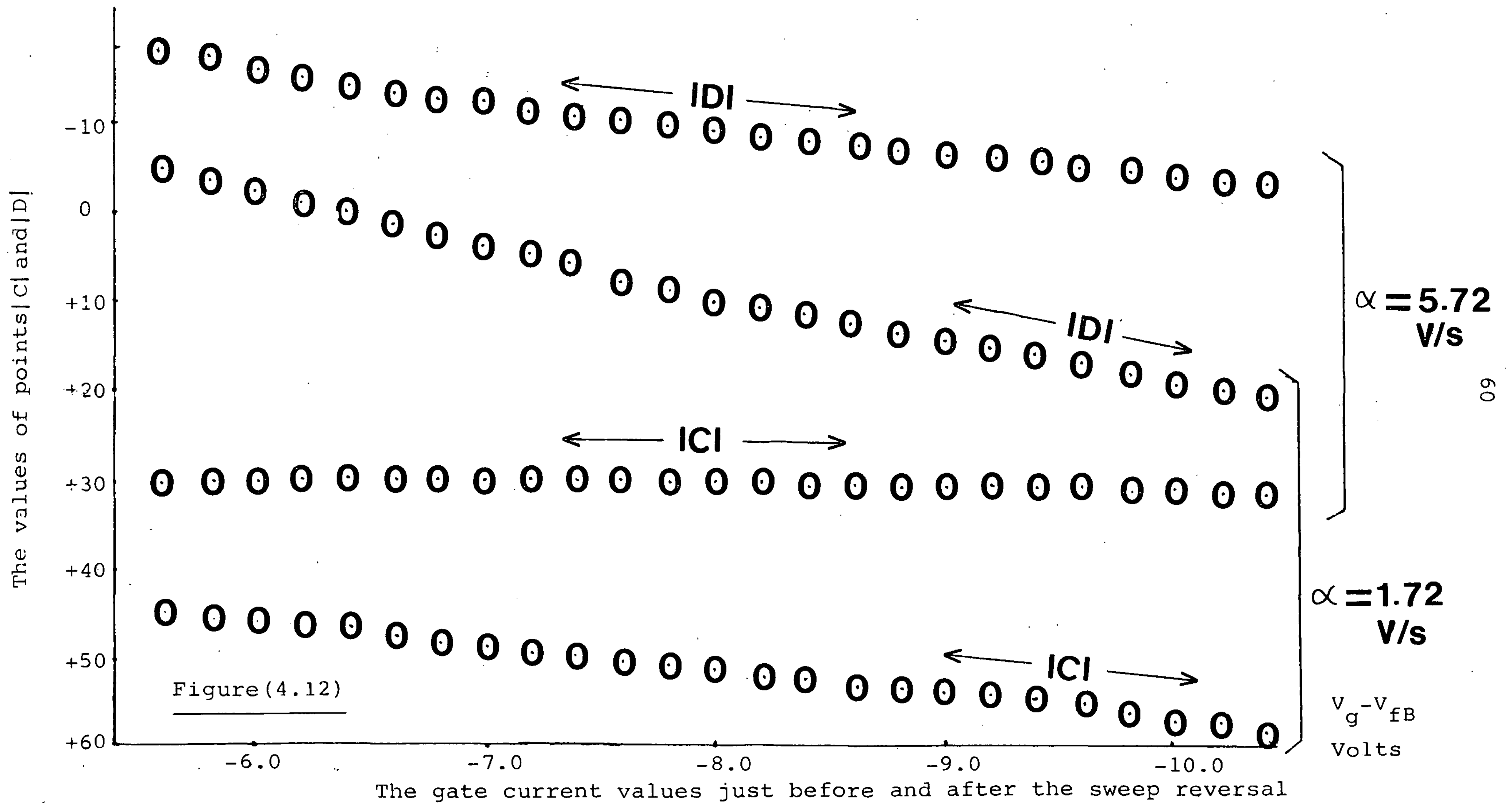

Figure (4.12)

The gate current values just before and after the sweep reversal :this is represented digitally by points |C| and |D| versus the applied gate voltage V_g for an n-type MOS device at two sweep rate values of 5.72V/s and 1.72V/s.

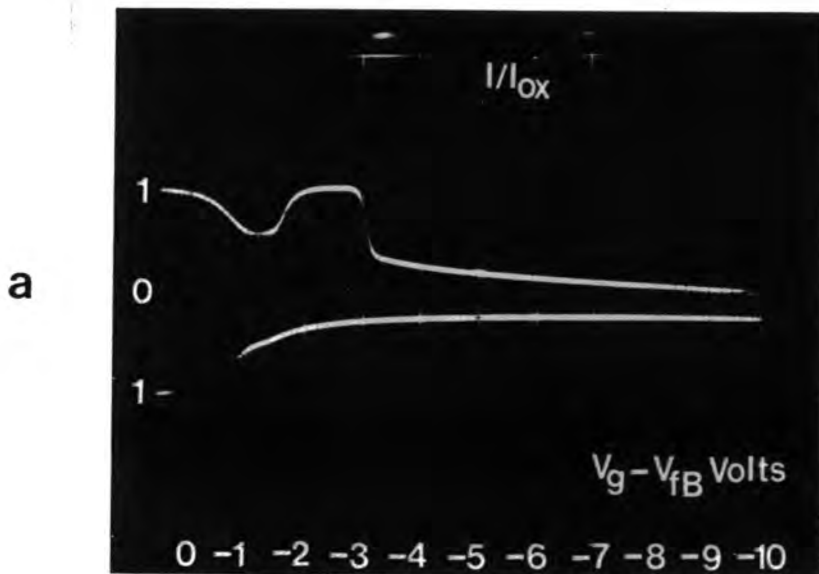

Figure(4.13a) The I-V curve for the n-type MOS device at a sweep rate value of 5.72V/s(the electrometer range is $0.1x10^{-8}$A.).

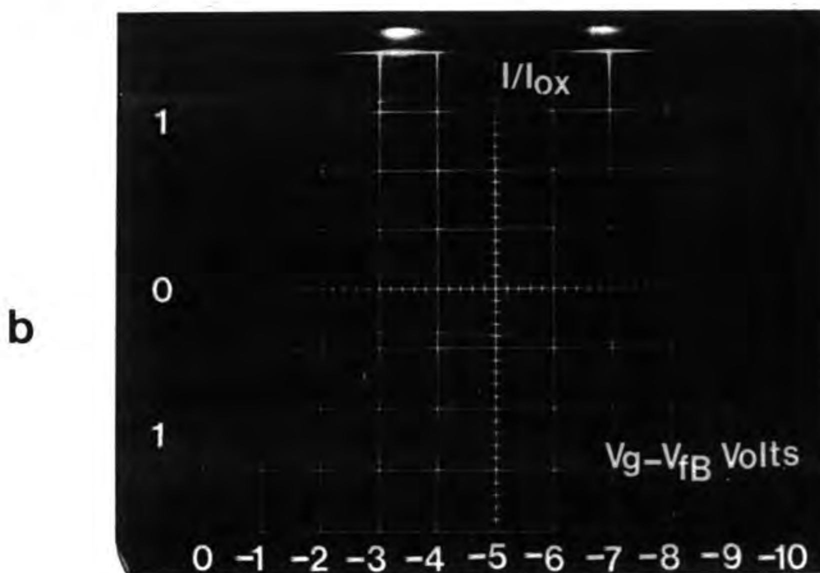

Figure(4.13b) The I-V curve for the n-type MOS device at a sweep rate value of 1.72V/s(the electrometer range is $0.3x10^{-9}$A.).

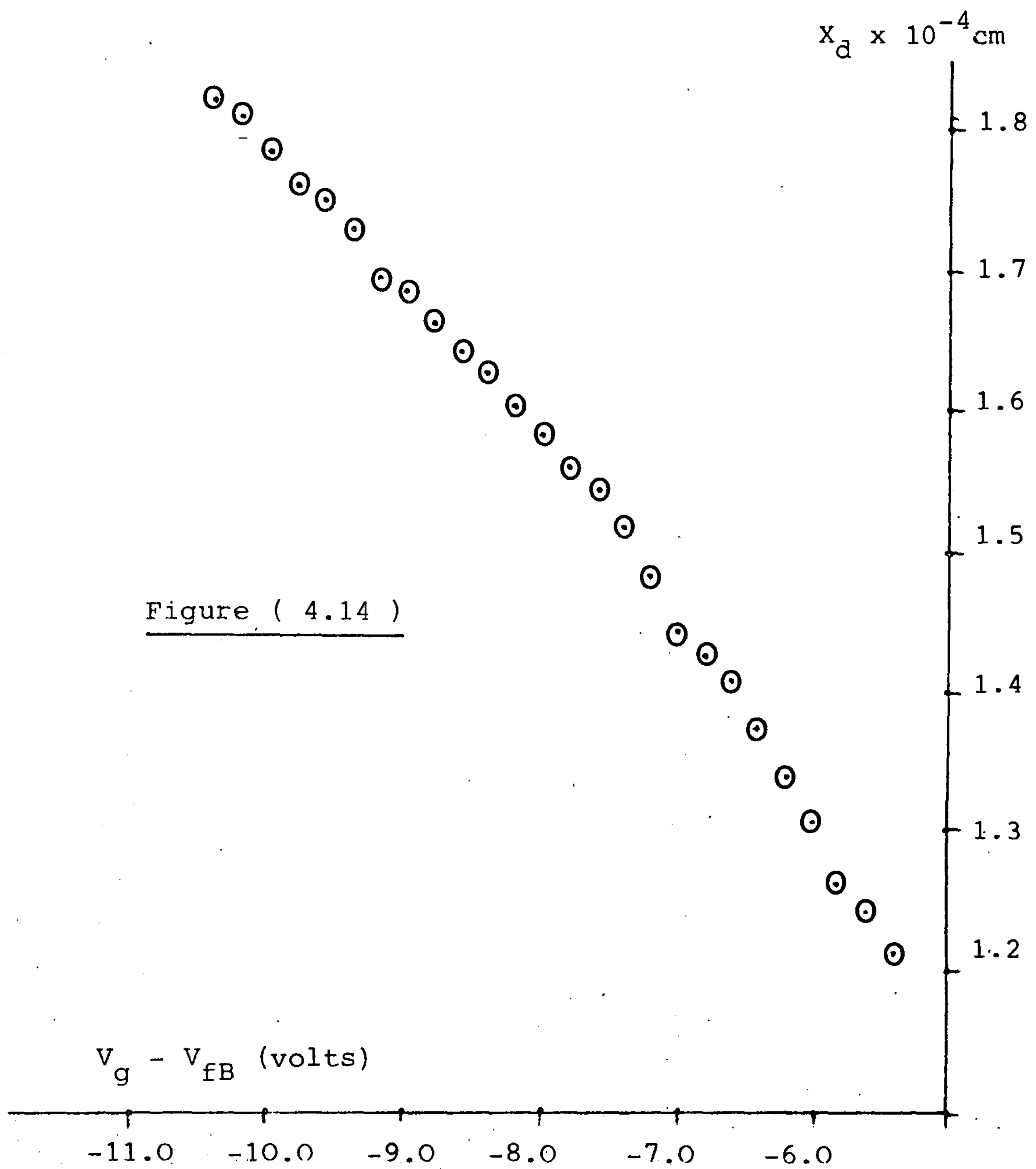

The depletion width X_d versus the applied gate voltage V_g for the n-type MOS device at a sweep rate of 5.72V/s as obtained by the drop-back technique.

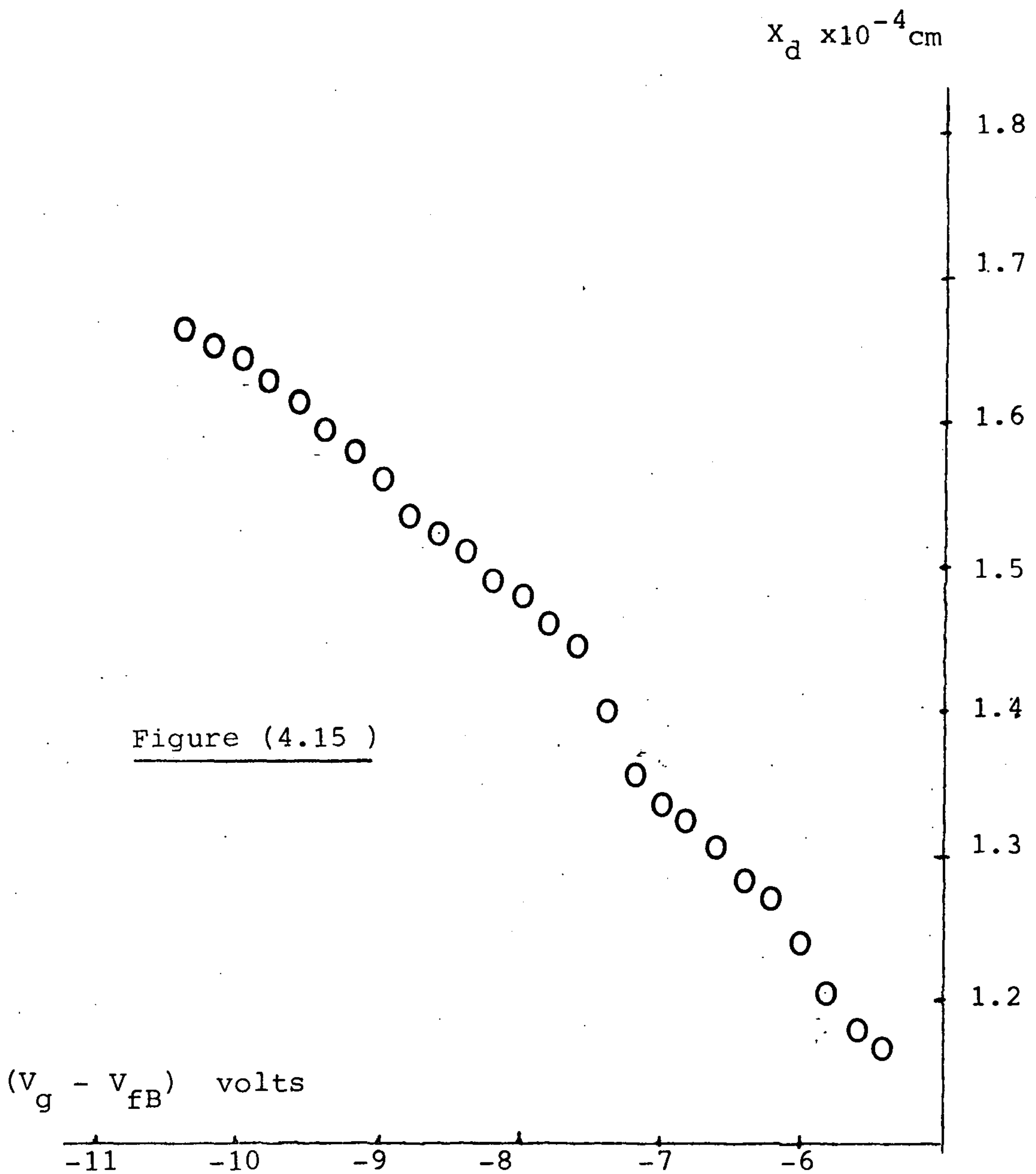

The depletion width X_d versus the applied gate voltage V_g curve for the n-type MOS device at a sweep rate of 1.72V/s as obtained by the drop-back technique.

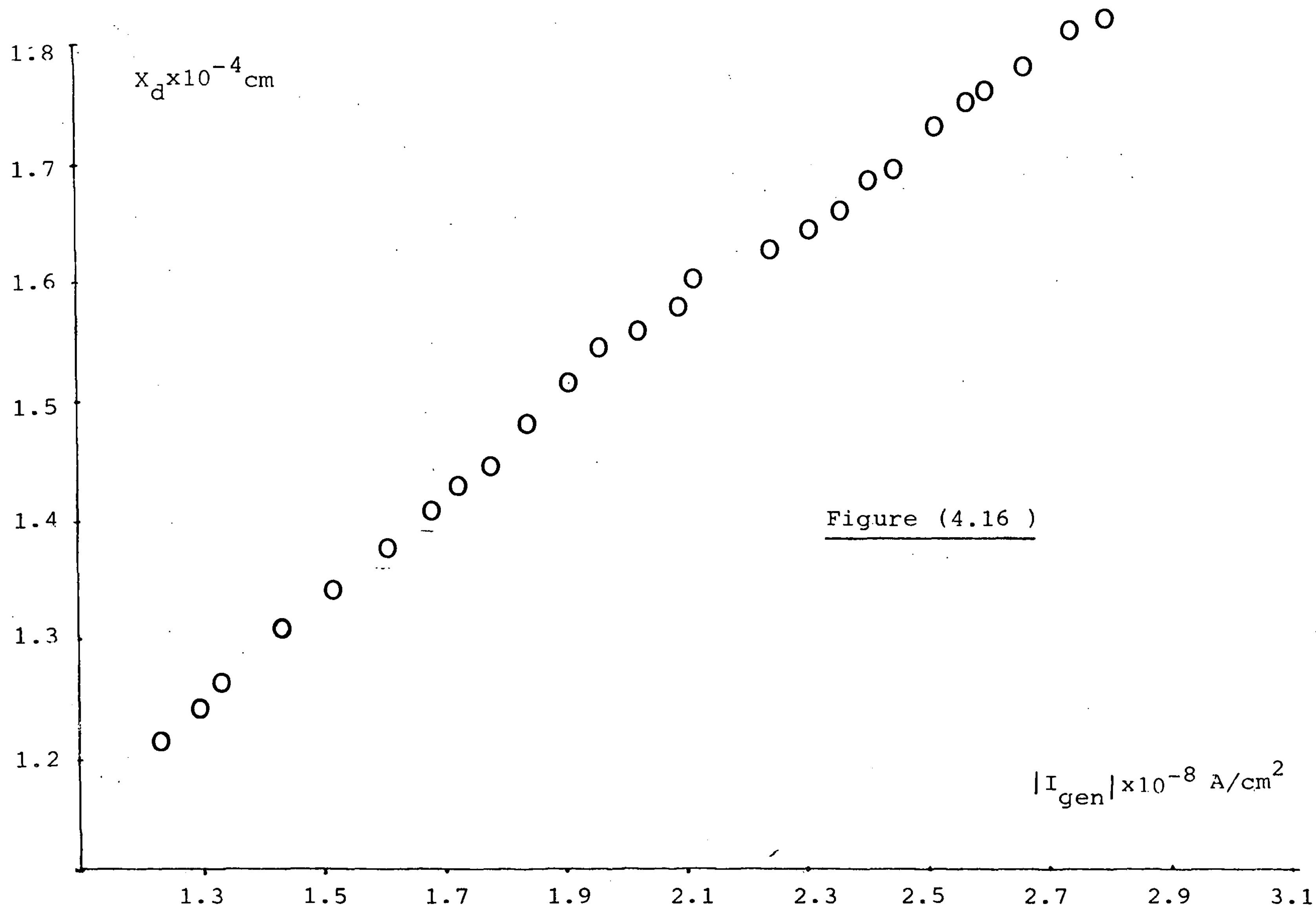

Figure (4.16)

The depletion width X_d versus the generation current $|I_{gen}|$ for the n-type MOS device at a sweep rate of 5.72V/s.

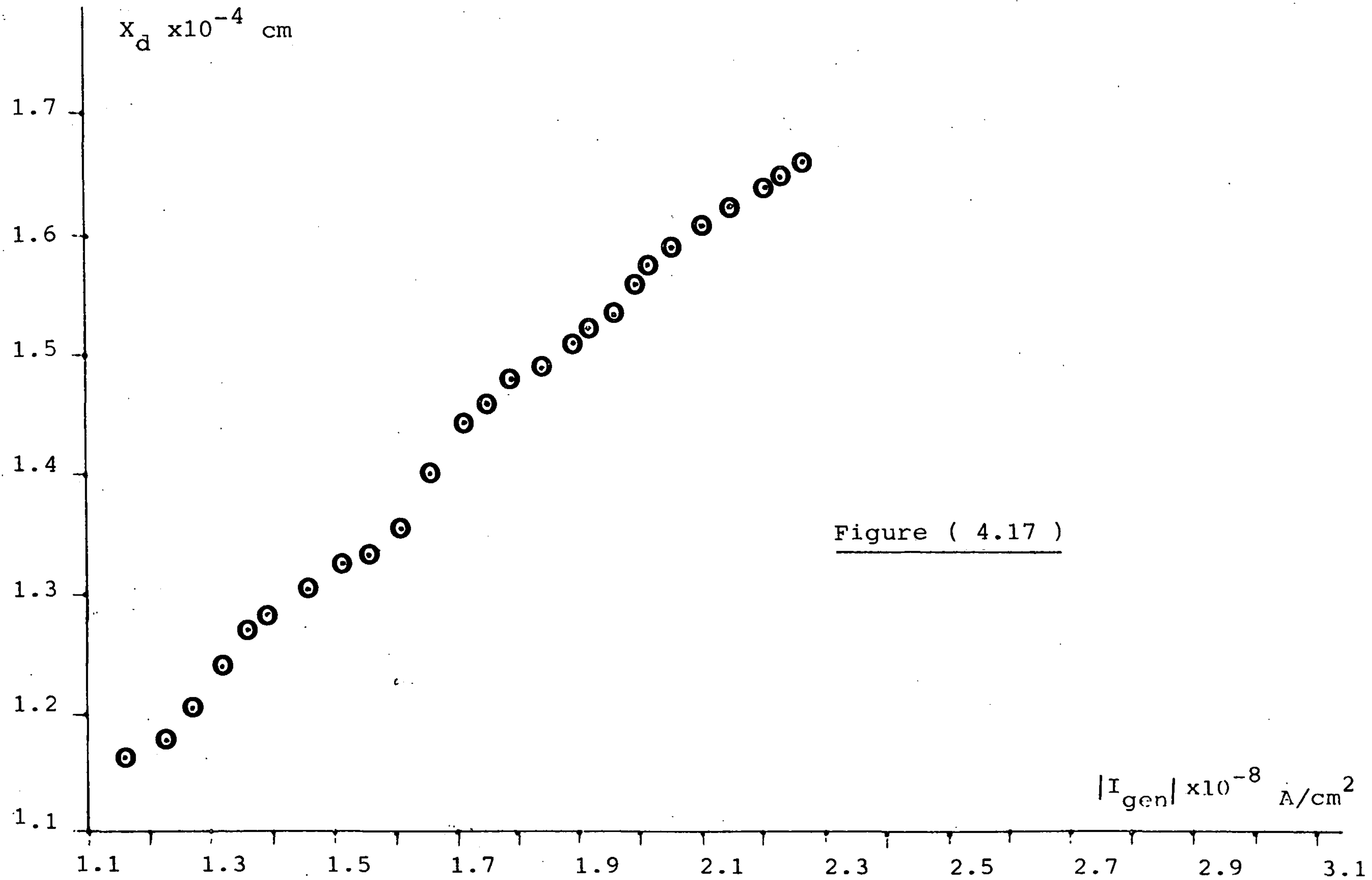

The depletion width X_d versus the generation current $|I_{gen}|$ curve for the n-type MOS device at a sweep rate of 1.72V/s.

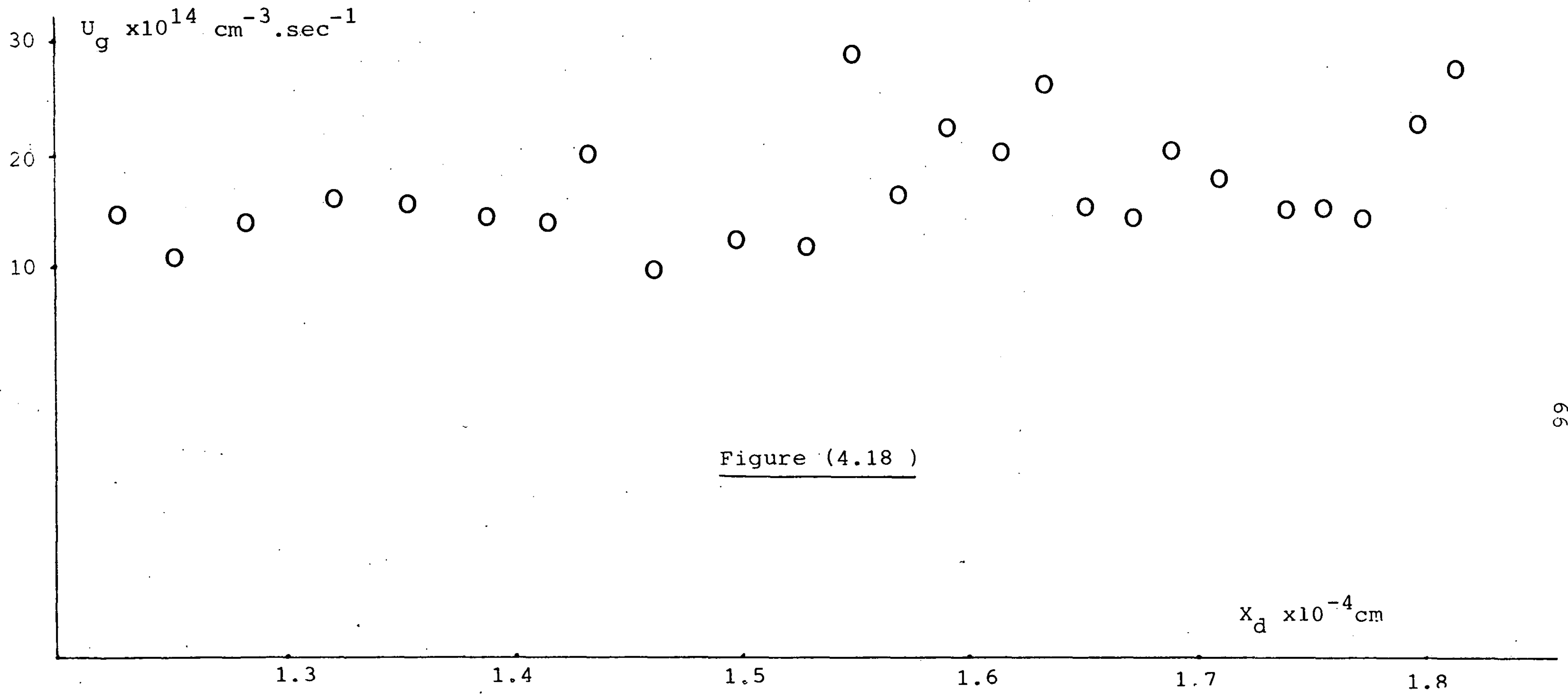

The bulk generation rate U_g versus the dep-etion width X_d for the n-type MOS device at a sweep rate of 5.72V/s.

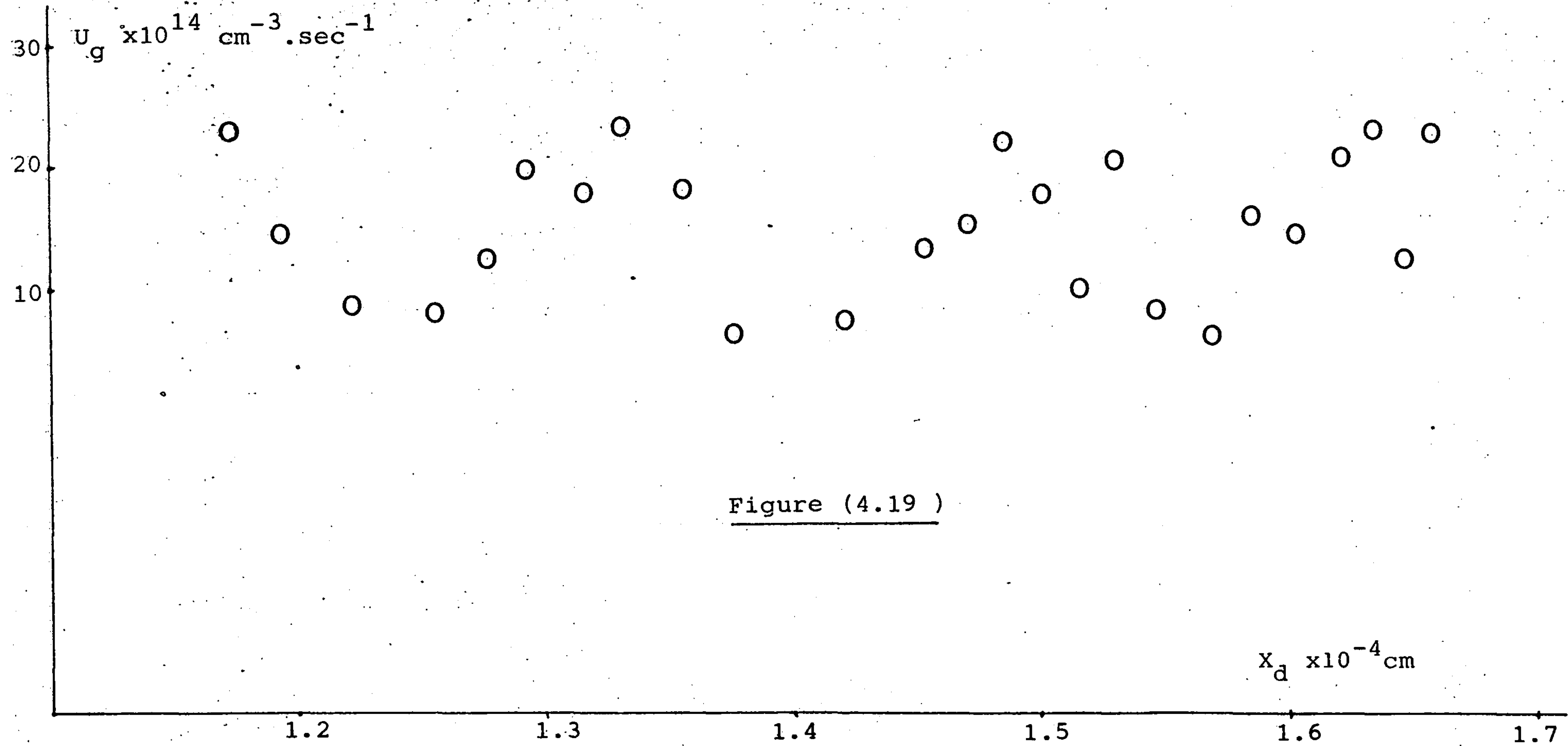

The bulk generation rate U_g versus the depletion width X_d for the n-type MOS device at a sweep rate of 1.72V/s.

The average value of the generation rate at a sweep rate of 5.72 V/s is 1.74 x $10^{15}cm^{-3}sec$,while at a sweep rate of 1.72 V/s it is 1.57 x $10^{15}cm^{-3}sec^{-1}$.This gives an overall average of 1.61 x $10^{15}cm^{-3}sec^{-1}$.

4.4 Surface potential measurements

a) The p-type MOS device:-The surface potential values ψ_s are calculated by substituting the depletion width X_d values calculated by the drop-back measurement into equation(4.9),that is,

$$\psi_s = \frac{q \cdot N_A}{2 \cdot \varepsilon_s} \cdot X_d^2 \qquad \text{------------------------4-9}$$

The surface potential can also be determined by use of the experimental technique mentioned in chapter three(see figure 3.3).

The resultant experimental curve are shown in figure (4.20)at different sweep rates.They were obtained by using a value of external variable resistance of R_1=856Ω and feed-back capacitance of C_f=1 x 10^4 pF.Figure(4.21)shows the surface potential versus the gate voltage curve obtained from the drop-back technique and figure(4.22)shows the corresponding curve obtained from the ψ_s-V_g experimental setup of Tonner & Simmons mons[ref 27]at a sweep rate of 3.05V/s.

Figures(4.23)and(4.24)show the corresponding curves at a sweep rate value of 1.03 V/s.The two sets of curves are very similar showing the consistency between the two experimental measurements.

b) n-type MOS device:-The $\psi_s$versus V_g curves are shown in figure (4.25).These being obtained by using the experimental setup mentioned in chapter three(see figure 3.3).In this case the external variable resistance R_1 is 162$\Omega$and the feed-back capacitance

a

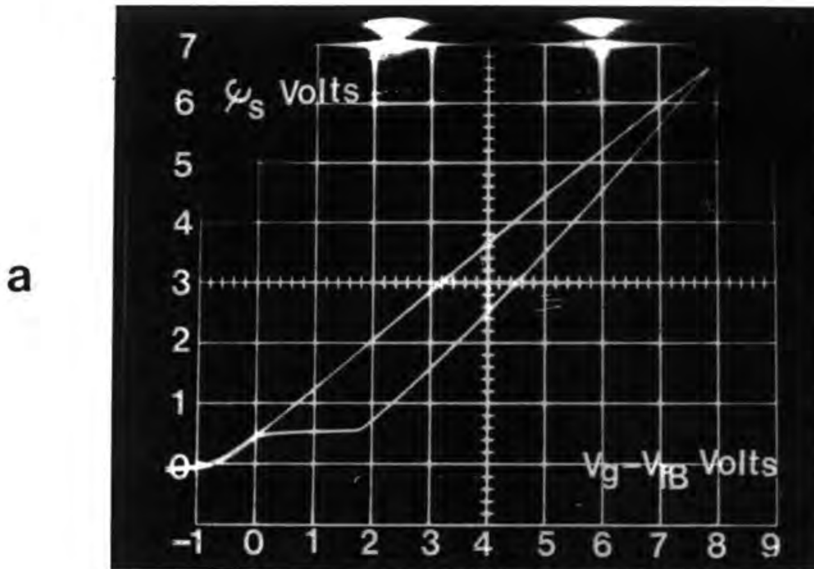

b

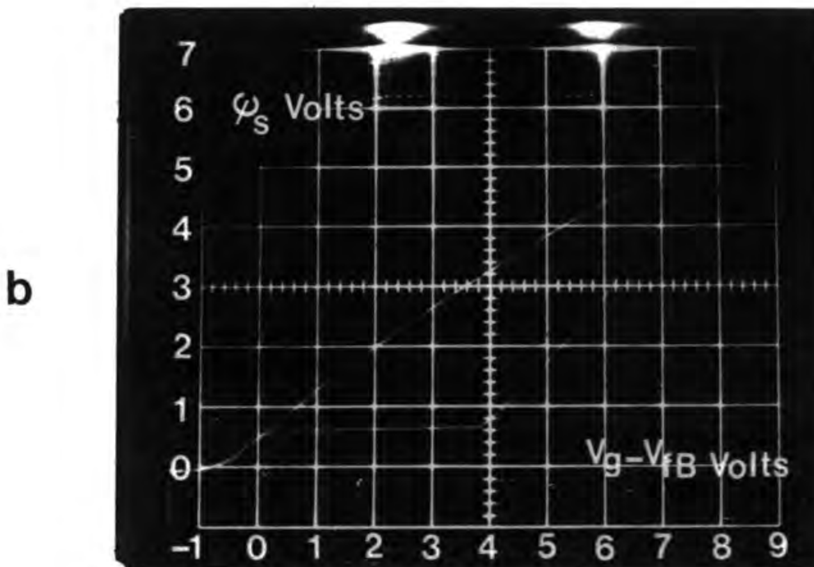

Figure(4.20) The experimental ψ_s-V_g curves for the p-type MOS device obtained by using Tonner & Simmons experimental setup at two different sweep rate values: a) At 3.05V/s. b) At 1.03V/s.

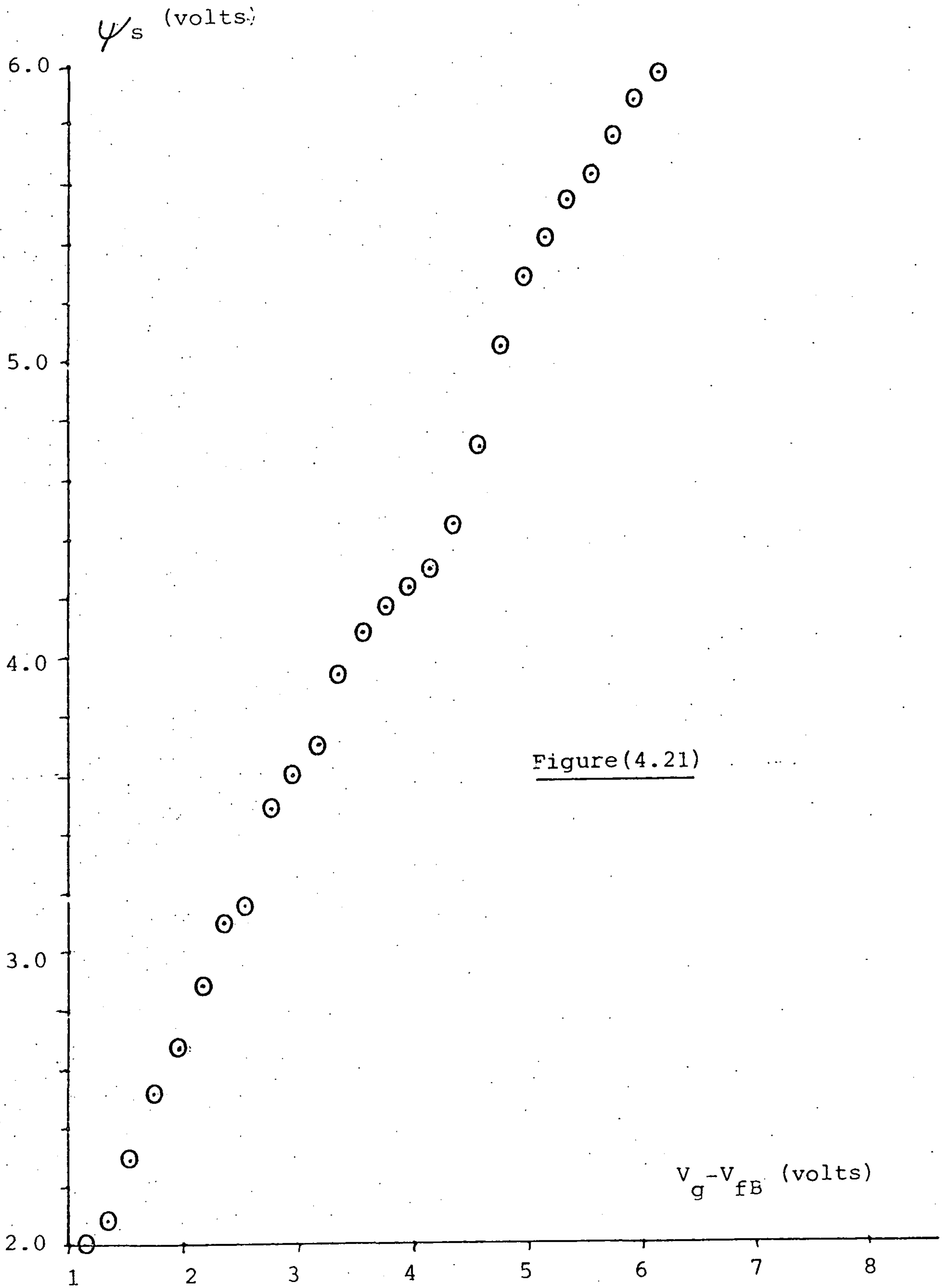

The non-equilibrium ψ_s-V_g curve for the p-type MOS device at a sweep rate of 3.05V/s as obtained by the drop-back technique.

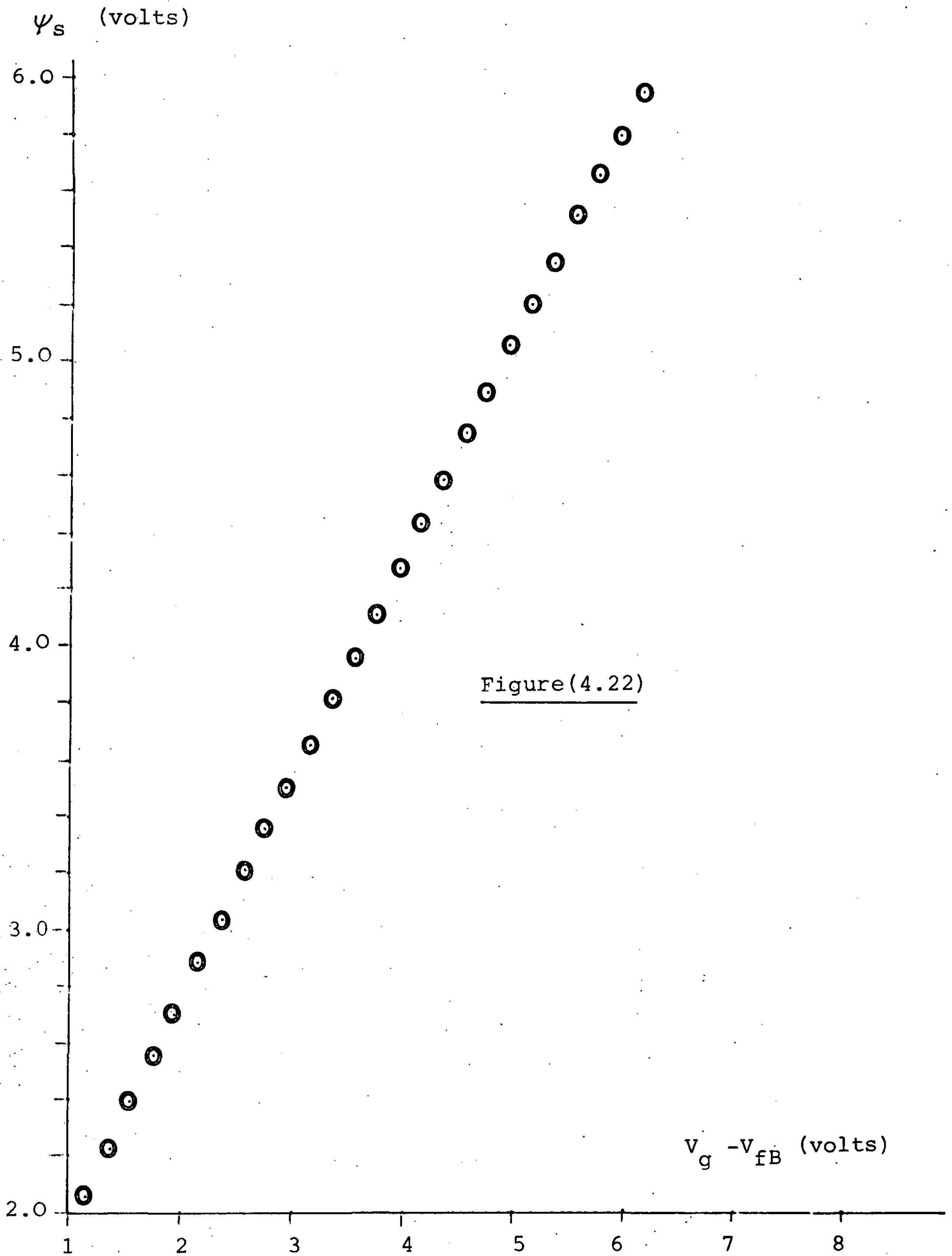

The non-equilibrium ψ_s-V_g curve for the p-type MOS device at a sweep rate of 3.05V/s as obtained directly from the experimental setup of Tonner & Simmons.

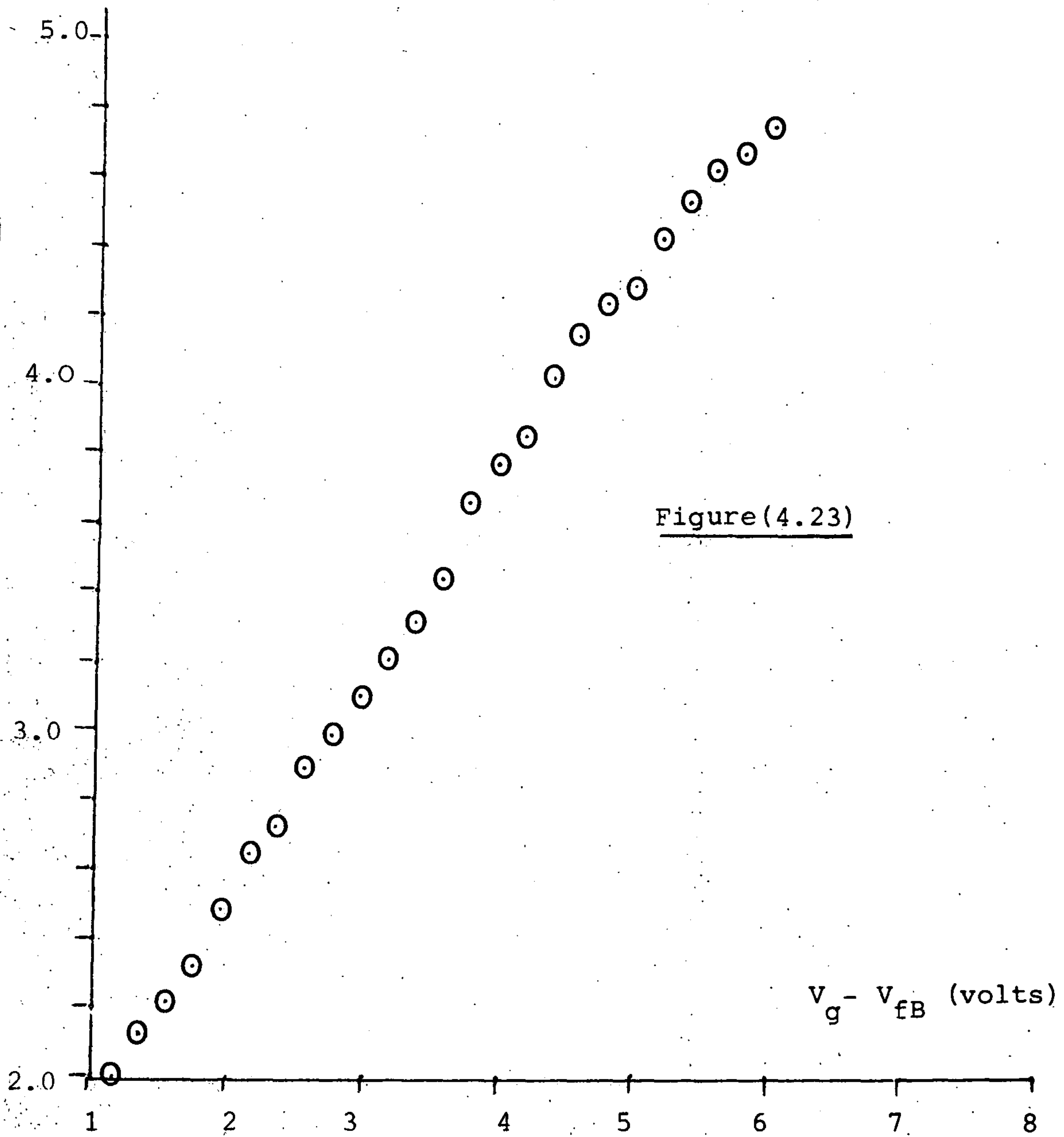

The non-equilibrium ψ_s-V_g curve for the p-type MOS device at a sweep rate of 1.03V/s as obtained by the drop-back technique.

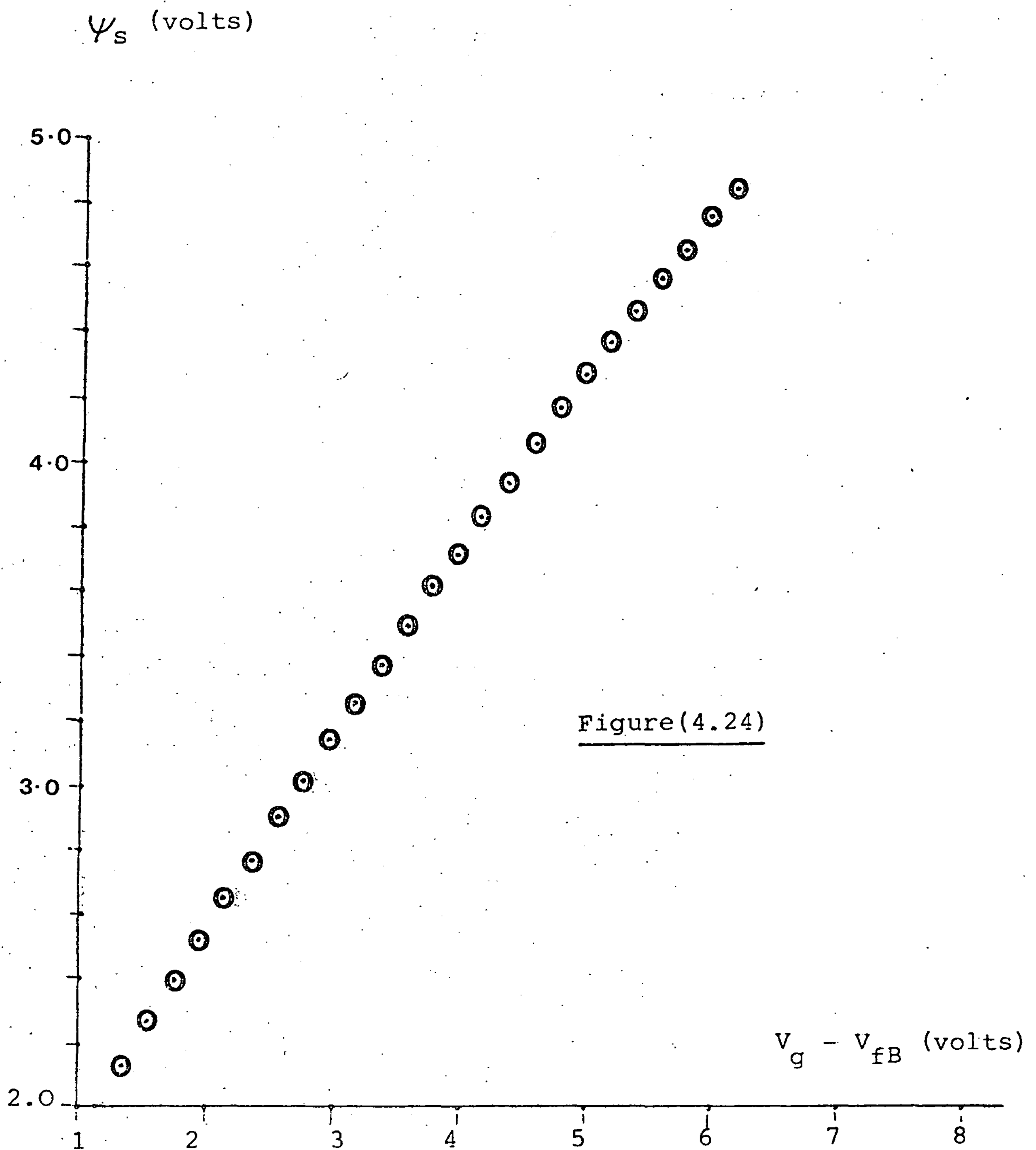

The non-equilibrium ψ_s-V_g curve for the p-type MOS device at a sweep rate of 1.03V/s as obtained directly from the experimental setup of Tonner & Simmons.

a

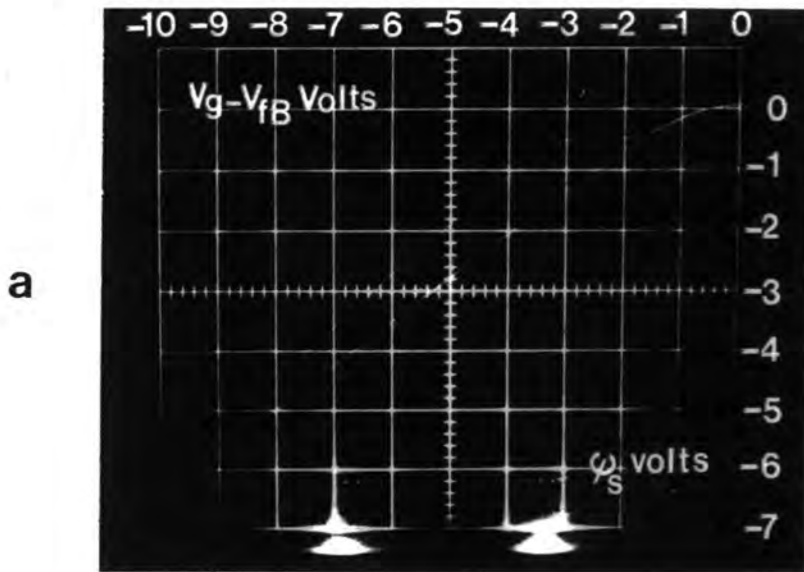

b

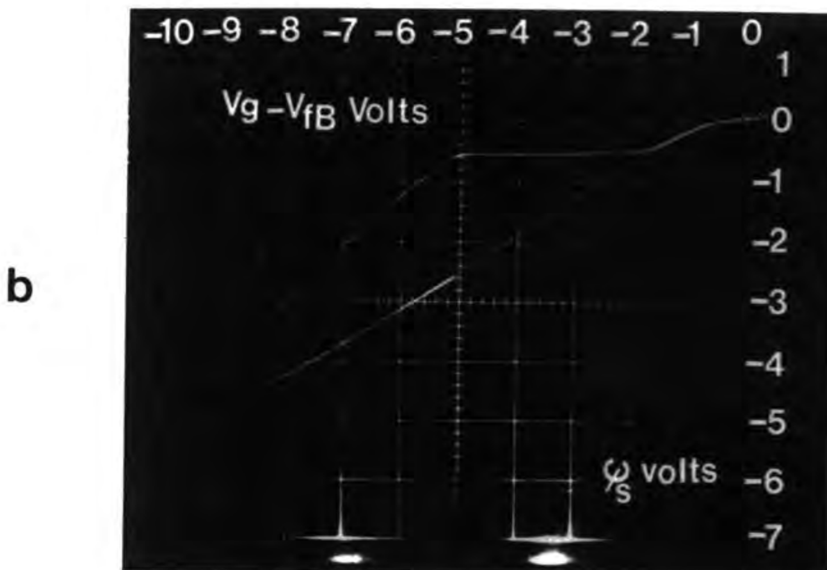

Figure(4.25) The experimental ψ_s-V_g curves for the n-type MOS device obtained by using Tonner & Simmons experimental setup at two different sweep rate values:

a) At 5.72V/s. b) At 1.72V/s.

The non-equilibrium ψ_s-V_g curve for the n-type MOS device at a sweep rate of 5.72V/s as obtained by the drop-back technique.

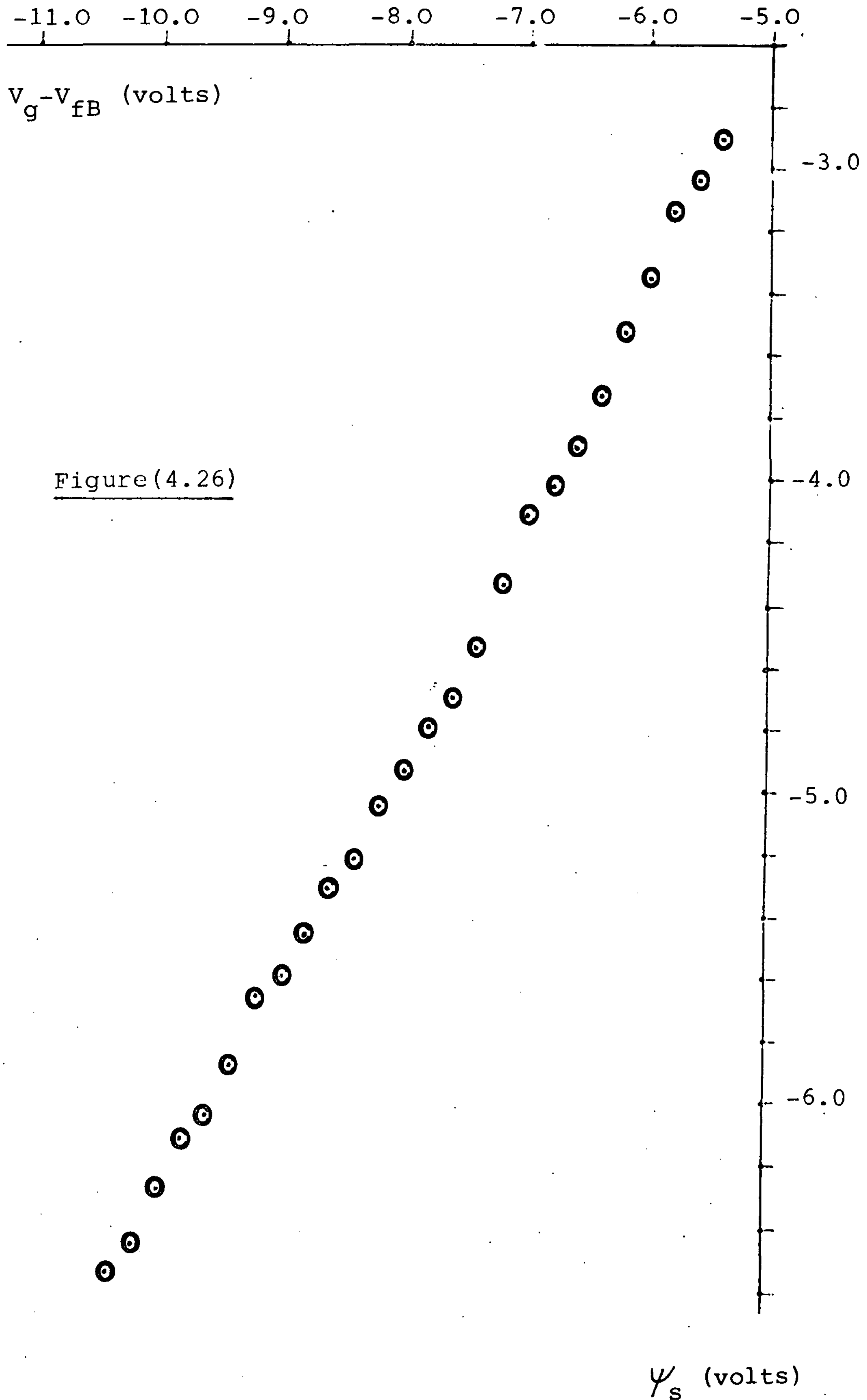

Figure(4.26)

The non-equilibrium ψ_s-V_g curve for the n-type MOS device at a sweep rate of 5.72V/s as obtained directly by using the experimental setup of Tonner & Simmons.

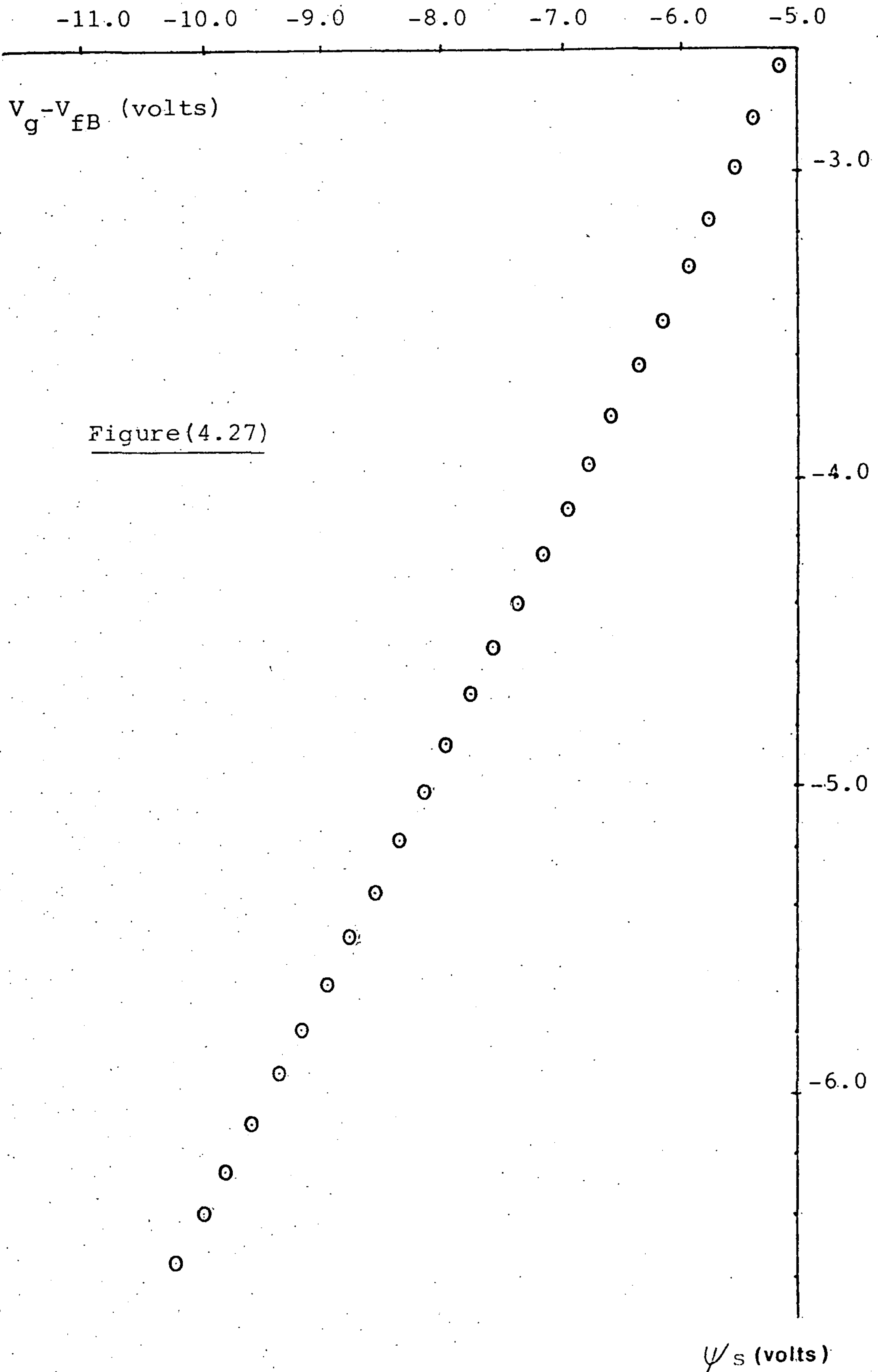

Figure(4.27)

The non-equilibrium ψ_s-V_g curve for the n-type MOS device at a sweep rate of 1.72V/s as obtained from the drop-back technique.

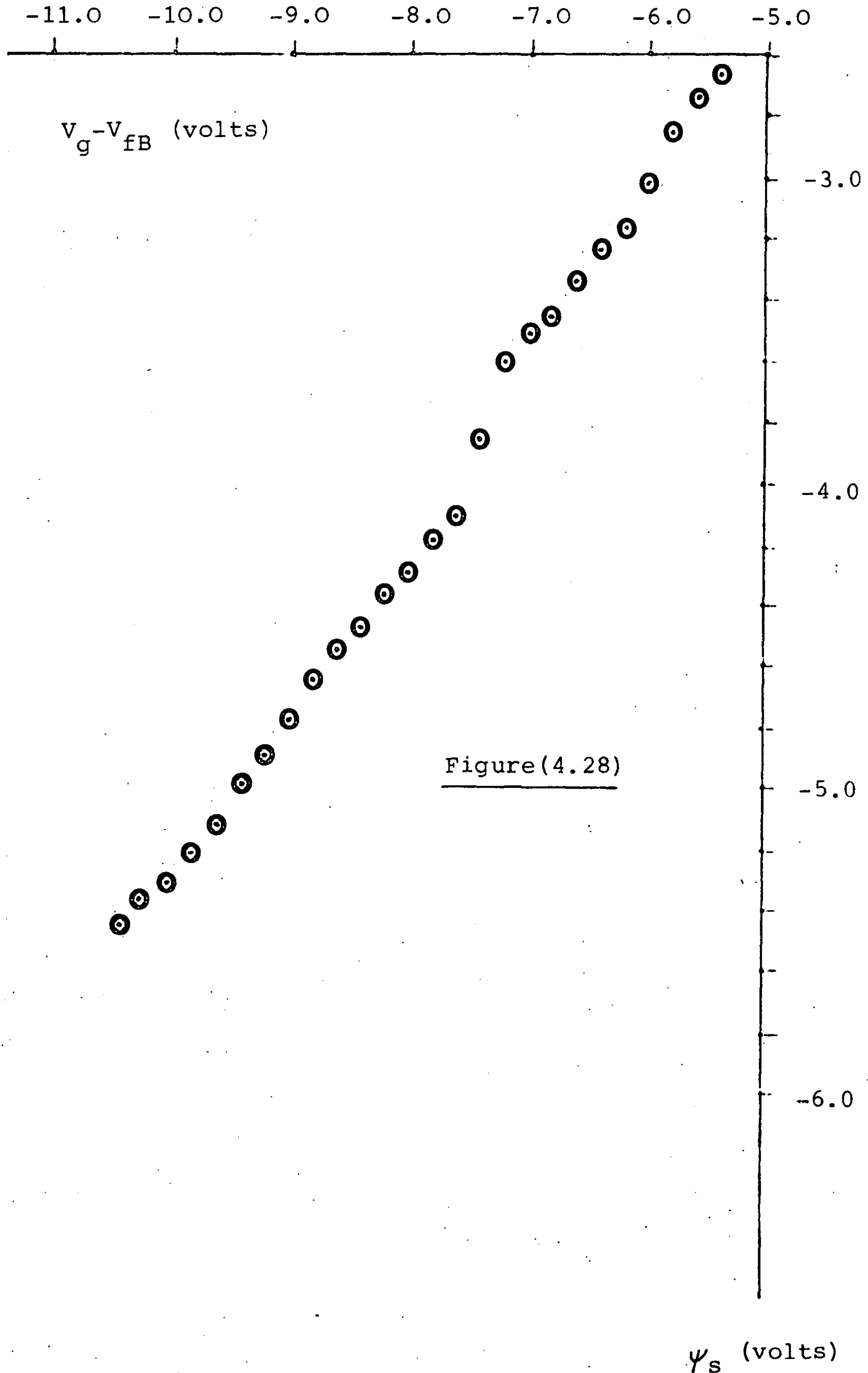

Figure(4.28)

The non-equilibrium ψ_s-V_g curve for the n-type device at a sweep rate of 1.72V/s as obtained directly from the experimental setup of Tonner & Simmons.

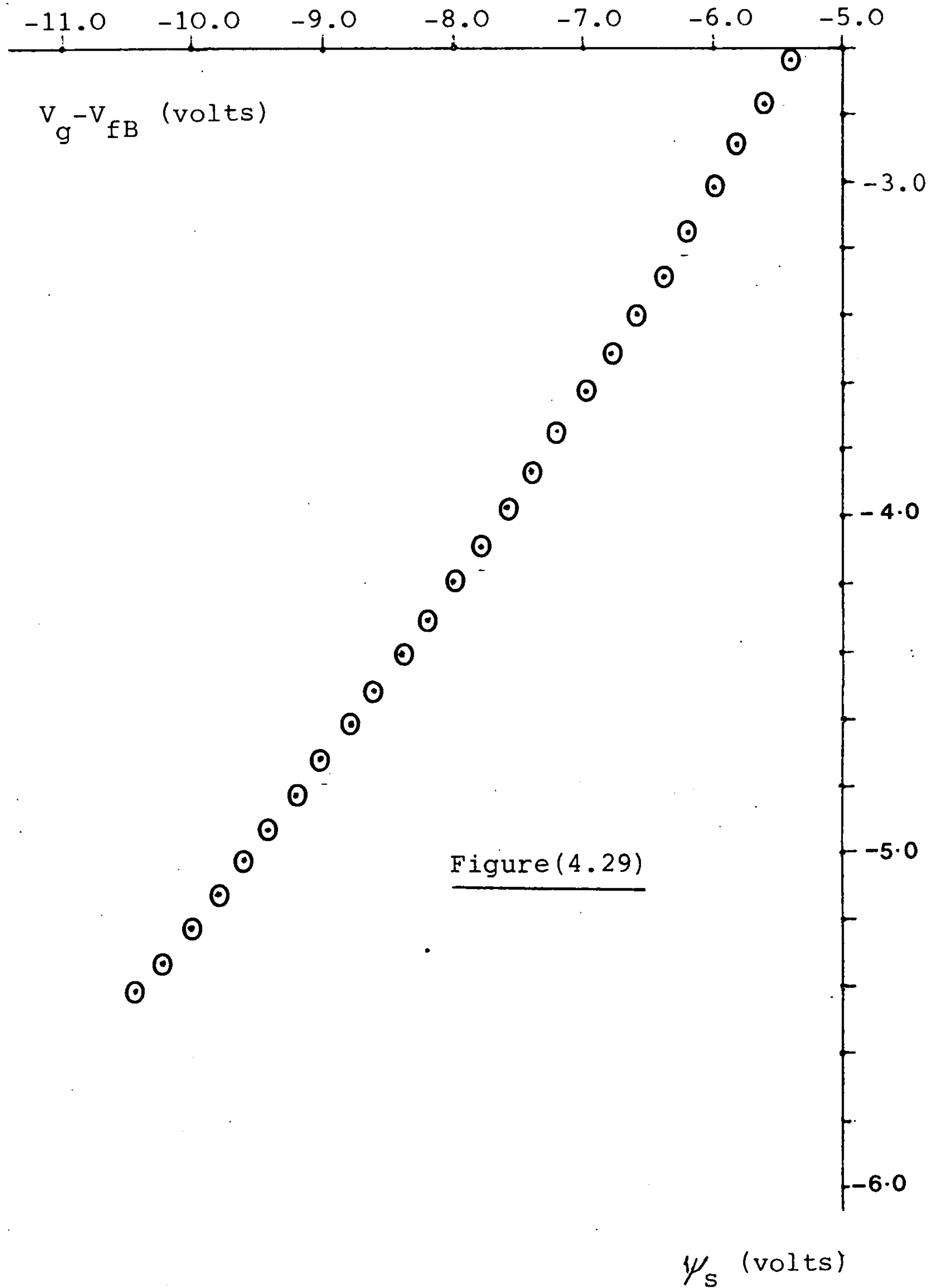

Figure(4.29)

C_f is $1x10^4$pF.Figure(4.26)shows the ψ_s-V_g characteristics obtained from the drop-back measurements and equation(4.9).whereas the corresponding curve obtained from the ψ_s-V_g experimental setup of Tonner & Simmons is shown in figure(4.27)at a sweep rate value of 5.72V/s.Figures(4.28)and(4.29)show the characteristics obtained at a sweep rate value of 1.72 V/s.Again,the closeness between the two experimental techniques is demonstrated.

4.5 Discussion

An experimental investigation into the drop-back technique has been carried out in this chapter and important information has been gained about the MOS devices under study.

The depletion width,generation current and generation rate values have been obtained by the use of a simple data logging and analysis program using a desk top computer.

Finally,the depletion width values obtained from the drop-back technique were compared to those obtained using the ψ_s-V_g experimental setup developed by Tonner and Simmons [ref 27] .The two sets of results were shown to be in very close agreement.

CONCLUSION

The work presented in this thesis is concerned with the application of a newly developed theoretical and experimental method(called the drop-back technique)to the study of MOS device non-equilibrium characteristics.

The technique is intimately related to the fast ramp technique,which consists of applying a triangular voltage wave-form to an MOS device of such a frequency as to take the device into the non-equilibrium mode of operation.The resulting I-V characteristic is logged on a desk top computer and the region of interest,the end of the forward voltage sweep,is analysed in detail.In particular,this means measuring the gate voltage and gate current just before sweep reversal and gate current just after sweep reversal.It has been shown to be possible to obtain directly plots of generation rate U_g versus depletion width X_d thus yielding a semiconductor bulk trap profile.

In the particular devices considered the average values of the generation rate U_g were seen to be fairly constant.The variation about this average is probably due to errors in measurement rather than real bulk trap effects.Standerd high frequency C-V measurements were performed in order to obtain such useful information about the device as the doping density value(N_A for the p-type and N_D for the n-type),the flat band voltage shift and the oxide capacitance.

Finally,the validity of the drop-back technique for measuring the depletion region width was verified by comparing the measurements against the direct measuring with the ψ_s-V_g experimental setup.

The limitation to the accuracy of the measurement technique has been mentioned before.This is due to the small size of the current drop and the concommitant problems ass-

ociated with measuring this.Some preliminary measurements have been performed using the analogous drop-back associated with the constant current technique.The drop measured in this case is much larger and should therefore lead to much higher accuracy.This will be the case of further experimental study.

REFERENCES

1- K.Board and J.G.Simmons.Solid State Electronics,20,859(1979).

2- J.L.Moll.Wescon Convention Record.Part 3,page 32(1959).

3- W.G.Pfann and C.G.B.Garrett.Proc.IRE,47,2011(1959).

4- D.R.Frankel.Solid State Electronics,2,285(1962).

5- R.Lindner.Bell System Technical.J,41,803(1962).

6- L.M.Terman.Solid State Electronics,5,285(1962).

7- P.V.Gray and D.M.Brown.Appl Physics.Lett,8,31(1966).

8- E.H.Nicollian and A.Goetzberger.Bell System Technical.J 46,1055(1966).

9- C.N.Berglund.IEEE Trans Electron Devices.ED-13,701(1966).

10-M.Kuhn.Solid State Electronics,13,873(1970).

11-G.Rupprecht.Phys.Rev,111,75(1958).

12-C.Jund and R.Poirier.Solid State Electronics,9,315(1966).

13-M.Zerbst and Z.Angew.Phys,22,30(1966).

14-F.P.Heiman.IEEE Trans.Electron Devices.ED-14,781(1967).

15-J.S.T.Huang.Proc.IEEE,1849(1970).

16-S.R.Hofstein,IEEE Trans Electron Devices.ED-14,785(1968).

17-P-Kuper and C.A.Grimbergen.Solid State Electronics,21,549 (1978).

18-R.Board,J.G.Simmons and P.G.C.Allman.Solid State Electronics, 21,1157(1978).

19-P.G.C.Allman and J.G.Simmons.IEE PROC,127,3,140(1980).

2 20-P.G.C.Allman and j.G.Simmons.IEE Proc,127,6,312(1980).

21-W.Shocklet and W.T.Read.Phys ical.Rev,87,835(1952).

22-P.M.Chirlian"Analysis and Design of Integrated Circuits".

23-A.P.Malvino"Digital Computer Electronics".

24-J.Millman"Microelectronics".

25-C.A.Holt"Electronic Circuits".

26-S.M.Sze"Physics of Semiconductor Devices".

27-P.D.Tonner and J.G.Simmons.Rev Sci.Instrum,51(10),oct(1980).

28-K.Board,P.G.C.Allman and J.G.Simmons.Solid State and Electron Devices,3,(1979).

29-D.D.Givone and R.P.Roesser"Microprocessors/Microcomputers: An Introduction".

30-A.S.Grove,B.E.Deal,E.H.Snow,and C.T.Sah.Solid State Electronics,8,145(1965).

APPENDIX ONE

A-1 The Clock Circuit

This circuit consists of two parts:

(a) The Quartz Crystal

The quartz crystal has two electrodes plated on opposite faces.When a potential is applied between these two electrodes forces will be exerted on the bound charges within the crystal.If this device is properly mounted deformations take place within the crystal and an electromechanical system is formed which will vibrate when properly excited [ref 23].

(b) 7400N Chip

Figure(A.1)shows two NAND gates connected in series and a quartz crystal with generating sinusoidal wave input to the first NAND gate,the output of the gate being a square wave with 180° phase shift.This output is fed to the second NAND gate which will change the phase again by 180°.The output is then in phase with the input signal,i.e the loop phase is 360°.This type of closed circuit ensures that oscillation will take place.

A-2 Some Electronic Circuit Fundamentals

An operational amplifier(figure A.2) is defined as a multistage configuration with a differential input stage and is characterized by high voltage gain,high input impedence and low output impedence.It is widely used in many different types of linear and non-linear circuits.

The main characteristics of the ideal operational amplifier are:

1) Very high input resistance($R_i = \infty$),so the voltage difference between the two inputs is zero.

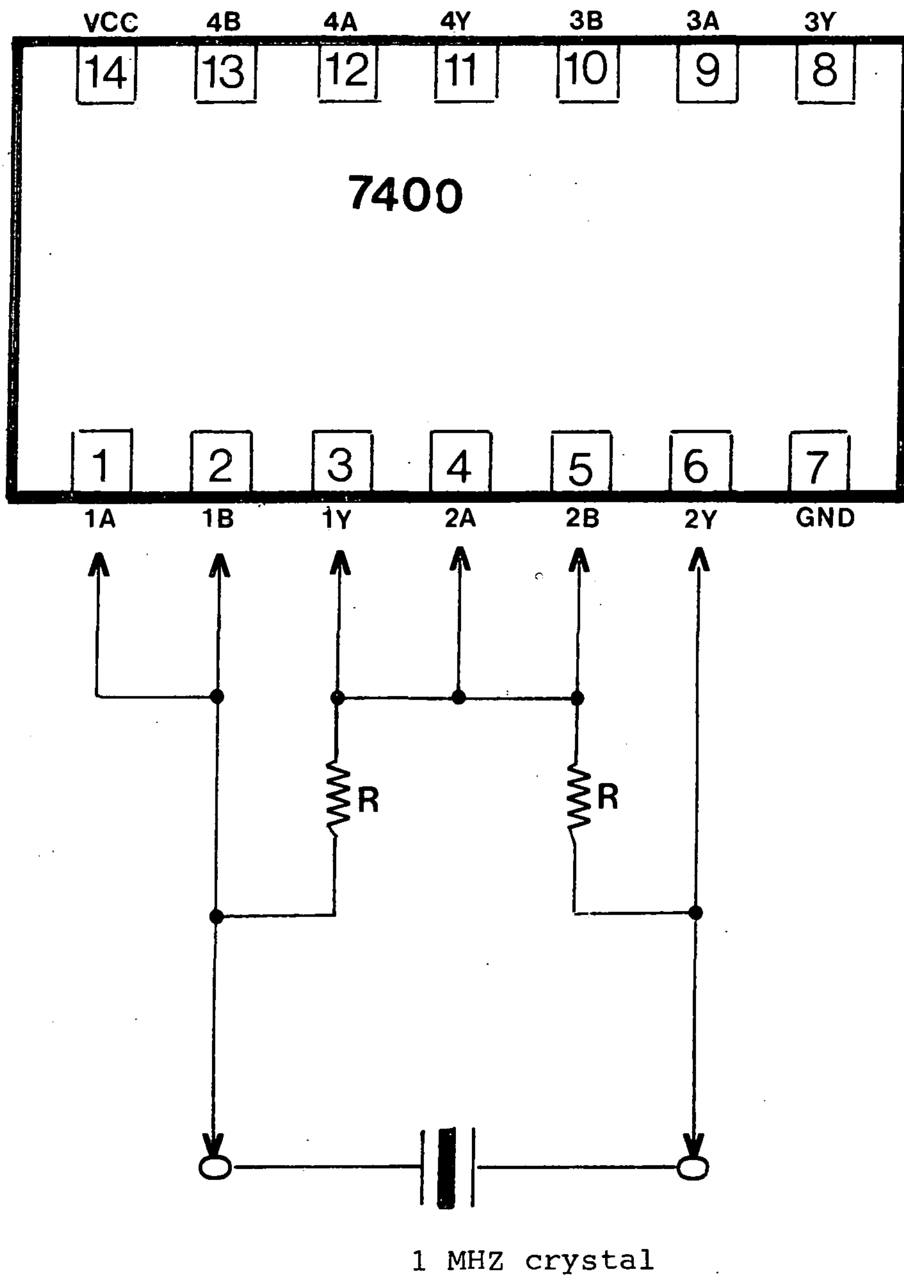

Figure(A.1)

Clock General Circuit.

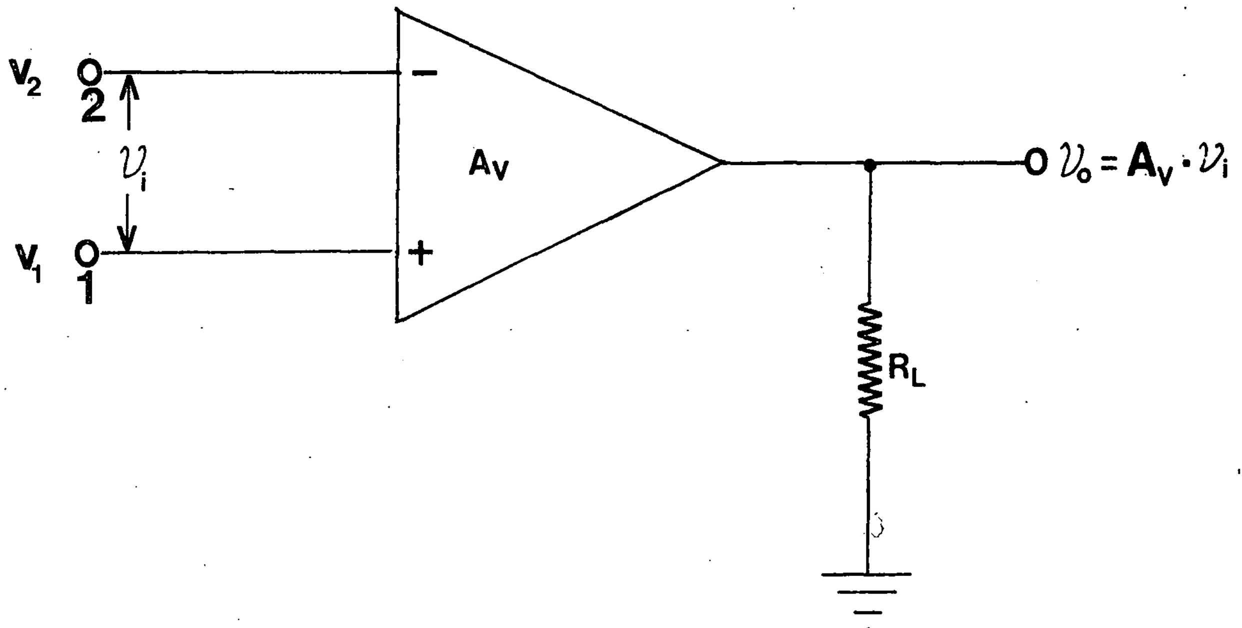

Figure(A.2a) Basic operational amplifier.

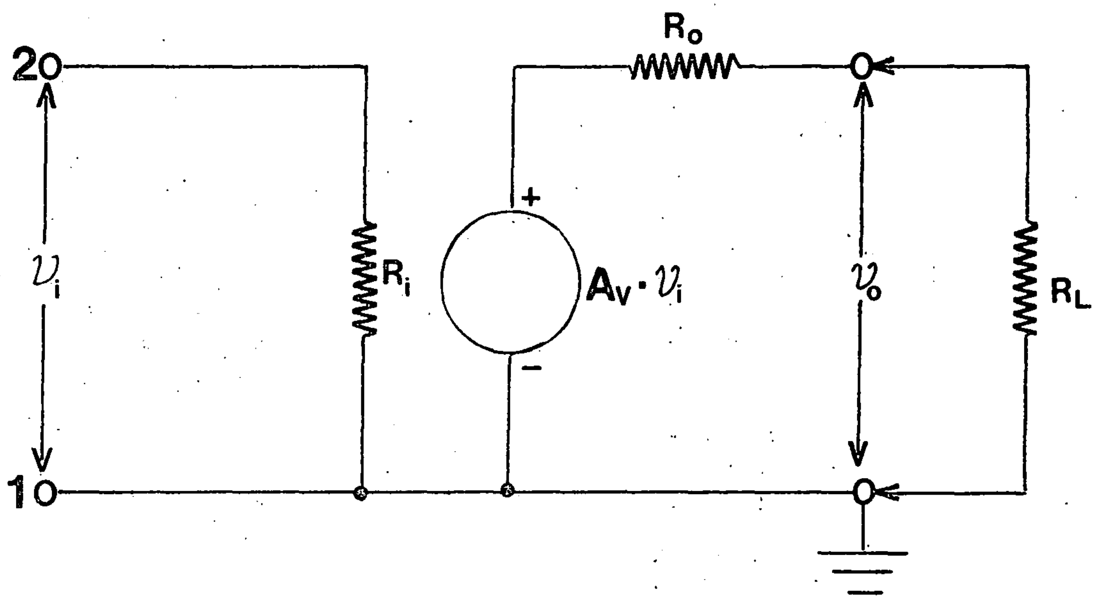

Figure(A.2b) Low frequency circuit model of the operational amplifier.

2) Very low output resistance(R_o=0).

3) V_o=0 when $V_1 = V_2$, where V_o is the output voltage.

Figure(A.2) shows the diagram of the operational amplifier circuit where the voltages V_1 and V_2 are applied to the inverting and non-inverting terminals. The voltage gain($A_v = \frac{V_o}{V_i}$) is positive if V_1 is greater than V_2 and negative if V_2 is greater than V_1.

The operational amplifier can be used for many useful things, e.g., a comparator, integrator, inverter, differentiater, voltage follower [ref 24].

1. The Analogue Comparator

The analogue comparator has two inputs, one is a reference voltage V_R and the other is a time varying signal V_i as shown in figure(A.3). The output voltage (for the ideal comparator) $V_o = \mathbf{V}(0)$ if $V_i < V_R$ and a different constant value $V_0 = \mathbf{V}(1)$ if $V_i > V_R$. That is, the input is compared with the reference and the output is digitized into one of the two states:

(a) Low(0) level of voltage $\mathbf{V}(0)$.

(b) High(1) level of voltage $\mathbf{V}(1)$.

i.e the comparator behaves as a 1-bit analogue to digital converter.

2. The integrator

The integrator is a circuit which consists of the operational amplifier and a capacitor connected in parallel, and a resistance R. This circuit performs the mathematical operation of integration, the equivalent circuit being shown in figure(A.4).

The output voltage $V_o = \frac{-1}{C} \int i \, . \, dt$.

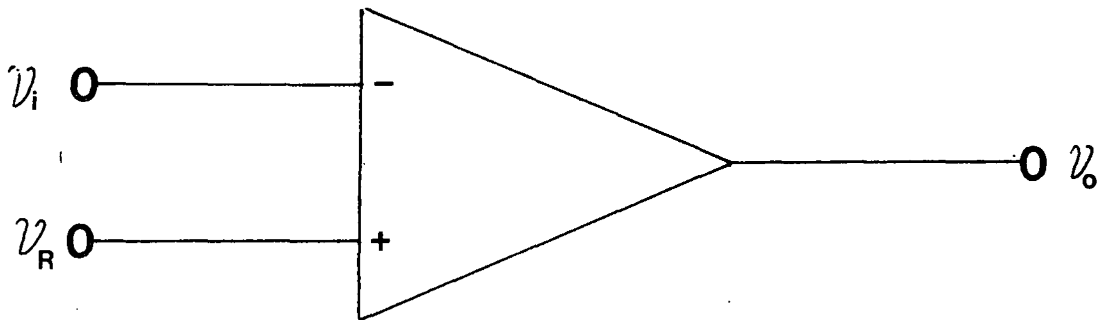

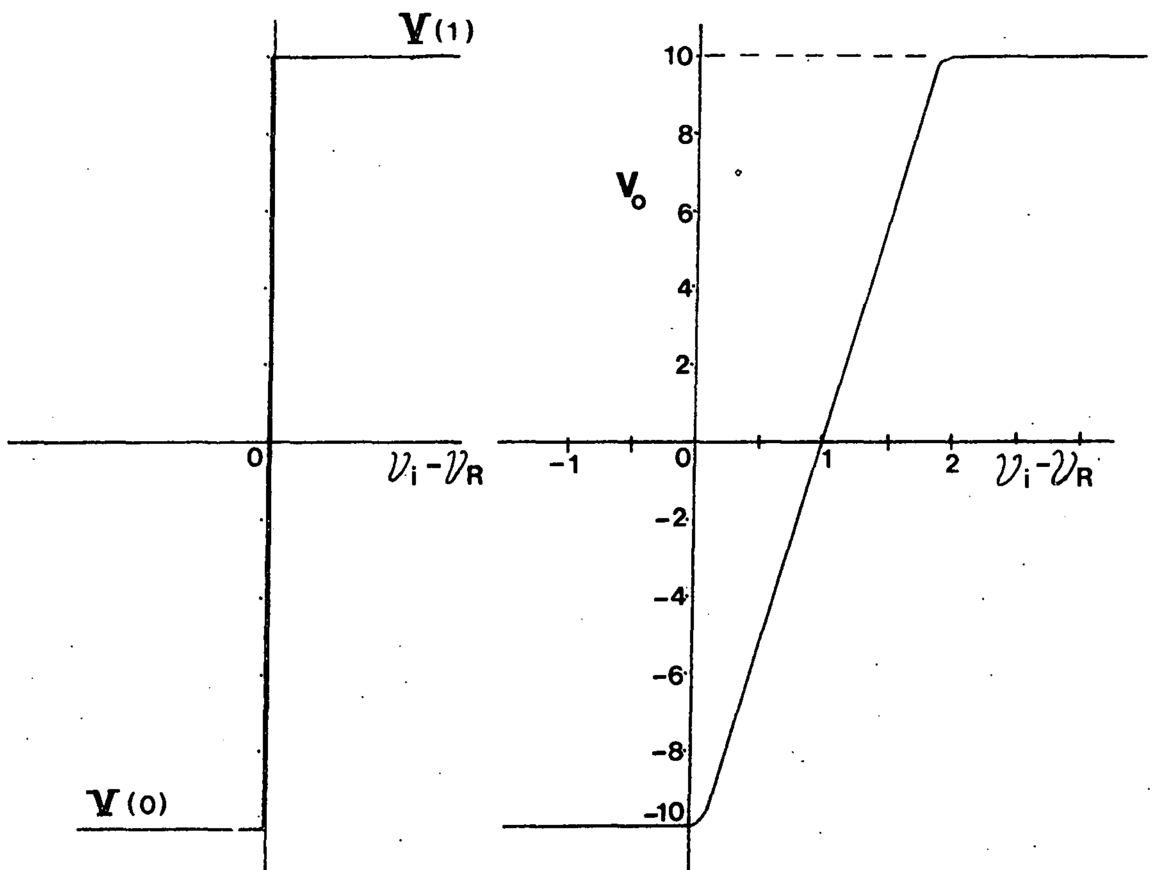

a) Ideal comparator b) Practical comparator .

Figure(A.3)

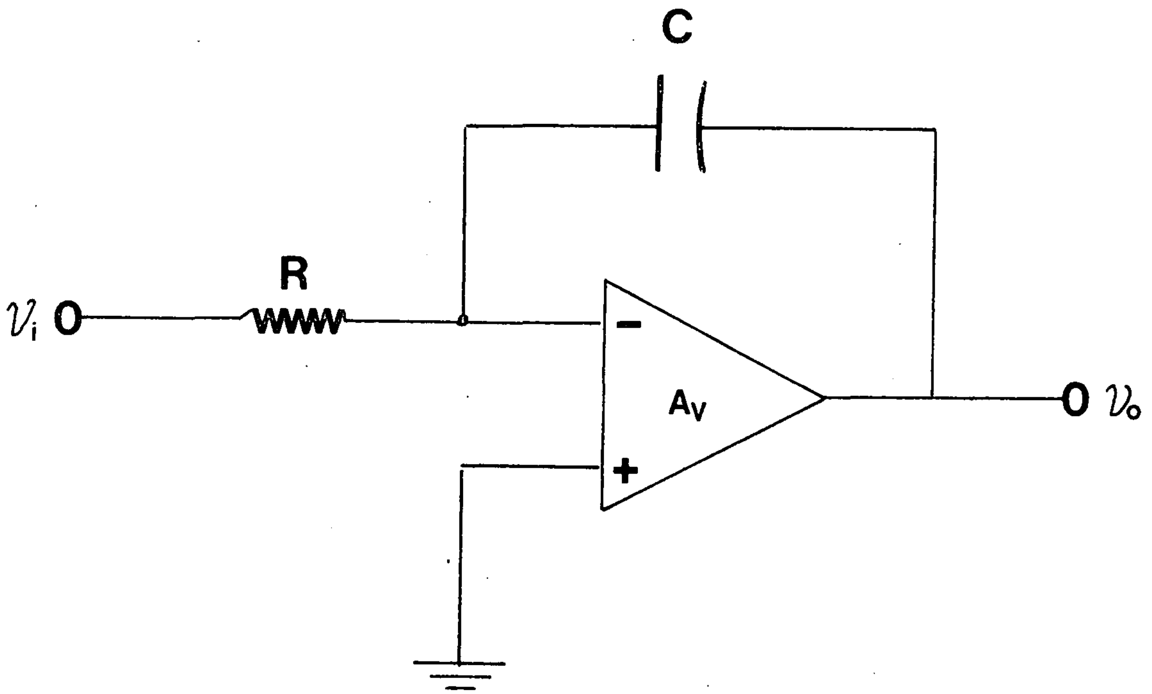

a) Operational integrator circuit.

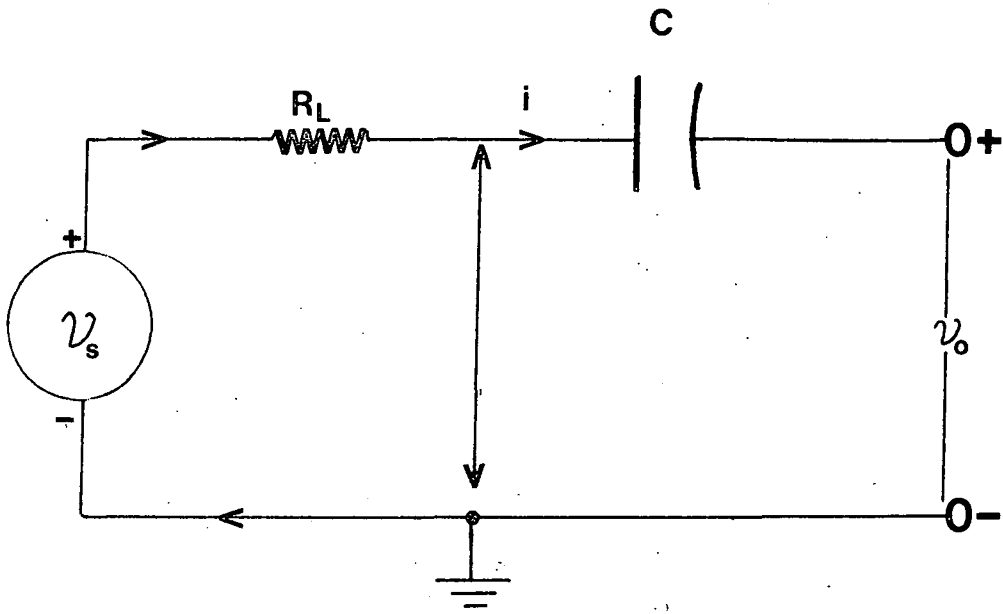

b) Equivalent circuit of the integrator (Ideal)

Figure(A.4)

$$\mathcal{V}_o = -\frac{1}{R \cdot C}\int \mathcal{V}_i \cdot dt$$

i.e.,the output voltage is proportional to the integral of **the** input voltage.When the input voltage is constant $\mathcal{V}_i = \mathbf{V}$ the output voltage becomes

$$\mathcal{V}_o = -\frac{\mathbf{V} \cdot t}{R \cdot C}$$

3. <u>The non-inverting amplifier configuration</u>

This circuit consists of an operational amplifier with resistors connected as shown in figure(A.5).The feed-back current which flows back to the input circuit is zero because $R_{in} = \infty$,so the feed-back voltage V_f across points B and C in figure(A.5)is equal to

$$\frac{\mathcal{V}_o}{R_1 + R_2} \cdot R_2$$

and since the input circuit is an open circuit

$$\mathcal{V}_i = \frac{\mathcal{V}_o}{R_1 + R_2} \cdot R_2$$

$$\frac{\mathcal{V}_o}{\mathcal{V}_i} = \frac{R_1 + R_2}{R_2} = A_v$$

$$A_v = 1 + \frac{R_1}{R_2}$$

So by manipulating the R_1 and R_2 values,The A_v value can be controled.

The voltage follower is a non-inverting amplifier configuration with $R_2 = \infty$ i.e.,open circuit and is used as

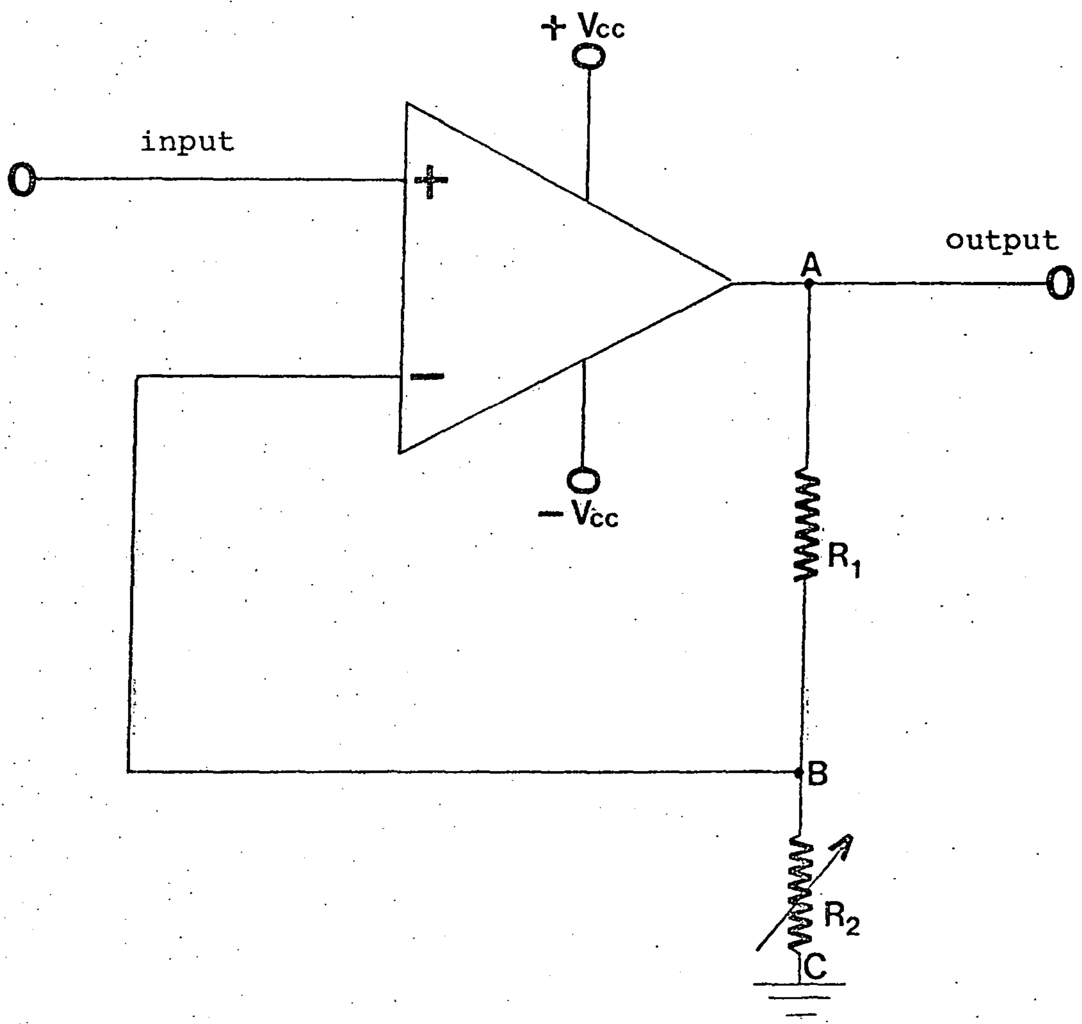

Figure (A. 5)

The non-inverting amplifier configuration .

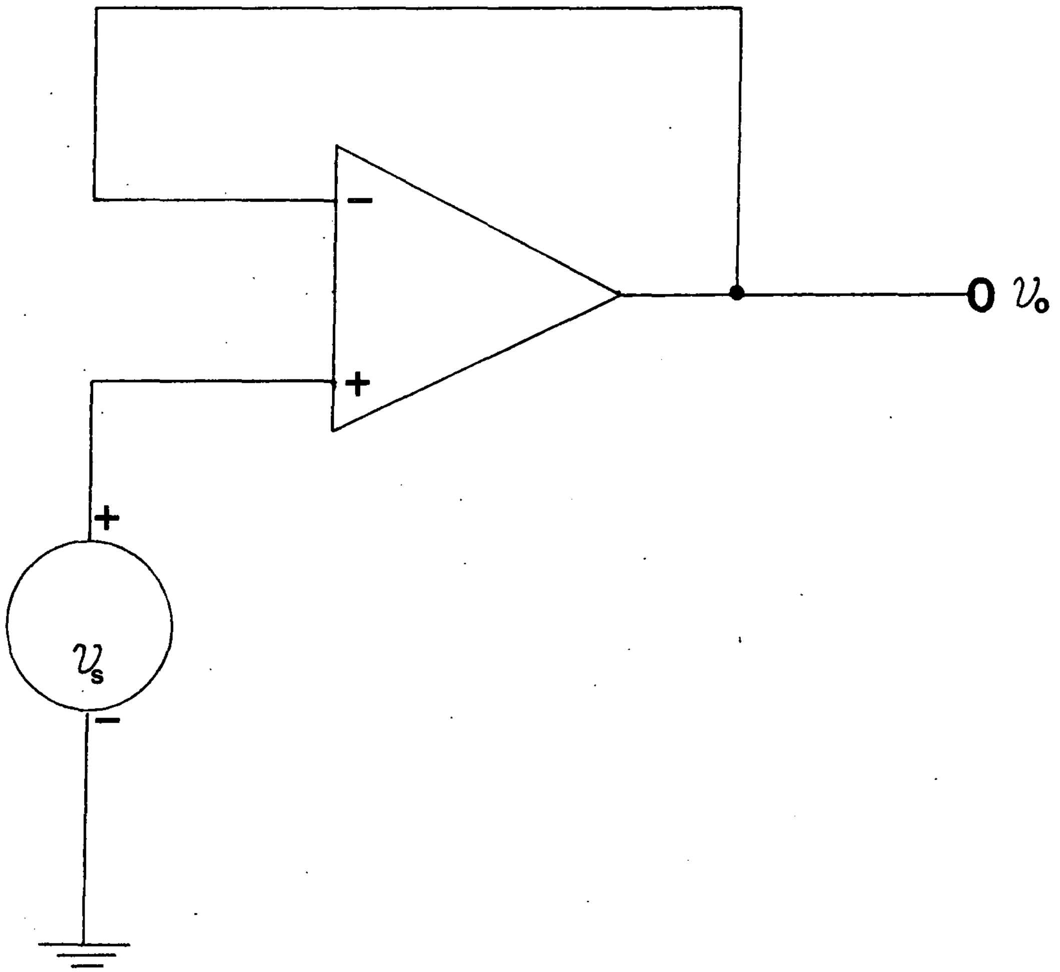

Figure(A.6)

Voltage follower with $v_o = v_s$.

an impedence matching network between two stages,(see figure A.6).

A-3 The Analogue to Digital Converter ADC Circuit

The ADC(see figure A.7)has the ability to digitize analogue signals or to translate the analogue information into the digital form.The analogue signal enters the ADC input and after a finite conversion time the digital output is available for use.There are many types of converter circuits, the four most popular systems being:

(1) The counting analogue to digital converter ADC.

(2) The successive approximation ADC.

(3) The parallel comparator ADC.

(4) The dual-slope integrator ADC.

The system which we employed is the successive approximation ADC which offers an enhanced rate of conversion with a high accuracy.The block diagram of the ADC based circuit which was constructed is shown in figure(A.8).This consists of an inverter and clock circuit with an ADC chip(RS 427).
The ADC chip is eight-bit based and incorporates;

1. A fast comparator.
2. A voltage switching digital to analogue converter.
3. A 2.5V precision reference.
4. Tri-state output buffers.
5. Approximation logic.

Figure(A.9)shows the internal block diagram of the converter where the R-2R ladder and the analogue voltage switches represent the control logic circuit.At the start of conversion(on the first clock pulse edge),the most significant bit MSB sets to 1(high) with all the other bits set to 0(low).This produces a voltage output from the DAC of $V_{ref\ in}$ which is co-

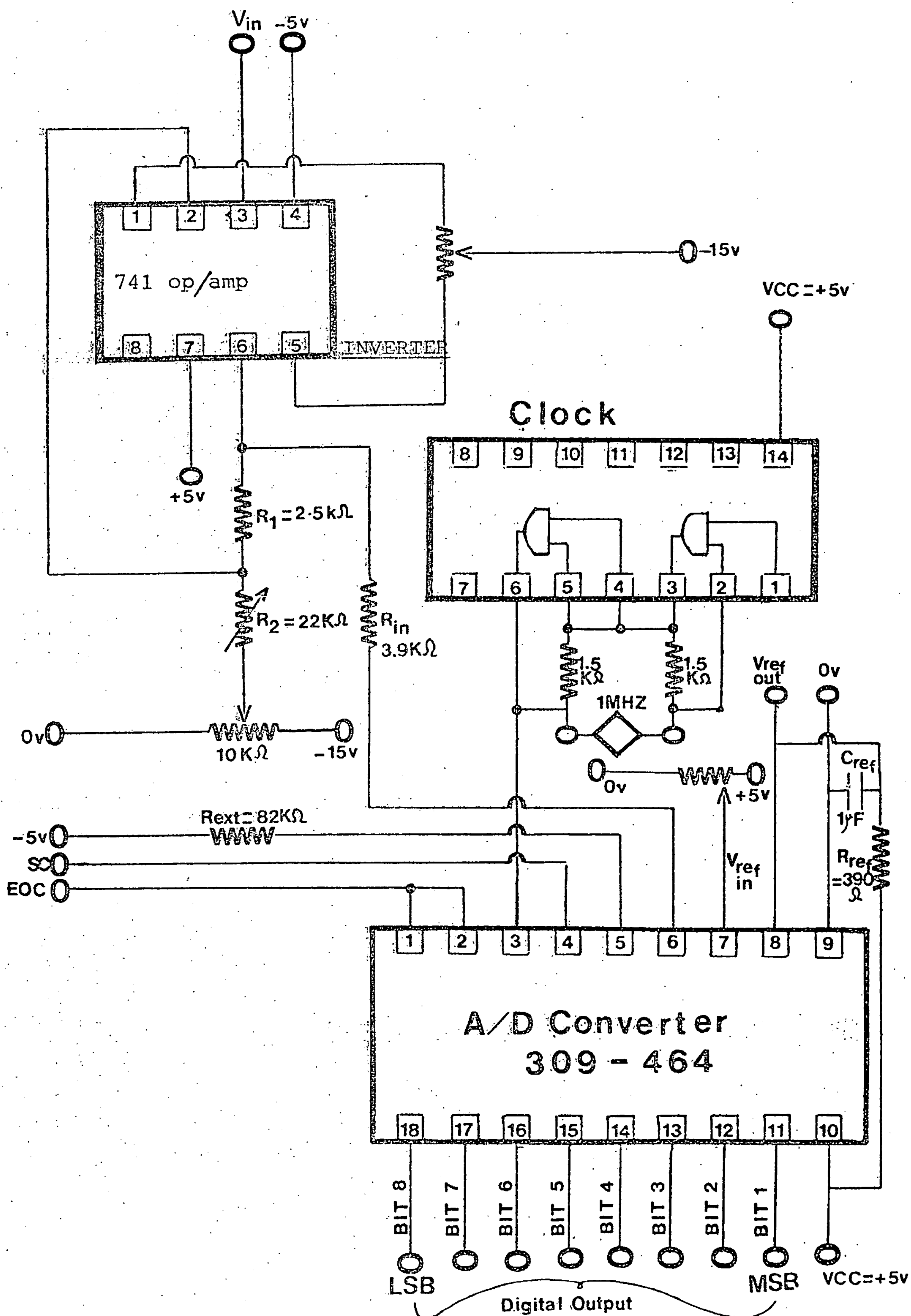

Figure(A.7)

Typical analogue to digital converter circuit.

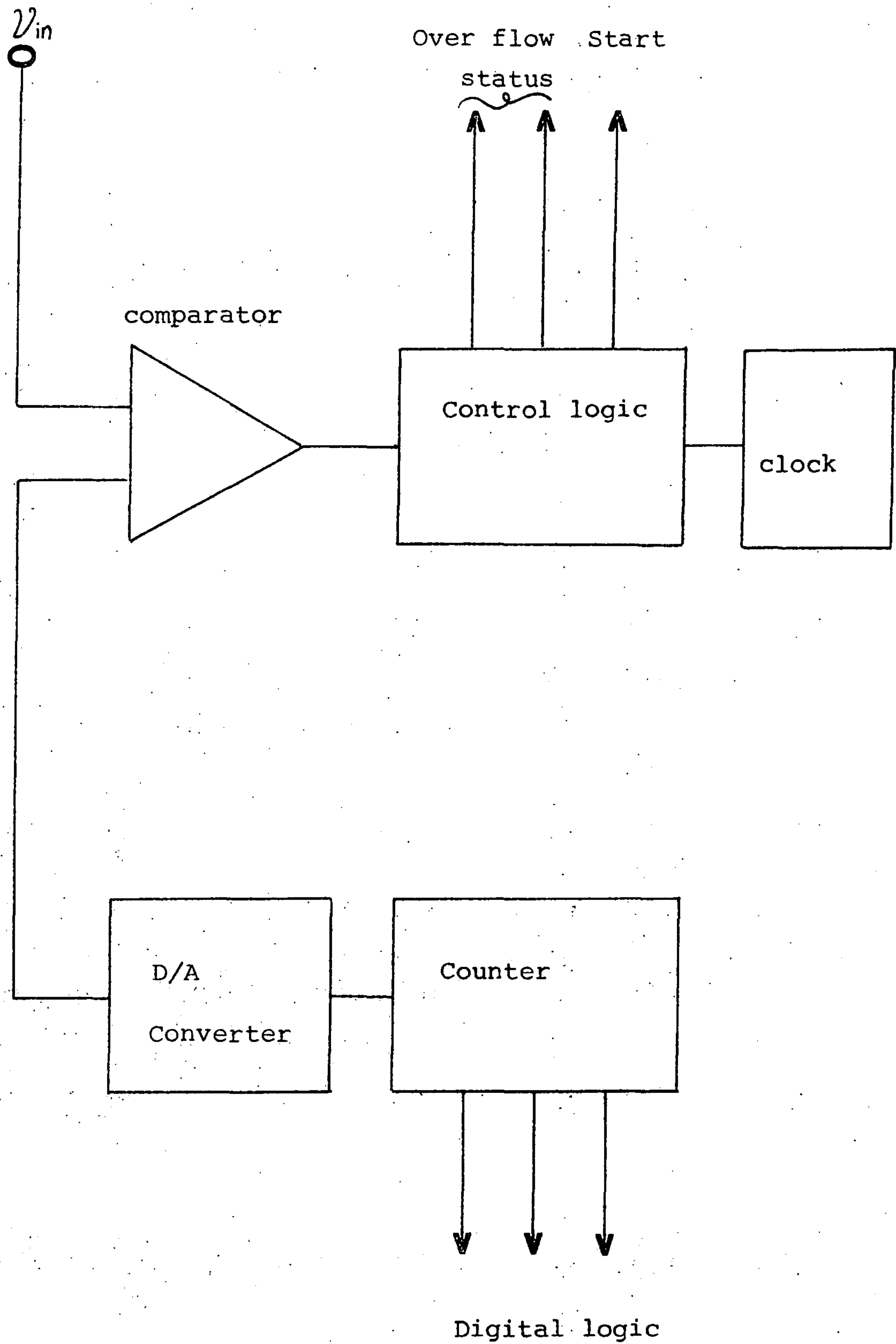

Figure (A.8)

Block Diagram of a successive approximation ADC.

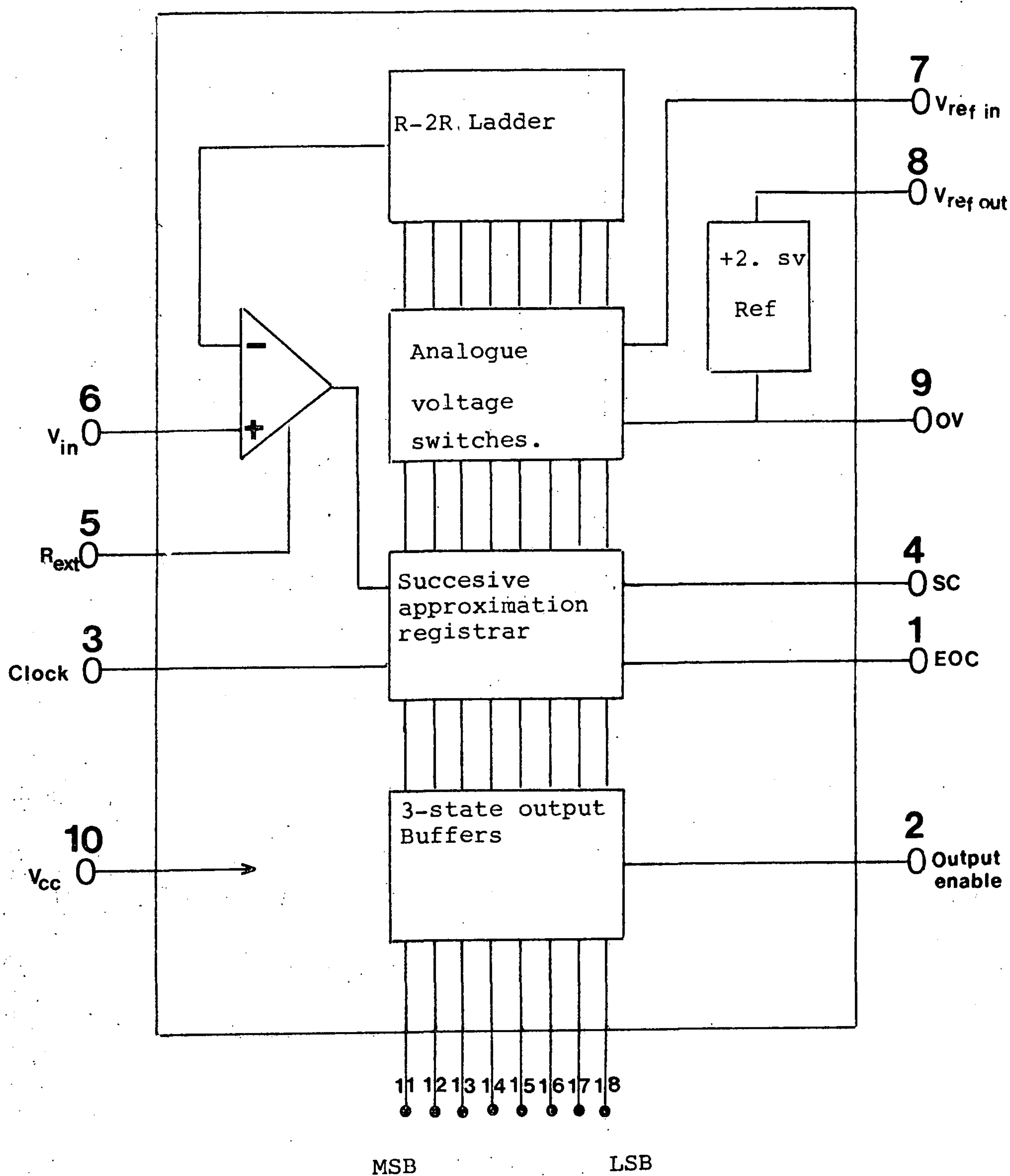

Figure(A.9)

The internal block diagram of the RS 427.

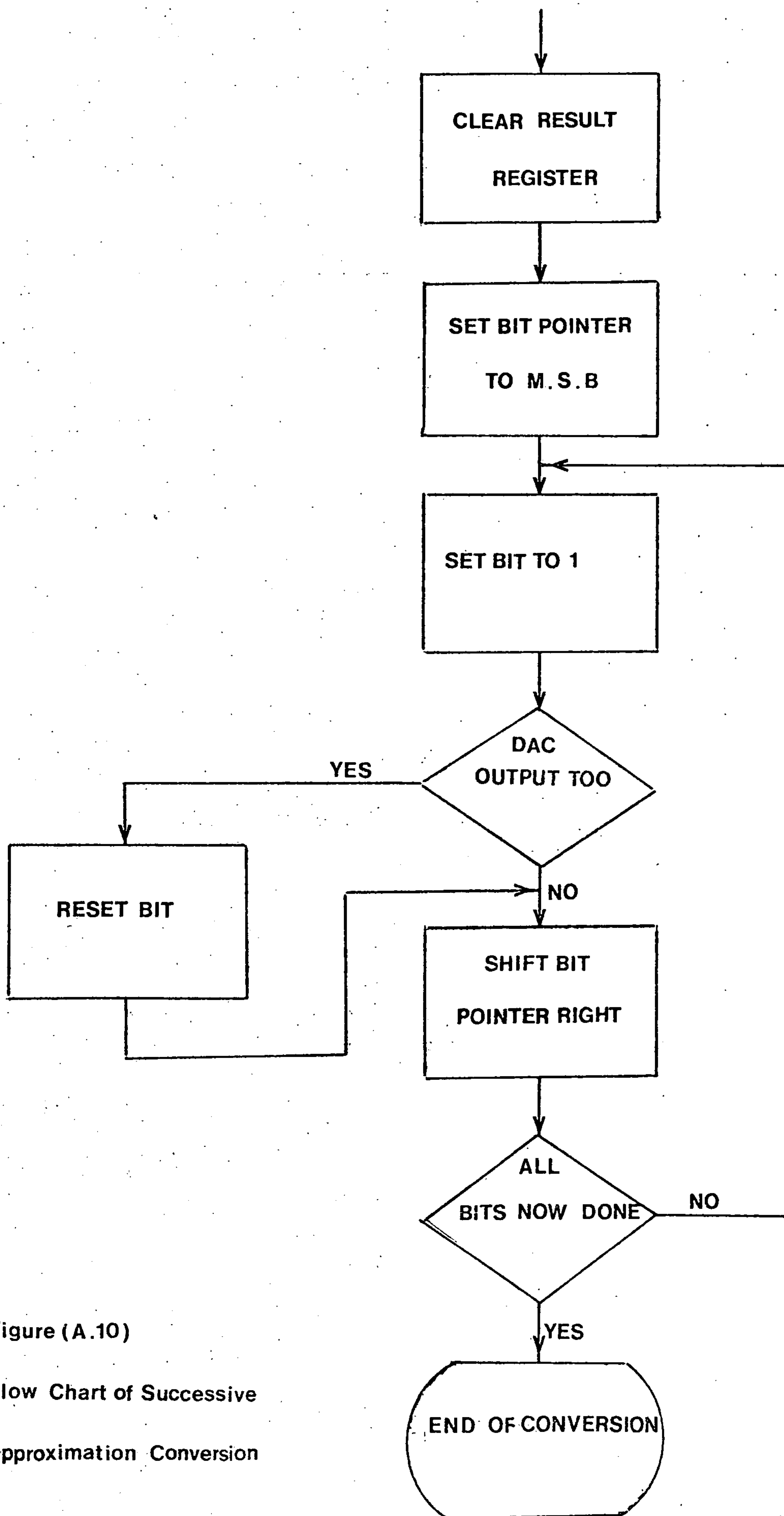

Figure (A.10)

Flow Chart of Successive

Approximation Conversion

mpared with the analogue input signal V_{in}.So,if the DAC output is larger,then the MSB sets to 0(**low**) and bit(2) is switched to a 1(high).This process is repeated for all the eight bits; then the EOC(end of conversion)output goes high and the digital output from the converter is a valid representation of V_{in}.The flow diagram explaining this operation is shown in figure(A.10).

Since the reference voltage is +2.5V,we need the input voltage to be within the range $0 \leftrightarrow +2.5V$.However,the supplied output voltage,which drives into the ADC,from the electrometer is within the range $+1V \leftrightarrow -1V$.It was therefore necessary to construct a circuit to convert the $\mp 1V$ to the voltage range of $0 \leftrightarrow +2.5V$.The circuit to perform this level shifting operation is shown in figure(A.11).

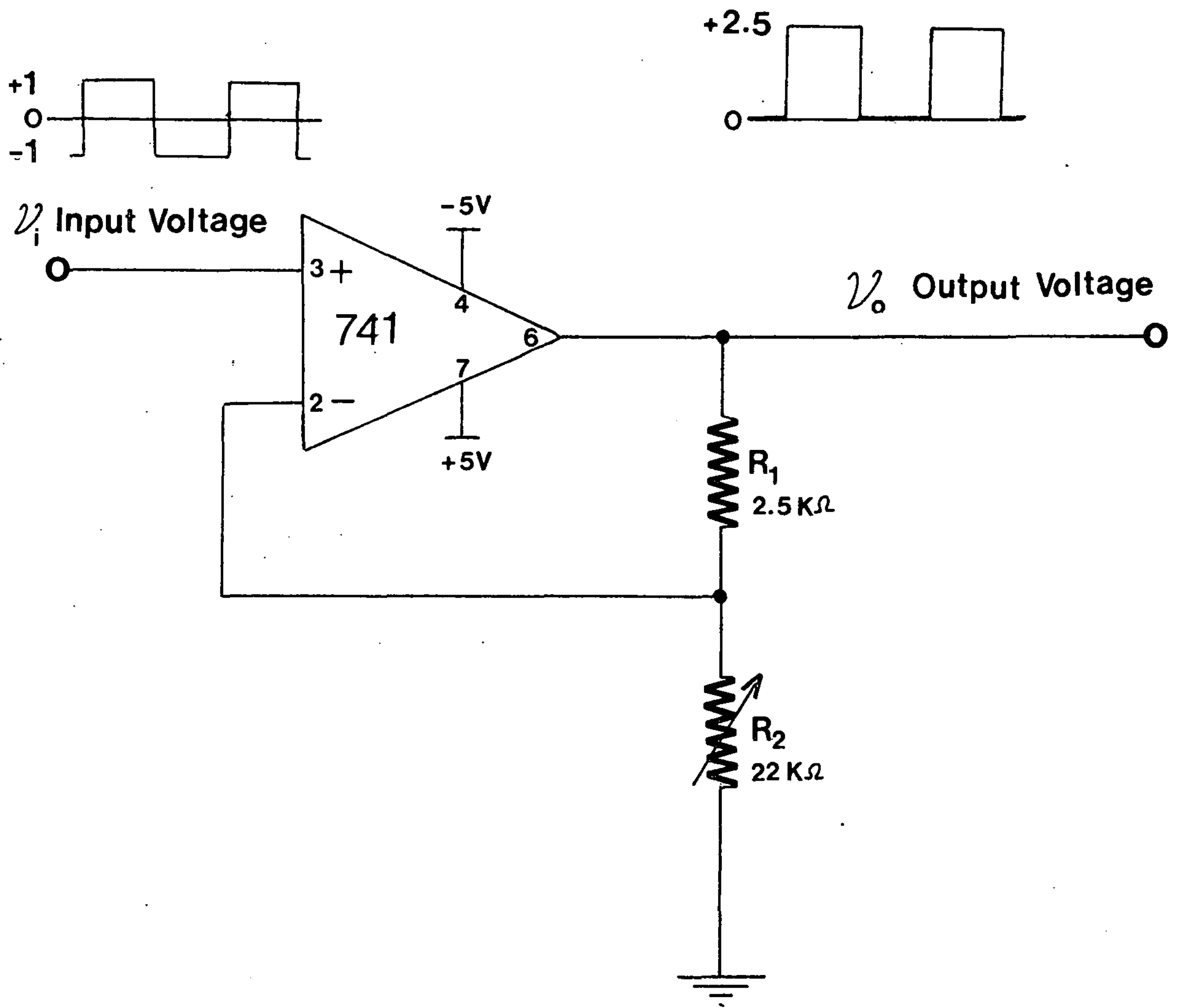

Figure(A.11) The the non-inverting amplifier circuit used **for** voltage level shifting operation.

APPENDIX TWO

LISTING OF THE EXPERIMENTAL RESULTS

p-type MOS device   Sweep rate α=3.05V/s   Electrometer range ER=0.3x10^{-8}A

	V_g Volts	V_g-V_{fB} Volts	C	D	|C|+|D|	|C|-|D|	X_d x10^{-4}cm	$\|I_{gen}\|$x10^{-8}A/cm^2	ψ_s Volts Drop-back.	ψ_s Volts Tonner & Simmons.
1	2.0	1.15	21.1	-7.1	28.2	14.0	1.530	1.025	1.989	2.06
2	2.2	1.35	21.5	-6.1	27.6	15.4	1.565	1.124	2.081	2.23
3	2.4	1.55	21.9	-4.6	26.5	17.3	1.642	1.255	2.290	2.39
4	2.6	1.75	22.0	-3.4	25.4	18.6	1.724	1.341	2.525	2.56
5	2.8	1.95	22.1	-2.7	24.8	19.4	1.771	1.395	2.665	2.71
6	3.0	2.15	22.3	-1.6	23.9	20.7	1.842	1.487	2.883	2.89
7	3.2	2.35	22.7	-0.5	23.2	22.2	1.908	1.584	3.093	3.04
8	3.4	2.55	23.0	0.0	23.0	23.0	1.927	1.639	3.155	3.20
9	3.6	2.75	23.2	1.2	24.4	22.0	2.024	1.730	3.480	3.35
10	3.8	2.95	23.7	2.0	25.7	21.7	2.056	1.820	3.591	3.50
11	4.0	3.15	24.0	2.6	26.6	21.4	2.088	1.881	3.704	3.65
12	4.2	3.35	24.1	3.2	27.3	20.8	2.154	1.925	3.942	3.81
13	4.4	3.55	24.5	4.1	28.6	20.4	2.192	2.016	4.082	3.95
14	4.6	3.75	25.0	4.7	29.7	20.3	2.215	2.089	4.168	4.11

P-type MOS device Sweep rate $\alpha = 3.05 V/s$ Electrometer range $ER = 0.3 \times 10^{-8} A$

(Continued)

	V_g Volts	$V_g - V_{fB}$ Volts	C	D	$\|C\|+\|D\|$	$\|C\|-\|D\|$	$X_d \times 10^{-4}$ cm	$\|I_{gen}\| \times 10^{-8} A/cm^2$	ψ_s Volts Drop-back	ψ_s Volts Tonner &Simmons.
15	4.8	3.95	25.3	5.2	30.5	20.1	2.232	2.150	4.233	4.27
16	5.0	4.15	25.7	5.7	31.4	20.0	2.248	2.205	4.293	4.42
17	5.2	4.35	26.2	6.5	32.7	19.7	2.297	2.293	4.444	4.58
18	5.4	4.55	26.7	7.5	34.2	19.2	2.352	2.392	4.700	4.74
19	5.6	4.75	27.0	8.4	35.4	18.6	2.435	2.469	5.038	4.89
20	5.8	4.95	27.5	9.3	36.8	18.2	2.493	2.562	5.280	5.04
21	6.0	5.15	28.0	10.0	38.0	18.0	2.523	2.643	5.408	5.19
22	6.2	5.35	28.5	10.7	39.2	17.8	2.554	2.724	5.542	5.34
23	6.4	5.55	28.8	11.1	39.9	17.7	2.570	2.771	5.612	5.50
24	6.6	5.75	29.2	11.7	40.9	17.5	2.602	2.838	5.752	5.65
25	6.8	5.95	29.7	12.4	42.1	17.3	2.630	2.920	5.877	5.79
26	7.0	6.15	30.1	12.9	43.0	17.2	2.651	2.982	5.971	5.94

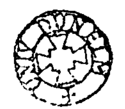

p-type MOS device   Sweep rate α=3.05V/s   Electrometer range ER=0.3 $\times 10^{-8}$A

	$X_E \times 10^{-4}$cm	$U_g \times 10^{15}$ sec^{-1}
1	1.547	1.765
2	1.603	1.061
3	1.683	0.654
4	1.747	0.717
5	1.806	0.808
6	1.875	0.917
7	1.917	1.806
8	1.975	0.585
9	2.04	1.755
10	2.072	1.189
11	2.121	0.416
12	2.173	1.494
13	2.203	1.981
14	2.223	2.239
15	2.240	2.145
16	2.267	1.408
17	2.319	0.950
18	2.393	0.579
19	2.464	1.000
20	2.508	1.685
21	2.538	1.631
22	2.562	1.833
23	2.586	1.306
24	2.616	1.828
25	2.640	1.842

average value of $U_g = 1.343 \times 10^{15}$ sec^{-1}

p-type MOS device Sweep rate α =1.03V/s Electrometer range ER=0.1×10^{-8}A

	V_g Volts	$V_g - V_{fB}$ Volts	C	D	|C|+|D|	|C|-|D|	X_d $\times10^{-4}$cm	$\|I_{gen}\|$ $\times10^{-8}$A/cm^2	ψ_s Volts Drop-back.	ψ_s Volts Tonner &Simmor
1	2.0	1.15	38.0	9.5	47.5	28.5	1.535	1.158	2.002	2.00
2	2.2	1.35	39.2	11.4	50.6	27.8	1.579	1.229	2.118	2.15
3	2.4	1.55	40.4	13.1	53.5	27.3	1.612	1.296	2.207	2.27
4	2.6	1.75	41.3	14.6	55.9	26.7	1.654	1.350	2.324	2.40
5	2.8	1.95	42.3	16.4	58.7	25.9	1.710	1.415	2.484	2.52
6	3.0	2.15	43.4	18.2	61.6	25.2	1.765	1.477	2.647	2.65
7	3.2	2.35	44.4	19.5	63.9	24.9	1.789	1.530	2.721	2.77
8	3.4	2.55	45.5	21.3	66.8	24.2	1.847	1.594	2.898	2.90
9	3.6	2.75	46.6	22.7	69.3	23.9	1.873	1.651	2.982	3.01
10	3.8	2.95	47.7	24.2	71.9	23.5	1.909	1.710	3.097	3.14
11	4.0	3.15	48.9	25.8	74.7	23.1	1.946	1.773	3.217	3.26
12	4.2	3.35	50.3	27.5	77.7	22.8	1.974	1.841	3.312	3.37
13	4.4	3.55	51.6	29.3	80.9	22.4	2.013	1.913	3.445	3.49
14	4.6	3.75	52.3	30.5	82.8	21.8	2.075	1.953	3.659	3.61
15	4.8	3.95	53.5	32.0	85.5	21.5	2.107	2.013	3.772	3.72
16	5.0	4.15	54.8	33.5	88.5	21.3	2.129	2.077	3.851	3.83
17	5.2	4.35	56.1	35.2	91.3	20.9	2.174	2.144	4.015	3.94
18	5.4	4.55	57.1	36.5	93.2	20.6	2.208	2.185	4.145	4.06
19	5.6	4.57	58.2	37.8	96.0	20.4	2.232	2.249	4.233	4.17
20	5.8	4.95	59.2	38.9	98.1	20.3	2.244	2.285	4.281	4.27
21	6.0	5.15	59.7	39.7	99.4	20.0	2.281	2.324	4.423	4.37
22	6.2	5.35	60.9	41.1	102.0	19.8	2.306	2.382	4.522	4.47
23	6.4	5.55	62.2	42.6	104.8	19.6	2.332	2.445	4.623	4.57
24	6.6	5.75	63.1	43.6	106.7	19.5	2.345	2.489	4.675	4.66
25	6.8	5.95	64.2	44.8	109.0	19.4	2.363	2.541	4.744	4.76
26	7.0	6.15	65.4	46.2	111.6	19.2	2.385	2.599	4.837	4.85

p-type MOS device Sweep rate α=1.03V/s Electrometer range ER=0.1×10^{-8}A

	$X_E \times 10^{-4}$ cm	$V_g \times 10^{15}$ sec^{-1}
1	1.557	1.007
2	1.595	1.267
3	1.633	0.8025
4	1.682	0.7245
5	1.737	0.7036
6	1.777	1.378
7	1.818	0.6887
8	1.860	1.368
9	1.891	1.023
10	1.927	1.062
11	1.960	1.515
12	1.993	1.152
13	2.044	0.4027
14	2.091	1.170
15	2.118	1.815
16	2.151	0.9293
17	2.191	0.7527
18	2.220	1.664
19	2.238	1.872
20	2.262	0.6579
21	2.293	0.5243
22	2.319	1.176
23	2.338	1,200
24	2.354	1.595
25	2.374	1.418

average value of $U_g=1.114\times10^{15}$ sec^{-1}

n-type MOS device   Sweep rate $\alpha = 5.72$ V/s   Electrometer range $ER = 0.1 \times 10^{-8}$ A

	V_g Volts	$V_g - V_{fB}$ Volts	C	D	|C|+|D|	|C|-|D|	$X_d \times 10^{-4}$ cm	$\|I_{gen}\| \times 10^{-8}$ A/cm^2	ψ_s Volts Drop-back.	ψ_s Volts Tonner & Simmor
1	-5.0	-5.42	30.3	-18.1	48.4	12.2	1.214	1.230	-2.899	-2.98
2	-5.2	-5.62	30.2	-17.3	47.5	12.9	1.242	1.295	-3.034	-3.12
3	-5.4	-5.82	30.1	-16.8	46.9	13.3	1.262	1.331	-3.132	-3.26
4	-5.6	-6.02	30.0	-15.6	45.6	14.4	1.307	1.432	-3.356	-3.41
5	-5.8	-6.22	30.0	-14.7	44.7	15.3	1.339	1.515	-3.526	-3.56
6	-6.0	-6.42	30.0	-13.7	43.7	16.3	1.376	1.606	-3.724	-3.70
7	-6.2	-6.62	30.0	-12.9	42.9	17.1	1.407	1.678	-3.893	-3.85
8	-6.4	-6.82	30.0	-12.4	42.4	17.6	1.427	1.723	-4.008	-3.99
9	-6.6	-7.02	30.0	-12.0	42.0	18.2	1.444	1.778	-4.101	-4.14
10	-6.8	-7.22	30.0	-11.1	41.1	18.9	1.482	1.838	-4.320	-4.29
11	-7.0	-7.42	30.0	-10.3	40.3	19.7	1.517	1.909	-4.528	-4.42
12	-7.2	-7.62	30.0	- 9.7	39.7	20.3	1.544	1.961	-4.693	-4.57
13	-7.4	-7.82	30.2	-9.2	39.4	21.0	1.558	2.026	-4.778	-4.71
14	-7.6	-8.02	30.3	-8.6	38.9	21.7	1.582	2.090	-4.925	-4.86
15	-7.8	-8.22	30.5	-8.0	38.5	22.5	1.602	2.162	-5.047	-5.00
16	-8.0	-8.42	30.7	-7.3	38.0	23.4	1.627	2.245	-5.206	-5.14
17	-8.2	-8.62	30.9	-6.8	37.7	24.1	1.642	2.309	-5.304	-5.29
18	-8.4	-8.82	31.0	-6.3	37.3	24.7	1.663	2.362	-5.439	-5.44
19	-8.6	-9.02	31.1	-5.8	36.9	25.3	1.684	2.412	-5.579	-5.58
20	-8.8	-9.22	31.2	-5.5	36.7	25.7	1.695	2.448	-5.650	-5.73

n-type MOS device   Sweep rate α=5.72V/s   Electrometer range ER=0.1×10^{-8}A

	V_g volts	V_g-V_{fB} volts	C	D	$\lvert C\rvert+\lvert D\rvert$	$\lvert C\rvert-\lvert D\rvert$	X_d $\times10^{-4}$cm	$\lvert J_{gen}\rvert$ $\times10^{-8}$ A/cm^2	ψ_s Volts Drop-back.	ψ_s Volts Tonner & Simmons
1	-9.0	-9.42	31.3	-4.8	36.1	26.5	1.728	2.517	-5.783	-5.88
2	-9.2	-9.62	31.4	-4.3	35.7	27.1	1.750	2.672	-6.028	-6.03
3	-9.4	-9.82	31.5	-4.0	35.5	27.5	1.762	2.602	-6.106	-6.18
4	-9.6	-10.02	31.6	-3.5	35.1	28.1	1.785	2.657	-6.271	-6.32
5	-9.8	-10.22	31.9	-2.8	34.7	29.1	1.809	2.746	-6.441	-6.48
6	-10.0	-10.42	32.1	-2.4	34.5	29.7	1.821	2.800	-6.528	-6.62

n-type MOS device   Sweep rate α=5.72V/s   Electrometer range ER=0.1×10^{-8}A

	$X_E \times 10^{-4}$cm	$U_g \times 10^{15}$ sec^{-1}
1	1.228	1.449
2	1.252	1.123
3	1.284	1.401
4	1.323	1.619
5	1.357	1.535
6	1.391	1.449
7	1.417	1.404
8	1.435	2.019
9	1.463	0.9856
10	1.499	1.266
11	1.530	1.202
12	1.551	2.898
13	1.569	1.664
14	1.592	2.247
15	1.614	2.072
16	1.634	2.663
17	1.652	1.575
18	1.673	1.486
19	1.689	2.043
20	1.711	1.828
21	1.739	1.560
22	1.756	1.560

	$X_E \times 10^{-4}$cm	$U_g \times 10^{15}$sec^{-1}
23	1.773	1.492
24	1.797	2.314
25	1.815	2.808

U_g(average) is 1.746×10^{15} sec^{-1}

n-type MOS device   Sweep rate α=1.72V/s   Electrometer range ER=0.3×10^{-9}A

	V_g Volts	V_g-V_{fB} Volts	C	D	|C|+|D|	|C| - |D|	X_d $\times10^{-4}$cm	$\|I_{gen}\|\times10^{-8}$ A/cm^2	ψ_s Volts Drop-back.	ψ_s Volts Tonner &Simmons
1	-5.0	-5.42	44.1	-6.1	50.2	38.0	1.164	1.159	-2.665	-2.64
2	-5.2	-5.62	44.8	-4.8	49.6	40.0	1.181	1.216	-2.743	-2.77
3	-5.4	-5.82	45.4	-3.4	48.8	42.0	1.205	1.272	-2.856	-2.89
4	-5.6	-6.02	45.8	-1.9	47.7	43.9	1.240	1.322	-3.024	-3.02
5	-5.8	-6.22	46.1	-0.7	46.8	45.4	1.270	1.361	-3.172	-3.15
6	-6.0	-6.42	46.4	0.0	46.4	46.4	1.283	1.388	-3.237	-3.28
7	-6.2	-6.62	47.3	1.5	48.8	45.8	1.304	1.456	-3.344	-3.39
8	-6.4	-6.82	48.1	2.9	51.0	45.2	1.325	1.517	-3.453	-3.51
9	-6.6	-7.02	48.7	3.8	52.5	44.9	1.336	1.559	-3.510	-3.63
10	-6.8	-7.22	49.4	5.0	54.4	44.4	1.354	1.612	-3.606	-3.74
11	-7.0	-7.42	49.8	6.6	56.4	43.2	1.400	1.661	-3.855	-3.86
12	-7.2	-7.62	50.3	8.2	58.5	42.1	1.444	1.714	-4.101	-3.97
13	-7.4	-7.82	50.8	9.1	59.9	41.7	1.461	1.752	-4.198	-4.08
14	-7.6	-8.02	51.4	10.1	61.5	41.3	1.478	1.795	-4.296	-4.19
15	-7.8	-8.22	52.1	11.1	63.2	41.0	1.491	1.842	-4.372	-4.30
16	-8.0	-8.42	52.8	12.2	65.0	40.6	1.508	1.891	-4.473	-4.40
17	-8.2	-8.62	53.1	12.8	65.9	40.3	1.522	1.914	-4.556	-4.51
18	-8.4	-8.82	53.8	13.8	67.6	40.0	1.536	1.961	-4.640	-4.61
19	-8.6	-9.02	54.2	14.7	68.9	39.5	1.559	1.994	-4.780	-4.71
20	-8.8	-9.22	54.4	15.3	69.7	39.1	1.577	2.013	-4.891	-4.81
21	-9.0	-9.42	55.0	16.2	71.2	38.8	1.592	2.053	-4.985	-4.92
22	-9.2	-9.62	55.7	17.3	73.0	38.4	1.612	2.101	-5.111	-5.01
23	-9.4	-9.82	56.5	18.4	74.9	38.1	1.627	2.153	-5.206	-5.11
24	-9.6	-10.02	57.4	19.6	77.0	37.8	1.642	2.210	-5.303	-5.21
25	-9.8	-10.22	57.7	20.1	77.8	37.6	1.652	2.231	-5.367	-5.31
26	-10.4	-10.42	58.5	21.1	79.6	37.4	1.663	2.272	-5.439	-5.40

n-type MOS device Sweep rate α=1.72V/s Electrometer range ER=0.3×10^{-9}A

	$X_d \times 10^{-4}$ cm	$U_g \times 10^{15}$ sec^{-1}
1	1.172	2.302
2	1.193	1.456
3	1.222	0.8917
4	1.255	0.8114
5	1.276	1.296
6	1.293	2.021
7	1.314	1.813
8	1.330	2.383
9	1.345	1.837
10	1.377	0.6649
11	1.422	0.7519
12	1.452	1.395
13	1.469	1.579
14	1.484	2.256
15	1.499	1.799
16	1.515	1.025
17	1.529	2.095
18	1.547	0.8956
19	1.568	0.6589
20	1.584	1.664
21	1.602	1.498
22	1.619	2.164
23	1.634	2.372
24	1.647	1.310
25	1.657	2.326

average $(U_g) = 1.570 \times 10^{15}$ sec^{-1}

APPENDIX THREE

THE PROGRAM LISTING

```
10 REM"THE DROP BACK PROGRAM"

20 REM POKE 59468,192:POKE 59468,224

30 REM Y=PEEK(59457)

40 REM PRINT Y

50 REM GO TO 10

60 DIM Y(255),T(255),D(255)

70 REM*****************(CONSTANTS)********************

80 SP=10.36E-13                     (ELECTRON PERMITTIVITY)

90 OP=3.46E-13                      (OXIDE PERMITTIVITY)

100 SR=3.05                         (SWEEP RATE)

110 ER=0.3E-8                       (ELECTROMETER RANGE)

120 AS=18.385E-3                    (GATE AREA)

130 FD=7                            (DROP FACTOR)

140 CX=47.158E-9                    (OXIDE CAPACITANCE)

150 QE=1.602E-19                    (ELECTRON CHARGE)

160 LET ER=ER/AS                    (ER PER UNIT AREA)

170 REM************************************************

180 INPUT"VOLTAGE DROP=";VD

190 T=0

200 J=0

210 M=0

220 CO=0

230 I=0

240 REM********************************************

250 POKE 59468,192:POKE 59468,224

260 Y(0)=PEEK(59457)

270 POKE 59468,192:POKE 59468,224

280 I=I+1

290 Y(I)=PEEK(59457)
```

```
300 IF (Y(I-1)-Y(I))>50 THEN 360

310 IF M=0 THEN 330

320 IF X <(TI-T(J-1) THEN 520

330 IF I<240 THEN 270

340 GO TO 230                    :REM RESTART

350 REM*******************(SENSING LOOP)*****************

360 FOR K=1 TO 5

370 I=I+1

380 POKE 59468,192:POKE 59468,224

390 Y(I)=PEEK(59457)

400 NEXT

410 IF(Y(I-6)-Y(I))>150 THEN (J)=TI:CO=CO+1:J=J+1:PRINT"SENSING"

420 REM**************************************************

430 IF CO=2 THEN TD=T(J-1)-T(J-2):GO TO 460

440 IF I<253 THEN 270

450 IF I>=253 THEN 510

460 X=(TD/2)*FD/10

470 T(J-1)=10*TI

480 M=1                         :REM READY FLAG

490 IF CO=2 GO TO 510

500 GO TO 220                   :REM RESTART

510 REM**************************************************

520 FOR I=1 TO 255

530 POKE 59468,192:POKE 59468,224

540 D(I)=PEEK(59457)

550 IF I<=5 THEN 610

560 IF T>0 THEN 590

570 IF D(I)-D(I-5)  10 THEN 590
```

```
580 GO TO 610
590 IF T=3 THEN 620
600 T=T+1
610 NEXT
620 C=127-D(I-8)
630 D=127-D(I)
640 KK=(2*ER)/255)
650 C1=KK*C
660 D1=KK*D
670 DI=C1+D1                                   (DI REPRESENTS |I|drop)
680 DR=C1-D1                                   (DR REPRESENTS Δ|I| )
690 XD=(2*SR*SP/DR)-SP/CX
700 F=1+(CX*XD/SP)
710 IG=DI/(2*(1-1/F))
720 OPEN 1,4
730 PRINT 1,"C="C,"D="D
740 PRINT 1,"C1="C1,"D1="D1
750 750 PRINT 1,"DI=C1+D1="DI,"DR=C1-D1="DR
760 PRINT 1,"XD="XD,"IG="IG,"VD="VD
770 CLOSE 1,4
```

****

****

******